THE ROLE OF LONG-CHAIN TRITHIOCARBONATES IN THE OPTIMISATION OF IMPALA PLATINUM'S FLOTATION CIRCUIT

BY

CORNELIUS FRANCOIS VOS

Submitted in partial fulfillment of the requirements for the degree

MASTERS IN ENGINEERING

(METALLURGICAL ENGINEERING)

in the Faculty of Engineering, Built Environment and Information Technology,
University of Pretoria

July 2006

Dedicated to My Beloved Parents

Francois and Aletta Vos

THE ROLE OF LONG-CHAIN TRITHIOCARBONATES IN THE OPTIMISATION OF IMPALA PLATINUM's FLOTATION CIRCUIT

by

Cornelius Francois Vos

Supervisor: Prof. J.C. Davidtz

Department Material Science and Metallurgical Engineering

Master in Engineering (Metallurgical Engineering)

Abstract

Trithiocarbonates (TTCs) with less than six carbon atoms per molecule historically have proved to be better bulk sulphide mineral collectors than conventional dithiocarbonates (DTCs). However, high vapor pressures of the short-chain mercaptan decomposition products prevented them from general industrial use.

Impala's commitment in TTC development changed in 2002 when the nC_{12}-trithiocarbonate indicated strong synergism when added to their existing flotation suite. A concerted research effort at the University of Utah followed, and in particular on their surface chemistry. To compliment current research and development at Impala, fundamental work regarding the surface hydrophobicity of pyrrhotite under electrochemically controlled conditions was undertaken at Utah University. Controlled contact angle measurements showed that the surface hydrophobicity of pyrrhotite can be increased by small additions of nC_{12}-trithiocarbonate to SIBX. It was also found that this improvement in the surface hydrophobicity with the SIBX-TTC mixture was more significant at lower oxidation potentials.

Work at Utah University further showed that a C_{12} decomposition product may or may not be present with an adsorbed TTC molecule.

External reflectance infrared spectroscopy in the mid infrared region suggested a "crowding" of the collectors at the surface when SIBX and TTC are combined. This was based on an increase in the absorbance of the -CH2- peaks in the mixed collector system.

In bench scale flotation tests on PGM bearing samples from the Merensky reef, it was found that a 5 molar percent replacement of SIBX with nC_{12}-trithiocarbonate improved the flotation activity relative

to the standard SIBX-DTP mixture.

Improvements were in the recoveries of PGMs, copper and nickel. The addition of TTC also increased the flotation rates of both slow and fast floating valuables as is predicted by the Kelsall equation. The optimum mixture for the pilot plant trials was thus a 5 molar percent replacement of the current collector suite with nC_{12}-TTC.
Based on the bench flotation results, research was extended to a pilot plant trial. At a depressant dosage of 100g/ton, the PGM concentrate grades from the first rougher cell improved from 120g/ton to 175g/ton when the TTC was introduced. This was achieved without any effect on the recovery from the first cell. This increase in concentrate grade is believed to arise from the nature of both:

- The mineral-collector surface state, and
- The bubble surface interaction.

Overall, the standard SIBX-DTP collector combination and the new SIBX-DTP-TTC collector combination (both at 100g/ton depressant) was also compared to pilot plant tests with SIBX-DTP at high (350g/ton) depressant dosages. The latter suite forms the currents reagent suite at Impala Platinum. When comparing the first two trials, at 100g/ton depressant, the addition of TTC as a ternary collector resulted in a recovery improvement of approximately 2.2% with a simultaneous increase in final concentrate grade from 57g/ton to 73g/ton. The result was a reduction in solids recovery from 5.3% to 4.1%. When comparing the TTC trial to the standard collector suite at high depressant dosages, only a small reduction (3.6% vs. 4.1%) in solids recovery was achieved with a final concentrate grade of 85g/ton. The PGM recoveries were very similar.

Based on current Merensky milling rates, depressant and TTC costs, and calculated replacements based on the pilot plant tests, a projected cost saving on chemicals is R9.6 million per annum. Financial impacts on processing, grade and kinetics have not been made.

It was also concluded that the detrimental effect of mild steel milling on the flotation activity of SIBX-DTP was diminished with the addition of the long-chain TTC with SIBX and DTP.

As part to this research, a preliminary plant trial on UG-2 underground material showed a reduced primary rougher chromite grade as well as a significant increase in PGM concentrate grade for the first two primary rougher cells. This is an important finding, especially for the melting process. In this final study a partial (5 molar percent) replacement of the standard collector used was also made. What was further realised was a significant increase in the final concentrate grade when compared to the standard conditions.

Acknowledgements

This thesis would not have been possible without great contributions from many individuals and selected institutions. I would like to take this opportunity to express my sincere gratitude towards:

- My Heavenly Father who gave me this extraordinary opportunity to be part of something great and for the opportunity to develop my abilities which He so lovingly bestowed upon me.
- My late grandfather Casper Matthee who taught me the life long values of patience and perseverance.
- My grandfather, Cor Vos, from whom both my father and I have learned life's lessons and for making us the men we are today. For teaching us the true values of faith, honesty and hard work.
- My parents who always stood by me during the tough times with kind works of motivation, their ideas and input into this thesis and for their prayers which carried me all the way.
- Prof. John Davidtz, my supervisor, for his friendship, encouragement, patience and guidance during my research and to his wife for her warm hospitality during my visits.
- Prof. Jan Miller of the College of Mines and Earth Science at the University of Utah, United States for his guidance and support during my visit.
- Doctors Jinshan Li, Zorroh Nicholov and Petersen from Utah University for their assistance with the fundamental investigations on pyrrhotite.
- To Impala Platinum for the financial assistance and to Johan Theron and Dave Marshall for their technical inputs.

Table of Contents

List of Figures

List of Tables

List of Abbreviations

$(DTC)_2$	Dixanthogen
Al_2O_3	Corundum
As	Arsenite
BC	Bushveld complex
C	Carbon atom
C_i	Thiocarbonate collector with i carbon atoms in the hydrocarbon chain
cm^2	Area, square centimeters
CMC	Carboxymethyl cellulose
$CO3^{2-}$	Carbonate ion
CR	Concentration ratio
Cr_2O_3	Chromite
Cu	Copper
CuS	Covellite
$CuSO_4$	Copper sulphate
DETA	Diethylenetriamine
dm	decimeter
DTC	Dithiocarbonates or xanthates
DTCB	Dithiocarbamates
DTP	Dithiophosphate
e^-	Electron
E	Potential (mV)
EDA	Ethylenediamine
ENT_i	Mineral entrainment
ERS	External reflectance spectroscopy
f,t,c	Indicates feed, concentrate and tails assays
FCTR	Floatability Characteristic Test Rig
$Fe_{(1-x)}S$	Pyrrhotite
$Fe(OH)_3$	Iron hydroxide
Fe^{2+}/Fe^{3+}	Ferrous/ferric ions
FTIR	Fourier Transform Infrared Spectroscopy

g/ton	PGM grade in grams per tone
H	Hydrogen atom
H_2O	Water
H_2S	Hydrogen sulphide
K	Initial flotation rate constant
Kf	Rate constant for fast floating minerals
kg	kilogram
KNO_3	Potassium nitrate
Ks	Rate constant for slow floating minerals
K_{sp}	Solubility product
L	Liter
m3	Cubic meter
MBS	Sodium meta-bisulphide
MF1	Mill-float once
MF2	Mill-float twice
mg	milligrams
min	Minutes
mol/L	Concentration in moles per liter
mV	Millivolts
nC_{12}	Normal carbon chain with twelve carbon atoms in chain
Ni	Nickel
nm	Nanometer
NRF	National research foundation
NSF	National science foundation
O_2	Oxygen
^oC	Temperature, degrees Celsius
OH^-	Hydroxide ion
Pb	Lead
$PbCO_3$	Lead carbonate
$PbNO_3$	Lead nitrate
PbS	Galena
$PbSO_4$	Lead sulphate
PGM	Platinum group minerals
Pn	Pentlandite

Po	Pyrrhotite
PZC	Point of zero charge
R	Ideal gas constant
r	Recovery at specific point in time
Ri	Final recovery
Rpm	Revolutions per minute
S	Sulphur
SAG	Semi-autogenous grinding
SCE	Standard calomel electrode
SG	Specific gravity
SHE	Standard hydrogen electrode
SIBX	Sodium isobutyl xanthate
SiO_2	Silica
SO_2	Sulphur dioxide
$SO4^{2-}$	Sulphate ion
STD	Standard test conditions (reference)
T	Temperature
t	Time
TOF-SIMS	Time of flight secondary ion mass spectroscopy
TTC	Trithiocarbonates
UG-2	Second chrometite layer of the upper group chrometite unit
V	Volts
X^-	ionic xanthate
X_2	Dixanthogen
Xi	Collector mole fraction
XPS	X-ray photon spectroscopy
XRD	X-ray diffraction
Xw	Water mole fraction
Zn	Zinc
ΔG^{ex}	Change in Gibbs Excess Free Energy
$\Delta\gamma$	Change in interfacial tension
ϕ	Equilibrium contact angle
ϕf	Fraction of fast floating minerals

ϕs	Fractions of slow floating minerals
γi	Activity coefficient of collector
γ_{ma}	Interface tension between mineral and air
γ_{mw}	Interface tension between mineral and water
γw	Activity coefficient of water
γ_{wa}	Interface tension between water and air
μA	Mikro-amperes
μm	Micrometer
π_{LG}	Surface tension between liquid (water) and gas (air)

CHAPTER 1

Introduction

1.1 Background

The trithiocarbonate (TTC) collectors were developed in the mid 1980's and from as early as 1985 Impala Platinum supported research that focused on the possibility of introducing the TTC as a collector for sulphide mineral beneficiation. These studies predominantly dealt with the short-chain (less than C_6) TTCs and the results repeatedly showed (Steyn, 1996; Coetzer, 1987; Slabbert, 1985) that when the TTC is adsorbed onto the mineral surface a much stronger hydrophobic state is obtained. An increase in rates and recoveries of PGMs were almost invariably found when compared to dithiocarbonates (DTCs), dithiophosphates (DTPs) or any combination of the latter two. The iso-propyl TTC in particular improved the rates and recoveries of base metals and PGMs. Its industrial application was however restricted due to hydrolysis and oxidation that produced a volatile mercaptan with an objectionable odour (Davidtz, 2004).

From a research point of view the short-chain TTCs were very interesting and rewarding. They resulted in an improved understanding of the science and in particular the chemistry of flotation systems. The added sulphur component in the carbonate series made it possible to systematically investigate the role of molecular structures, and in particular the effect of isomorphous replacements of sulfur, nitrogen and oxygen atoms in the polar group of the thiocarbonates. Using newer techniques, (Steyn, 1996), it became possible to calculate the surface activity coefficients of adsorbed molecules on sulphide minerals. By introducing a calculable thermodynamic function, the Gibbs Excess Free Energy (ΔG^{ex}), surface hydrophobicity and those structural factors that influenced it could be quantified (Davidtz, 1999; Steyn, 1996). A direct theoretical thermodynamic function, the contact angle, which is related to the Gibbs Excess Free Energy (equation 1.1), could now add to the understanding of molecular factors on the physical properties of the system.

$$\Delta G^{ex} = \pi_{LG}.(Cos\phi-1) \qquad (1.1)$$

where π_{LG} is the surface tension between liquid(water) and gas(air), and ϕ the equilibrium contact angle.

Continued research led to the development of water soluble long-chain (C_{10} and C_{12}) TTCs and with the funding from NRF (S.A), NSF (U.S.A), Utah and Pretoria Universities, it was possible to undertake fundamental studies to investigate the surface chemistry of short- and long-chain TTCs, and in particular the chemistry associated with pyrite surfaces (Du Plessis, 2003). This improved understanding of the surface chemistry showed the TTCs to differ markedly from the DTCs and DTCBs (dithiocarbamates). Furthermore, short- and long-chain TTCs also differed in their chemistry and physical effects on flotation (Davidtz, 2004). Being aware of these new developments in TTC collectors Impala Platinum agreed to sponsor an MSc project to re-investigate the application of the long-chain TTC in the beneficiation of PGM bearing ores, the results of which follow.

1.2 Research Objectives and Thesis Layout

The primary objective was to ***improve Impala's collector suite***. Since the interactions between the various flotation chemicals are not necessary independently variable, changes in collector combination could influence the function of other chemical additives such as activators, frothers and depressants. It is not possible to predict the effects of a newly added chemical so the testing of various combinations of long-chain TTCs with Impala's existing chemical suite was the most logical. This meant an R&D program on collector chemicals. The results would need special attention and interpretation on plant operations. This means observing and analysing circuit performance.

Various criteria, such as rougher grade, would for example have implications on downstream processing such as smelting. An integrated view of collector chemistry and overall effects on plant performance are necessary when evaluating findings on rates, recoveries and grades. So, an important objective was to ***search for and identify chemical factors as they influence plant performance***. This also meant the unraveling of those chemical factors that result in physical and operational changes.

Unusual fundamental properties of TTCs such as the ability to produce a strong hydrophobic state at very low oxygen partial pressures have to be capitalised on and the influence of oxygen presence and absence on chemical and mineral reactions have to be exploited. This means a different approach to investigating flotation activity (rate, recovery and selectivity) from laboratory scale, to pilot plant and finally to a full scale plant trial was possible.

The sub-processes and interactions (figure 1.1) during sulphide flotation as summarised by Chander (1999) shows many phases and interactions. From a physico-chemical point of view it was recognised that the flotation system is a multi-phase and multi-component system and it is necessary to reduce the many interacting components to only include the sulphide minerals, different reagents and the oxygen partial pressure.

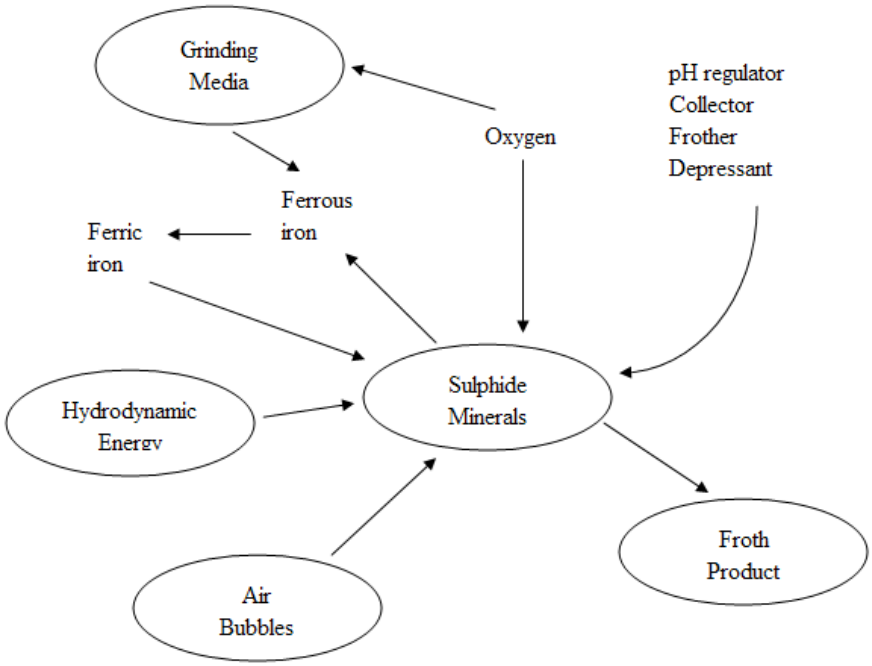

Figure 1.1: Schematic of interactions during the flotation of sulphide minerals (Chander, 1999).

Pyrrhotite readily oxidizes and at high pH it hydroxylates. A further objective was to ***establish the effect of copper and lead activation with combinations of TTC and xanthate on surface hydrophobicity of pyrrhotite***. This was done with captive bubble contact angle measurements under electrochemically-controlled conditions along with external reflectance spectroscopy (ERS).

A fourth objective was to ***define the amount of TTC required to improve PGM beneficiation*** for the ensuing pilot plant and eventual full-scale plant trial. The PGM-bearing Merensky reef was used and supporting laboratory bench flotation tests on Merensky reef samples were done.

All laboratory and pilot plant research focused on Merensky reef with the intention of following up with a plant trial on this ore. Unforeseen problems arose on the MF-2 section of the ***Central concentrator*** where the trial was planned. Because of this it was decided to evaluate the chemicals on a UG-2 plant trial although no preliminary research had been done on UG-2.

The current reagent suite at Impala Platinum on Merensky ore consists of: sodium isobutyl xanthate (SIBX) and sodium dithiophosphate (DTP) as collectors, copper sulphate as activator, KU-47 which is a CMC as depressant and Senfroth20 as a frothing agent. High chrome (~12%) grinding media is used in the SAG mills while the system is open to air. During a pilot plant trial the new TTC as co-collector at 100g/ton depressant was researched and compared to the standard collector suite at both normal (100g/ton) and high (350 g/ton) depressant dosages. The metallurgical evaluation was done in terms of valuable mineral flotation kinetics, final PGM recovery and PGM grade in the final concentrate.

The reagent suites used for treating UG-2 ores differ for the Central and UG-2 concentrator. The UG-2 concentrator makes use of a Mintek-type suite, consisting of high collector and low activator dosages. No DTP is used and the activator is only added to the primary section. At the Central concentrator lower collector dosages are used with DTP included as promoter. More activator is used and dosed to both the primary and secondary sections. Both concentrators use the same CMC depressant and frother.

The thesis is concluded with a summary of findings and recommendations for future research.

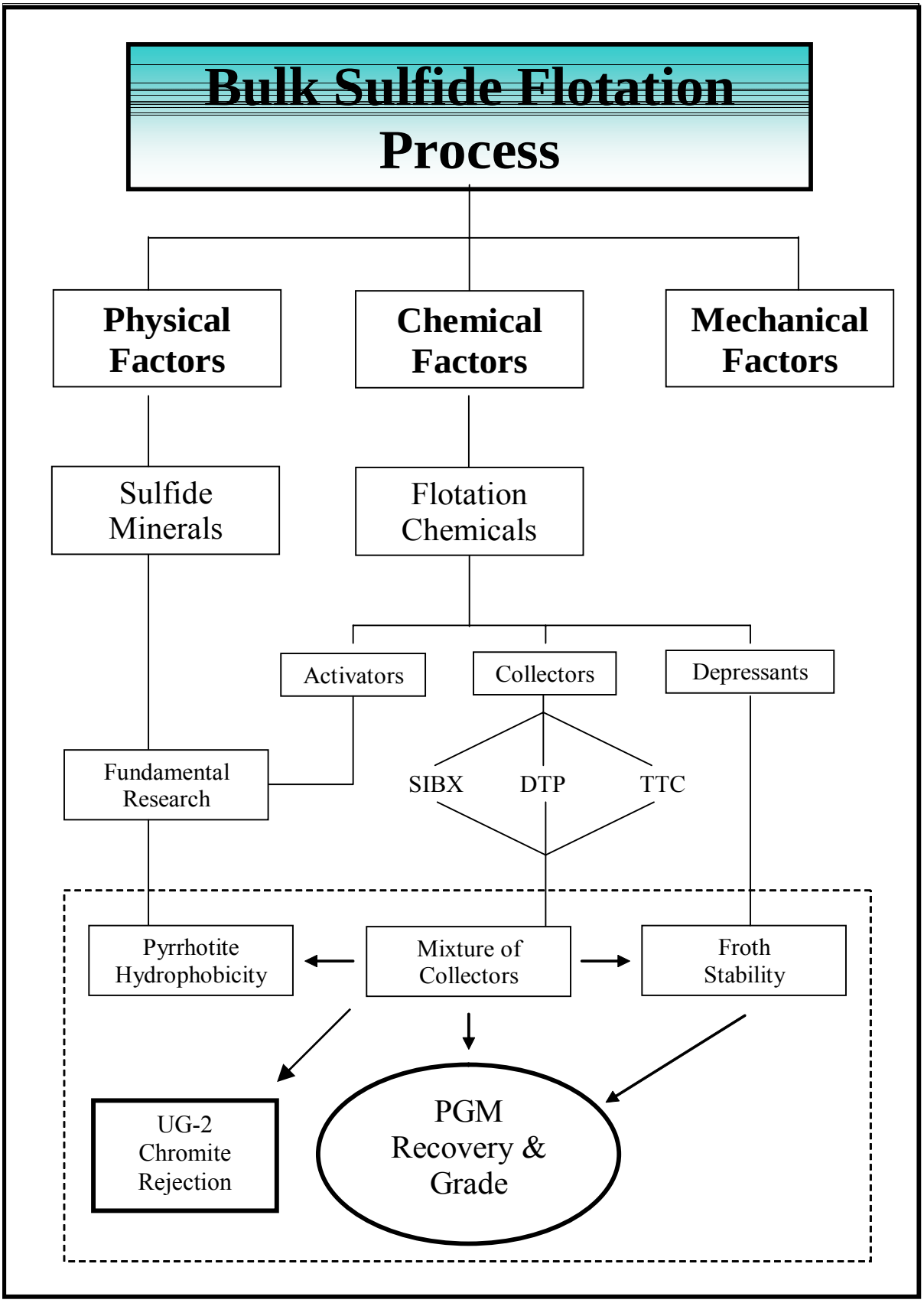

Figure 1.2: A schematic summary of the scope of this thesis.

CHAPTER 2

Literature Review

2.1 Introduction to PGM Beneficiation

The Bushveld Complex (BC) is the worlds largest know source of platinum group minerals (PGMs) with a very complex sulphide and PGM mineralogy. Depending on the reef type and geography of the BC, the predominant PGM mineral types and their associations can vary to a great degree (Cramer, 2001).

The most important sulphide minerals of interest in the BC, and subsequently in this investigation, are pyrrhotite, pentlandite, and chalcopyrite. Chalcopyrite and pentlandite are copper and nickel sulphides respectively, with low metal-xanthate solubility products (Chander, 1999). Iron-xanthate species however, are unstable and at high pH iron hydroxides are the preferred species (Fuerstenau, 1982b). As a rule then, chalcopyrite and pentlandite react strongly with sulfhydryl collectors and are readily floated. Pyrrhotite however is readily oxidised and the result is a varying surface state as a function of time after crystal fracture.

Table 2.1: Most common PGM minerals and base metal sulphides in the Merensky reef (Cramer, 2001).

PGM Minerals		**Base Metal Sulphides**	
Mineral	**Chemical Composition**	**Mineral**	**Chemical Composition**
Braggite	(PtPdNi)S	Chalcopyrite	$CuFeS_2$
Cooperite	PtS	Pentlandite	$(Ni,Fe)_9S_8$
Moncheite	$(PtPdNi)(TeBiSb)_2$	Pyrrhotite	FeS (ideal)
Kotulskite	$(PtPdNi)(TeBiSb)_2$		
Laurite	$(RuFeOsIrPt)S_2$		
Pt-Fe alloys	Unreported		

The PGMs in the float feed are primarily associated with the base metal sulphides, followed by their association with the different oxides and silicates (Vos, 2004; Cramer, 2001). To

concentrate the valuable minerals the mined ore is crushed, milled and subjected to bulk sulphide flotation prior to metalisation (melting and refining).

The design of such flotation circuits in part rely on the knowledge of the flotation kinetics of the different minerals present. Faster flotation kinetics of valuable minerals imply that less and/or smaller flotation cells (lower residence time) can achieve the required valuable mineral. Slower flotation rates of the valuable minerals then would imply that extended circuit residence time will be required to achieve the planned metal recoveries and in the majority of cases the addition of cleaning and re-cleaning stages is needed to achieve the desired final concentrate grades.

For a given flotation circuit and ore type the rates of recovery, and ultimately, the final metal grades and recoveries are influenced by numerous ***chemical factors***. They include: the type and flotation chemistry of the sulphide minerals (Göktepe, 2002; Chander, 1999; Klimpel and Isherwood, 1992; Woods, 1976), the role of various grinding media in comminution circuits (Forssberg et al, 1993; Adam et al, 1984; Iwasaki et al, 1983), the type of flotation reagents used (Grobler et al, 2005; Bulatovic, 2003; Klimpel, 2000) and the presence or absence of oxygen in the pulp - relating to pulp potential (Khan et al, 2004; Du Plessis, 2003; Kuopanportti et al, 1997; Poling, 1976). These factors and their relevance to this thesis are reviewed and discussed next.

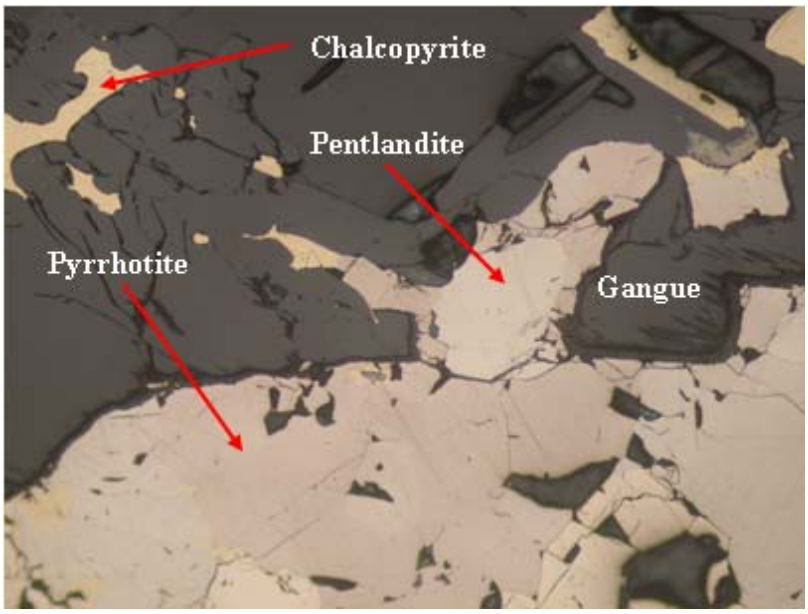

Figure 2.1: Microscope image of a Merensky reef sample indicating base metal sulphides and gangue.

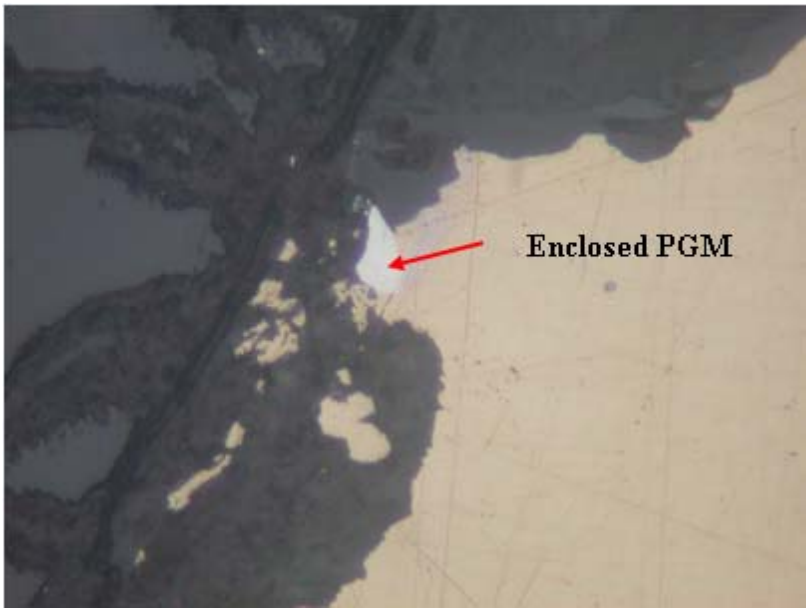

Figure 2.2: Microscope image indicating a PGM mineral included at the sulphide - gangue grain boundary.

2.2 Interacting Parameters in Sulphide Flotation

2.2.1 Reagents

2.2.1.1 Collectors

Collectors are surfactant molecules and in sulphide mineral flotation the polar functional group of the molecule attaches to the mineral surface. The non-polar or hydrophobic groups are not directly bonded to the surface and result in repulsive interactions with polar water molecules. This effect is then responsible for the hydrophobic state between the coated mineral surface and adjacent bulk water. When the hydrophobic chains are relatively long ($+C_6$), hydrophobic interactions can occur between adjacent adsorbed molecules. These are adsorbed "micelle" type of interactions and reduce the interaction with adjacent water relative to fully extended polar chains (Lovell, 1982).

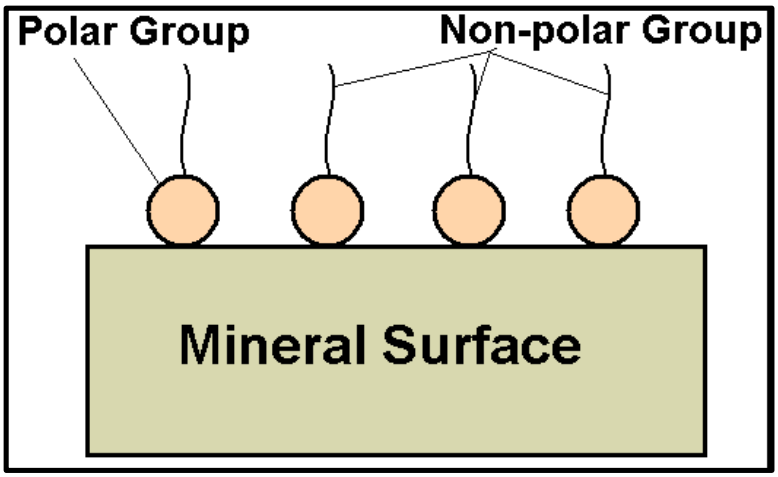

Figure 2.3: An illustration of collector adsorption at a mineral surface (Wills, 1997).

Depending on the sulphide mineral present and the electrochemical nature of the flotation system the collector can either attach via chemisorption, Van der Waals bonding or physisorption (Fuerstenau, 1982a). The accepted mechanisms of adsorption are discussed in more detail later on.

Dithiocarbonates (DTCs) and dithiophosphates (DTPs) are the most widely used collectors for sulphide flotation in the platinum industry. These are "bulk" collectors and this implies a non-selective interaction with sulphide minerals (Wiese, 2005 a, b; Fuerstenau, 1982b). Their

chemistry of adsorption has been well documented (Buckley et al, 2003; Bradshaw, 1997; Buckley et al, 1997; Fuerstenau, 1982a). On the other hand, the chemistry of trithiocarbonates (TTCs) (Du Plessis, 2003) and their flotation characteristics (Steyn, 1996; Slabbert, 1985) have only recently been reported and shown to be particularly effective in the beneficiation of gold and PGMs.

2.2.1.1.1 Single collectors systems

- Dithiophosphates

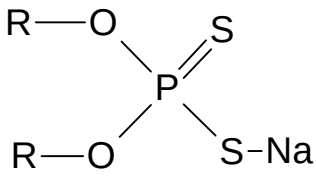

The applications of DTP collectors are primarily in the collection of sulphide minerals over a wide pH (4-12) range, but are most commonly applied in alkaline systems (Lovell, 1982).

Longer chain DTPs ($+C_4$) are known to exhibit both collecting and frothing properties. The former is due to the adsorbed state and the latter due to the alcohol decomposition product while the shorter chain DTPs are essentially non-frothing. When combined with xanthates, these mixtures are reported to be more selective than xanthate collectors alone by reducing the flotation of iron sulphides (Lovell, 1982, Poling, 1976).

A prominent feature of dithiophosphates when compared to xanthates is the adsorption via an ionic state (figure 2.4) at fairly high oxidation potentials (Chander, 1999). In relation to most other thiolates, oxidation of dithiophosphates to the corresponding dithiolate is more difficult. DTP alone however does not show very strong collection properties (Helbig et al, 2000).

- Dithiocarbonates

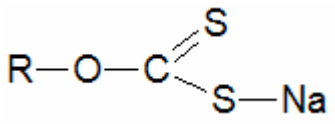

Dithiocarbonates are the only member of the thiocarbonate collectors that has found general application in the industry. There are a number of advantages (Klimpel, 1999; Lovell, 1982) in the selection of DTCs:

- They are relatively inexpensive,
- are easily manufactured, stored and transported,
- are highly soluble in water (2 to 8 mol/L),
- maintain good stability in alkaline solutions (pH > 8), and
- are very effective in the bulk flotation of sulphides.

Short-chain dithiocarbonates (e.g. ethyl xanthate), are predominantly used for the selective flotation of Cu-Zn, Pb-Zn and Cu-Pb-Zn ores (Coetzer et al, 1989; Lovell, 1982) while longer chain (Buckley et al, 2003; Coetzer et al, 1989; Lovell, 1982) DTCs display greater bulk sulphide collection properties.

At pH values below 8, the decomposition of xanthate is believed to first form xanthic acid ($ROCS_2H$) followed by further decomposition to carbon disulphide and the corresponding alcohol (Fuerstenau, 1982b). This low temperature decomposition becomes more prevalent as the pH of the system decreases.

- Trithiocarbonates

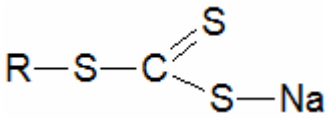

Short-chain trithiocarbonate chemistry in the presence of pyrite has extensively been studied by Du Plessis (2003). It was concluded that TTCs differed markedly from the corresponding dithiocarbonates. Furthermore, using thermodynamic calculations (Davidtz, 1999) it was

shown that the third sulphur atom reduces the polarity of this molecule and this increases the hydrophobic character considerably when compared to that of the corresponding DTC with an isomorphous substituted oxygen. Calculations of Gibbs Excess Free Energies, G^{ex}, for interactions between adjacent water and the corresponding thiocarbonate at equal densities of adsorption show the TTC and DTC to be 3030 and 1470 Joules per mole of interacting species, respectively. This means the TTC has a much weaker attraction for water with a more than double G^{ex}. The difference is due to the increased attraction of water by the oxygen in the butyl DTC and this reduces the hydrophobic state by over 100% if there is a direct relationship between G^{ex} and hydrophobicity (Davidtz, 1999).

One of the differences of the trithiocarbonate molecule when compared to dithiocarbonates and dithiophosphates is that the standard potential for dithiolate formation (figure 2.4) is much lower (Du Plessis, 2003; Chander, 1999) indicating that oxidation to the corresponding dithiolate is much easier. In relation to flotation this implies that provided the dithiolates contribute significantly to flotation activity, TTCs will more readily produce dithiolates on mineral surfaces at lower oxidation potentials (Du Plessis, 2003). Furthermore, the work (Du Plessis, 2003) on pyrite has suggested that one of the decomposition and catalysed adsorption products may be a mercaptan.

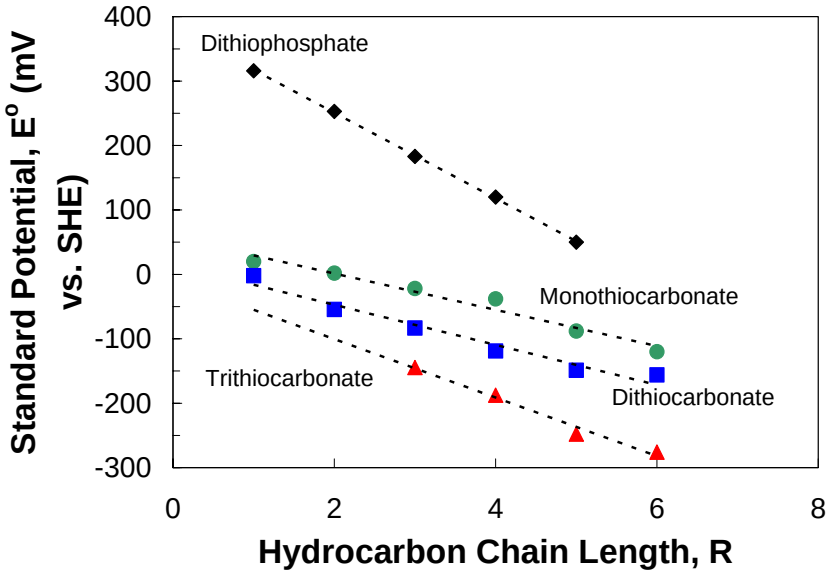

Figure 2.4: Standard redox potentials for thiocarbonate / dithiolate couples as a function of hydrocarbon chain length (Du Plessis, 2003; Chander, 1999).

QEM*SEM (Quantitative evaluation of minerals using scanning electron microscopy) analysis done on Merensky batch flotation tails samples (Steyn, 1996, Davidtz, 1998) for both xanthate and short chain TTC flotation tests indicated that iC3-TTC, when compared to iC4-DTC/DTP, improved the recovery of fine and course iron sulphides. The values of pyrrhotite, pentlandite and chalcopyrite in the flotation tails were reduced by 37.7%, 26.9% and 27.3% respectively. The TTC was thus concluded to be more effective in recovering iron bearing sulphide minerals than DTC-DTP.

2.2.1.1.2 Mixed collector systems

The use of co-collectors or promoters in flotation is well established (Grobler et al, 2005; Monte et al, 2004; Bradshaw, 1997) and these mixtures have often resulted in reduced collector costs without loss in metallurgical performance (Crozier et al, 1989; Leja, 1989; Hanumantha Rao et al, 1997).

Bulk sulphide flotation in PGM beneficiation, traditionally has employed a combination of xanthate and dithiophosphate (Wiese et al, 2005a,b; Bulatovic, 2003; Sweet, 1999). Helbig et al (2000) believed that the role of DTP in a mixture with xanthate was to promote the adsorption of collectors onto sulphide minerals and by doing so increases the collector surface coverage. However, batch flotation test work on PGM bearing Merensky reef samples by Wiese et al (2005b) also showed that DTC-DTP mixtures increased gangue recovery, especially when the collectors were added to the mill followed by copper sulphate addition.

It is believed that the addition of DTP with DTC also increases the selectivity of the process over that of common iron sulphides such as pyrite and pyrrhotite (Poling, 1976). This synergistic effect was attributed to high potentials (Chander, 1999), along with the fact that the metal salts of cuprous and nickel dithiophosphates are more soluble than those of the corresponding DTC salts (Fuerstenau, 1982b). However, it was shown by Wiese et al (2005b) that the presence of both copper sulphate and DTP resulted in improved iron sulphide recoveries.

Breytenbach et al (2003) found the long-chain TTC as a ternary collector with DTC and DTP to significantly improve sulphur grades and recoveries.

2.2.1.2 Depressants

Table 2.1 is a summary of common depressants.

Table 2.2: Common depressants in froth flotation.

Depressant	Application	Reference
Cyanide (CHN^-)	Depression of pyrite.	Du Plessis, 2003
Sodium meta-bisulphide (MBS)	Selective depression of pyrrhotite from a mixture with pentlandite.	Bozkurt et al, 1999
Ethylenediamine (EDA)	The managing of the inadvertent activation of pyroxene in a pyroxene-pentlandite system.	Shackleton et al, 2003
Diethylenetriamine (DETA) + SO_2	Selective depression of pyrrhotite from a mixed Cu-Ni ore.	Kelebek et al, 1996
Polyglucosides and sulfonates	Depression of silica and dolomites in base metal flotation.	Fuerstenau, 1982a
Carboxymethyl cellulose (CMC) and Guar Gum	Used to depress gangue in bulk sulphide flotation for PGM beneficiation.	Wiese et al, 2005b Bradshaw et al, 2006 Ekmekci et al, 2006

The function of depressants during flotation is primarily to increase the hydrophilic state of gangue minerals and thereby reduce their floatability (Kelly and Spottiswood, 1989). A difference between CMC and guar depressants used in PGM flotation, as described by Robertson et al (2003), is that CMC will ionise in solution to form an anionic polymer.

Once adsorbed the new negative mineral surface not only is more hydrophilic but the electrical double layers of similarly charged particles repel one another and thereby disperses or “cleanse” sulphide surfaces. The resultant, an increase in sulphide mineral surface area is exposed to collector molecules, and eventually bubble attachment. This also increases the rate of sulphide mineral flotation (Robertson et al, 2003). A smaller bubble in the froth zone was also identified and the explanation offered (Dippenaar, 1982) was that these highly hydrophobic sulphide minerals cause bubble rupture because no stable contact angle could be formed between sulphide particles and the liquid film.

2.2.1.3 Frothers

Frother molecules can be ionic or anionic. The polar end forms hydrogen bonds with water while the non-polar groups are hydrophobic and concentrates and aligns at the air-water interface within the bubble, making the frother much more powerful (Adamson, 1990).

When considering frothers, the main factors responsible for stable flotation froth formation according to Harris (1982) are:

- The activity of the frother molecule on the surface
- The rate at which the frother molecules can reach a newly extended surface
- The surface viscosity of adsorbed layers of the frother, and
- The bulk viscosity of the frother

An intention with frother addition is to have no interaction with solid surfaces or any of the other added reagents. However, these reactions occur and effect rheological properties of the froths that form (Harris, 1982). Leja and Schulman (1954) reported the co-adsorption of long-chain alcohols with long-chain DTCs at the air-liquid interface and this formed very stable films, which prevented mineral-bubble contact. Furthermore, Leja and Schulman (1954) also showed that frother molecules do interact with mineral surfaces.

Hanumantha Rao and Forssberg (1997) described the interaction between frother and collector molecules by acknowledging the presence of associated and unassociated collector and frother molecules at the interfaces. The film at the solid surface also differs from the film at the air-liquid interface in that the collector is said to adsorb irreversibly while the frother molecules are free to adsorb and desorb. A change in the local surface concentration and hydrophobic character of the solid surface will take place upon contact with a bubble and this is due to the penetration of the frother and collector molecules from the air-liquid interface into the diffuse monolayer at the solid. This strengthens the bubble-particle attachment due to a denser mixed monolayer at the air-liquid interface (Hanumantha Rao and Forssberg, 1997).

To summarise, the function of frothers are no longer seen as reagents solely for the production of froth. Continued research led to a better understanding of the interactions between collector and frother molecules, their influences on bubbles size and the rate of

bubble surface production as well as flotation kinetics (Grobler et al, 2005). The effect of different frothers on the flotation rate of various size fractions of specific ore types is also well known with properly defined optimal particle sizes and flotation recovery rates for the various individual frothers (Klimpel, 1999). To have a balanced system in terms of these variables many concentrators make use of a mix or blend of different frother types (Grobler et al, 2005).

2.2.2 The role of oxygen

2.2.2.1 Surface hydrophobicity

Short-chain DTC collectors are considered to be effective in the recovery of metal sulphides in the presence of oxygen and the explanation given for this is as follow: (Fuerstenau, 1982c):

- Because of the large size of the sulphide ion, (unlike oxygen) the sulphur will not readily form hydrogen bonds and are then naturally hydrophobic.
- The formation of insoluble salts between the short-chain collectors and the heavy metal ions occur at low concentrations.
- Some sulfhydryl collectors are known to undergo oxidation to the corresponding dithiolate at the mineral surface.

Early research work by Taggart et al (1934), Gaudin (1957), Plaksin et al (1957) and Leja (1968) reported the presence of oxygen as a prerequisite for thiol collector adsorption onto sulphide minerals and this was explained by Gaudin (1957) in terms of oxygen being a major component in the reactions between the collector and the sulphide surface. Furthermore, Woods (1971) reported dithiolates as a requirement for the development of a hydrophobic surface state with xanthates.

Although the dithiolate has been identified on most minerals investigated up until now, not all of the surfaces had this product present, yet a hydrophobic surface exists (table 2.3 and references within). Today, it is accepted that two mechanisms are present for thiol collector adsorption onto sulphide mineral surfaces (Woods, 1976).

The first mechanism is ***electrochemical*** and here the oxygen will act as a sink or source for electrons. In this case the oxidation of the thiol to the dithiolate takes place on the mineral surface via two separate reactions (Woods, 1976). The first is the anodic oxidation of the collector to the dithiolate:

$$2X^- \rightarrow X_2 + 2e^- \quad (2.1)$$

coupled with the cathodic reduction of oxygen:

$$H_2O + ½\ O_2 + 2e^- \rightarrow 2OH^- \quad (2.2)$$

Since sulphide minerals show good semi-conductive properties, the electron transfer is said to be via the specific mineral surface. As a result, these mineral surfaces catalise oxygen reduction and dithiolate formation (Woods, 1976).

The second mechanism is that of ***ionic interactions*** with immobilised adsorption and involves the precipitation of the metal dithiolate at the minerals surface (Buckley and Woods, 1997).

Fuerstenau (1982a) proposed the formation of lead-dixanthogen on galena using the following steps:

$$PbS(s) + 2O_2(g) \rightarrow PbSO4(s) \quad (2.3)$$

The equilibrium constant for this reaction is 10^{124} (Fuerstenau, 1982a) suggesting that an oxygen partial pressure of 10^{-62} atmosphere is required for this reaction to occur. This is exceeded by the oxygen present in the atmosphere and hence the oxidation of galena will produce thiosulphate and sulphate. Being open to air and dissolved oxygen, the presence of carbonates will result in the formation of lead carbonate:

$$PbSO_4(s) + CO_3^{2-} \rightarrow PbCO_3(s) + SO_4^{2-} \quad (2.4)$$

At the usual flotation pH (8-9) lead xanthate is more stable than lead carbonate, thiosulphate or sulphate and lead xanthate will form by the replacement (*ion exchange*) of the other lead species.

$$PbA\ (s) + 2X^- \rightarrow PbX_2 + A^{2-} \qquad (2.5)$$

where A represents CO_3 or SO_4.

However, as early as 1952 the suggestion has been that xanthate adsorption onto galena takes place in two stages. The first is the chemisorption of xanthate in mono-layers followed by the formation and adsorption of bulk lead xanthate that precipitates (Fuerstenau, 1982c and references within). It is only the latter part of this model that is described by the ion exchange mechanism.

Since reactions (2.1) and (2.2) are electrochemical with the anodic and cathodic reactions forming different processes there must be a *mixed potential* or *rest potential* at which the two processes both proceed at a finite rate (Woods, 1976). If the rest potential of a mineral-solution system is greater than the reversible potential for dithiolate formation, the formation of dixanthogen is favoured, however, if this is not the case, the formation of the metal xanthate is the only possible surface product (Kelly and Spottiswood, 1989; Woods, 1976). This reversible potential is dependant on the collector type and concentration as is discussed by Du Plessis (2003). To calculate this reversible potential, the Nerst equation is used:

$$E_{rev} = E^O - 0.059 \cdot \log\left(X^-\right) \qquad (2.6)$$

where E^o is the standard half cell potential (figure 2.4) and (X^-) the collector concentration (mol/L).

In a review on the electrochemistry of sulphide flotation, Woods (1976) summarised the rest potentials and xanthate surface species for various metal sulphides from the literature (table 2.3.). It is then suggested that there are two states in which xanthate can be found on the mineral surface. One is the original ionic xanthate adsorbed (metal-xanthate) and the other the dithiolate, which is a neutral molecule.

Using electrochemically controlled contact angle measurements Du Plessis (2003) confirmed that pyrite hydrophobicity with DTCs in oxygenated solutions could not be extended below the reversible potential for dithiolate formation. The metal xanthate species was not present as the hydrophobic species with oxygen at low potentials. However, when the same set of experiments were repeated for pyrite in the presence of TTCs it was found that pyrite hydrophobicity could be extended well below the reversible potential for dithiolate formation.

It was proposed that one of the decomposition products of trithiocarbonates (possibly the mercaptan) was also present at the mineral surface and that this species could contribute to surface hydrophobicity at reduced potentials. The presence of the mercaptan is still speculative due to difficulties in distinguishing between the mercaptan and the carbon disulphide peaks due to the low molar extinction of the mercaptan compared to carbon disulphide as well as the location of the mercaptan peak (206.5nm) to that of carbon disulphide (230nm). It was also reported that trithiocarbonate decomposition was responsible for an increase in pH and this further supported her hypothesis that one of the possible products might be the mercaptan. It has further been suggested by Davidtz (2004) that the formation of mercaptan and its adsorption onto the surface would probably be catalysed by an adsorption step since the mercaptan on its own is a poor synergistic collector with DTCs.

When tests were carried out in the absence of oxygen (nitrogen as flotation gas) the hydrophobicity of pyrite was extended well below the reversible potential for dithiolate formation for both collectors. Infrared spectroscopy identified the presence of iron-dithiolate species on the surface (Du Plessis, 2003).

In this thesis emphasis is placed on iron bearing sulphide minerals (particularly pyrrhotite) during the fundamental studies since copper containing sulphide minerals that do not have iron in the lattice do not have dixanthogen as a surface product but rather it appears to be the metal xanthate. The same can be said for iron bearing sulphide minerals in the absence of oxygen (Du Plessis, 2003). Although the dithiolate/mercaptan issue is still unresolved, Du Plessis (2003) concluded that the creation of hydrophobic surfaces with a TTC is less sensitive to the electrochemical conditions in the pulp than for xanthates.

Table 2.3: Rest potentials (vs. SHE) of sulphide minerals in 6.25x10-4 molar KEX.

Mineral	**Structure**	**Rest Potential and *Xanthate Product**	**Source**
Sphalerite	ZnS	-0.15 - MX	Polling, 1976
Galena	PbS	0.06 - MX	Woods, 1976 Vreugdenhil et al, 1997
Chalcocite	Cu_2S	0.06 - MX	Polling, 1976; Zdziennicka et al, 1998 Buckley et al, 1993
Covellite	CuS	0.05 - X_2	Woods, 1976 Poling, 1976
Chalcopyrite	$CuFeS_2$	0.14 - X_2 MX / X_2	Woods, 1976 Polling, 1976 Hicyilmaz et al, 2004 Mielczarski et al, 1998
Pyrrhotite	$Fe_{1-x}S$	0.21 - X_2	Woods, 1976 Bozkurt et al, 1999; Poling, 1976
Pyrite	FeS_2	0.22 - X_2	Poling, 1976 Hicyilmaz et al, 2004
Arsenopyrite	FeAsS	0.22 - X_2	Polling, 1976

2.2.2.2 Sulphide mineral oxidation

In general, metals and sulphur have a range of oxidation states and because of this sulphide minerals are thermodynamically unstable and oxidation of the surface will begin immediately upon exposure to dissolved oxygen (Vaughan et al, 1997). The extent of oxidation is dependant on the total surface area exposed, the temperature and the time of exposure (Chander, 1999).

Figure 2.5 presents the stability diagram for iron oxides and sulphides in water. Under Impala's flotation conditions (indicated by large circle), open to air, pyrrhotite is reported to be unstable (Garrels and Christ, 1990). The stability of pyrrhotite is only found in a very small region (pH 7-9 and at potentials between -0.37 and -0.54 V vs.SHE). When the potential is increased the pyrrhotite surface structure will first change to that of pyrite (FeS_2) and eventually that of hematite (Fe_2O_3).

Montalti (1994) investigated the rate of iron release from the mineral lattice for various iron containing sulphides. It was reported that pyrrhotite was the least stable mineral and that it produces a significantly higher amount of iron in solution, even at very low potentials (figure 2.6).

Various authors have investigated the development of hydroxide species on pyrrhotite due to oxidation (Khan et al, 2004; Buswell et al, 2002). From their work they summarised the oxidation of pyrrhotite according to:

$$Fe_{(1-x)}S + 3yOH^- \rightarrow Fe_{(1-x-y)}S + yFe(OH)_3 + 3ye^- \quad (2.6)$$

In flotation (alkaline pH) where oxygen is the primary oxidant, Nicholson and Scharer (1994) proposed the following oxidation reactions:

- Oxidation of pyrrhotite to form ferrous ions:

$$Fe_{1-x}S + (2 - \tfrac{1}{2}\, x)O_2 + xH_2O \rightarrow (1-x)Fe^{2+} + SO_4^{2-} + 2xH^+ \quad (2.7)$$

- Oxidation of ferrous ions to ferric ions and ferric hydroxide precipitation:

$$Fe^{2+} + ¼\ O_2 + 2H^+ \rightarrow Fe^{3+} + ½\ H_2O \quad (2.8)$$

$$Fe^{3+} + 3H_2O \rightarrow Fe(OH)_{3(s)} + 3H^+ \quad (2.9)$$

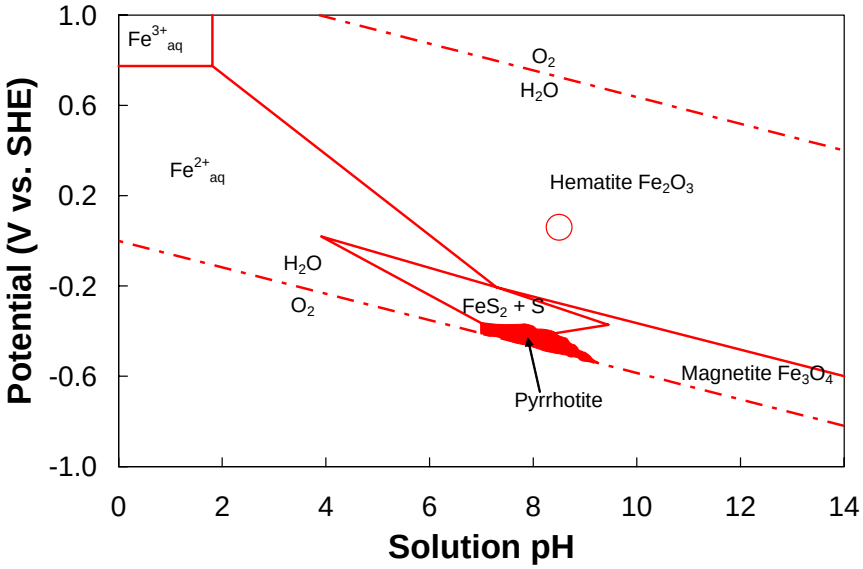

Figure 2.5: Stability regions of iron oxides and sulphides in water at 25 °C and 1 atmosphere pressure. Sulphur concentration is $1x10^{-6}$ mol/l and that of iron is $1x10^{-6}$ mol/l (Garrels and Christ, 1990).

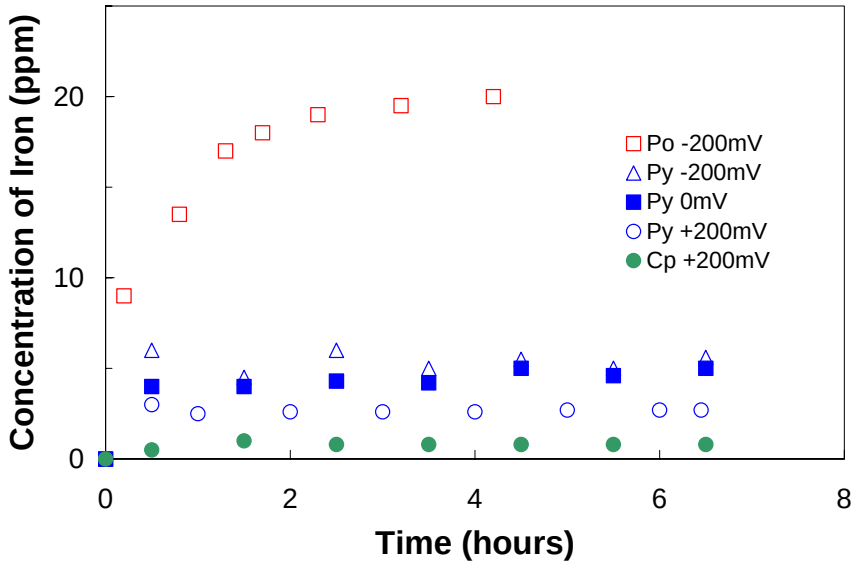

Figure 2.6: Dissolution of iron from iron containing sulphides as a function of time (Montalti, 1994).

During research on a South African pyrrhotite sample, Buswell and his co-workers (2002) identified two distinct peaks in the current density of a pyrrhotite electrode (figure 2.7).

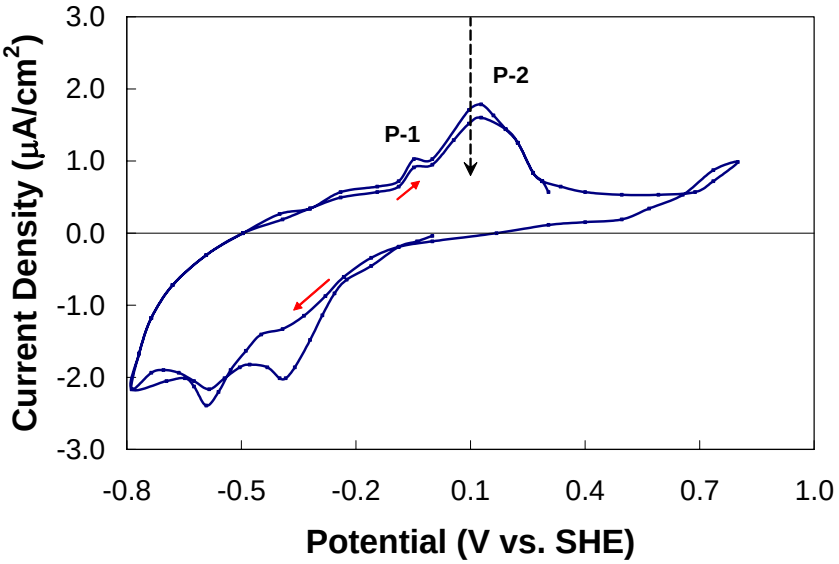

Figure 2.7: Cyclic voltammetry diagram of a South African pyrrhotite electrode at pH 9.2 in a xanthate-free solution (Buswell et al, 2002).

The first peak (P-1) they attributed to reactions (2.6 to 2.8) while the second peak (P-2) was said to be the continued oxidation of pyrrhotite by ferric ions according to:

$$Fe_{1-x}S + (8-2x)Fe^{3+} + 4H_2O \rightarrow (9-3x)Fe^{2+} + SO_4^{2-} + 8H^+ \qquad (2.10)$$

The dashed line (vertical arrow) indicates the potential (108mV vs. SHE) at which dixanthogen formation begins in an oxygenated solution for 10^{-4} molar SIBX.

2.2.2.3 The role of grinding media

Comprehensive studies on the influence of grinding media type during the flotation of sulphide minerals are reported in the literature (Forrsberg et al, 1993; Klimpel et al, 1992; Adam et al, 1984; Iwasaki et al, 1983). It was found (Iwasaki et al, 1983) that during autogenous milling the recovery of copper, nickel and cobalt exceeded those recoveries obtained with conventional ball milling. The residual sulphur in the flotation tails was also lower in the former case. Forrsberg et al (1993) reported similar trends for a copper-lead-zinc circuit using autogenous and conventional grinding.

Iron is almost always present in the flotation feed, either from the grinding media or from the mill lining (Forrsberg et al, 1993). Early work by Fuerstenau et al (In Fuerstenau, 1982b) indicated that the oxidation of DTC to $(DTC)_2$ by ferric ions does not occur at a pH of 6 and above. In alkaline slurries ferric hydroxides are the stable iron species and DTC oxidation will thus not occur (Fuerstenau, 1982b). This is because the formation of ferric hydroxides scavenges oxygen which lowers the pulp potential and by doing so impair DTC oxidation (Chander, 1999). Iron hydroxide species are also hydrophilic which further hinders sulphide mineral flotation (Forrsberg et al, 1993).

2.2.3 Sulphide minerals

It has been established that iron bearing sulphide mineral flotation with dithiocarbonate collectors differ from those having no iron in the mineral lattice (table 2.3). Apart from the surface reactions taking place the electrochemical conditions under which flotation is achieved in aerated solutions seem to dependant on the amount of iron (figure 2.8) in the mineral lattice (Richardson and Walker, 1985). Resent work (Vermaak, 2005) also confirmed different floatabilities for chalcopyrite, pyrite and pyrrhotite with SIBX as the collector using micro flotation tests on particles ranging in size from 38 to 106 um. The results indicated that chalcopyrite is the fastest floater followed by pyrite and lastly pyrrhotite.

Therefore, in order to understand the flotation response of bulk sulphides with sulfhydryl collectors it is important to consider the type of iron bearing sulphide mineral in the system as well as dissolved oxygen content.

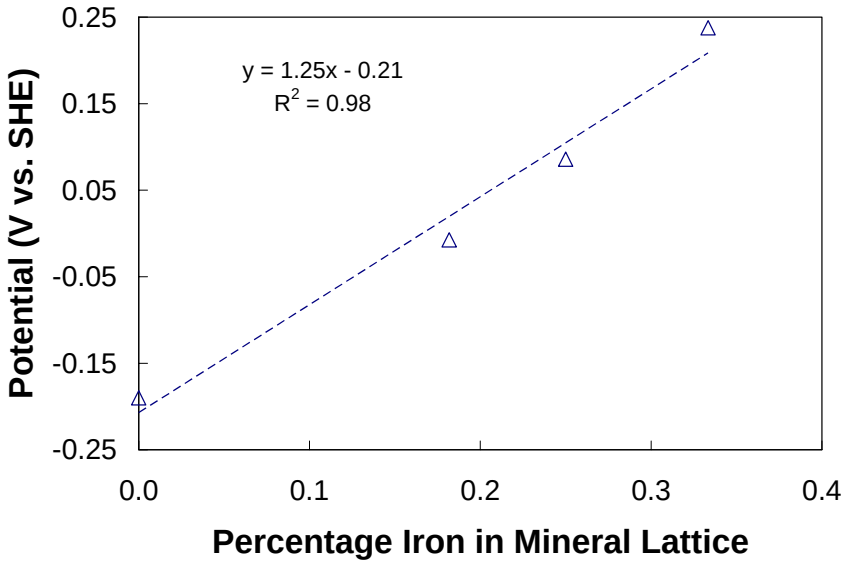

Figure 2.8: The relationship between the amount of iron in the mineral lattice and the potential required to achieve 20% recovery for various sulphide minerals (Richardson and Walker, 1985).

2.2.3.1 Natural floatability of iron bearing sulphides

Although the addition of collectors is general during sulphide flotation it is recognised that some sulphide minerals can be floated in the absence of collectors (Chander, 1999).

Only a small number of sulphide minerals are naturally floatable without collectors while the rest are reported to have intrinsic hydrophobic characters due to mild oxidation in the presence of oxygen (Fuerstenau and Sabacky, 1981). The authors based this native floatability on the fact that the sulphide-lattice ions do not have very strong water interactions because of weak hydration. Miller (1988) however argued that sulphide minerals are thermodynamically unstable and that sufficient oxygen is present in the system to oxidise the mineral(s) which leads to the formation of elemental sulphur. Woods (1987) argued that mild oxidation of sulphide minerals lead to the formation of metal-deficient sulphur layers and that they could be considered to be hydrophobic. Buckley et al (1985) reported similar results.

The natural floatability of sulphides is important since their selectivity against iron sulphides is good. This is because chalcopyrite for instance forms sulphur rich surfaces as it oxidises while pyrite will form an iron rich surface (Klimpel, 1999). Electrochemical studies by Pang and Chander (1993) have shown that, unlike for pyrite, the iron oxides/hydroxides than form

during chalcopyrite oxidation will not coat the surface and by doing so form an iron-deficient surface layer.

Heyens and Trahar (1984) claimed that the natural floatability of pyrrhotite is a result of mild oxidation which produces metastable complexes which they modeled as metal hydroxy-polysulphides. However, upon prolonged exposure to air pyrrhotite will oxidise, covering its surface in hydroxides (Heyens and Trahar, 1984) which inhibit its floatability.

$$Fe_{1-x}S + (7-3x)H_2O \leftrightarrow (1-x)Fe(OH)_3 + SO_2^{4-} + (11-3x)H^+ + (9-3x)e^- \quad (2.11)$$

2.2.3.2 Reactions with thiol collectors

Interactions of DTC with chalcopyrite have extensively been investigated (Andreev et al, 2003; Guo et al, 2003; Mielczarski et al, 1998; Mielczarski et al, 1996; Woods, 1976). Woods (1976) showed that compared to pentlandite and pyrite (figure 2.9) chalcopyrite is more readily oxidised but less than pyrrhotite.

It was established by Woods (1976) that the addition of DTC does not have an effect on the chalcopyrite current density below the reversible potential for dithiolate formation and concluded that this served as evidence that no electrochemical reaction was taking place resulting in no formation of the hydrophobic species dixanthogen. An increase in the current density was however observed above the reversible potential for dithiolate formation, indicating an electrochemical reaction which was associated with dixanthogen formation (Woods, 1976).

Hydrophobic surface products for a xanthate-chalcopyrite system were also shown to be cuprous xanthate complexes but this product was only present at low xanthate concentrations. As the concentration of xanthate increased dixanthogen was also identified as a surface product (Andreev et al, 2003; Mielczarski et al, 1996).

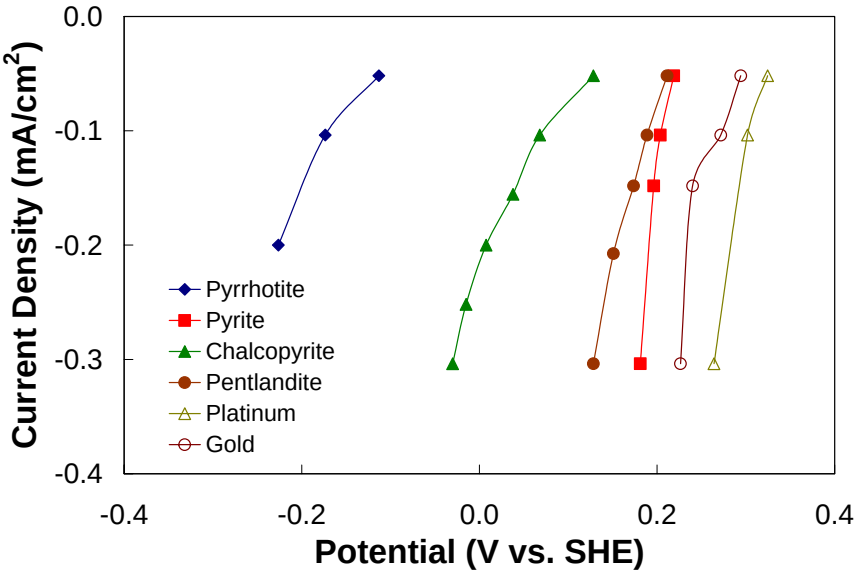

Figure 2.9: Current-potential curves for oxygen reduction on some base metal sulphide electrodes (Woods, 1976).

For pentlandite, figure 2.9 suggests that the electron transfer reaction (electrochemical mechanism) results in DTC oxidation and thus dithiolate formation on the surface (Woods, 1976).

However, electrochemical investigations by Hodgson and Agar (1989) suggested that xanthate adsorbs onto pentlandite via a two-step process:

- Chemisorption of xanthate ions onto nickel sites.

$$Pn|| + X^- \leftrightarrow Pn||X + e^- \quad (2.12)$$

- Dixanthogen formation.

$$Pn||X + X^- \leftrightarrow Pn||X_2 + e^- \quad (2.13)$$

Khan et al (2004) and Bozkurt et al (1998) did not detect chemisorption of xanthate by pyrrhotite. They proposed the following sequence of reactions where anionic xanthate is believed to physi-sorb onto the pyrrhotite surface as an initial step.

$$Po||(OH)[S]^+ + X^- \leftrightarrow Po||(OH)[S][X] \quad (2.14)$$

The xanthate on the surface will then be oxidised to dixanthogen accordingly:

$$Po||(OH)[S][X] + X^- \leftrightarrow Po||(OH)[S][X_2] + e^- \quad (2.15)$$

Buswell et al (2002) also found that pyrrhotite reacted slowly with xanthate. A small change in the potential for the pyrrhotite electrode was observed when xanthate was added, confirming that pyrrhotite is a very poor catalyst for oxygen reduction which is an essential step for the formation of dixanthogen in traditional flotation systems.

2.2.3.3 Activation with heavy metal ions

It was found (Hicyilmaz et al, 2004; Du Plessis, 2003; Mendiratta, 2000) that the addition of metal ions such as copper, lead or nickel prior to collector addition greatly improved the surface hydrophobicity of iron bearing sulphides. Fuerstenau (1982d) summarised the response of various metal sulphides with collectors from the literature (table 2.4).

Table 2.4: Response of metal sulphides with xanthate type collectors (Adapted from Fuerstenau, 1982d).

Mineral	Methyl Xanthate	Sodium Aerofloat	Ethyl Xanthate	Butyl Xanthate	Amyl Xanthate	Hexadecyl Xanthate	Potassium DTP
Sphalerite	Respond with collector only with activation						
Pyrrhotite							
Pyrite							
Galena							
Chalcopyrite							
Bornite	Respond with collector without activation						
Covellite							
Chalcocite							

It shows that pyrrhotite only responds to long chain collector molecules while the flotation of chalcopyrite is achieved with short chain collectors. However, the use of an activator renders pyrrhotite susceptible to flotation even with short chain collector molecules. The reason for this can be explained from the solubility products of the metal xanthate species (figure 2.10). Copper xanthate species are several orders of magnitude less soluble than say nickel or lead xanthate and forms a much more stable surface product.

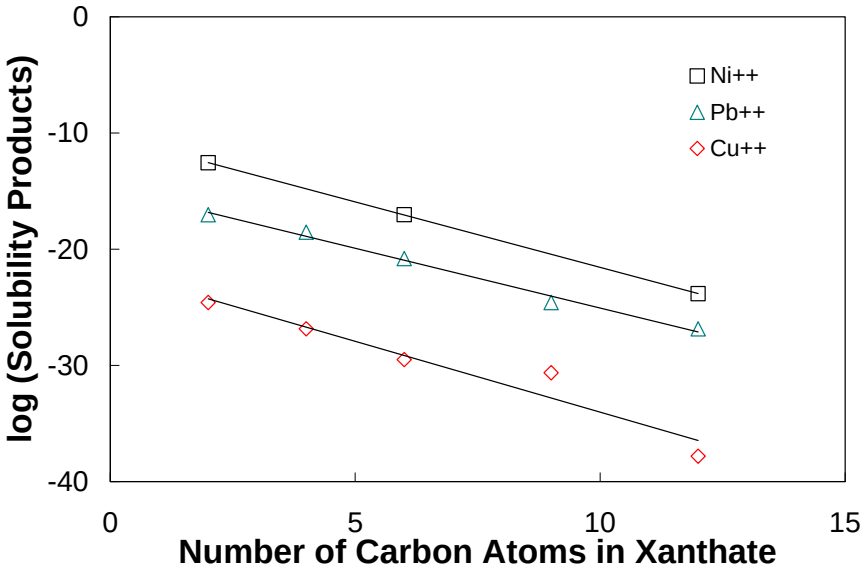

Figure 2.10: Solubility products of various metal xanthates (In Chander, 1999).

In a detailed experiment Chang et al (1954) investigated the activation of pyrrhotite with copper ions at pH 5.1. They found that under these conditions the copper directly exchanged with the ferrous ions at the surface and this greatly improved pyrrhotite floatability. The amount of copper, iron and sulphur in solution was measured with time (figure 2.11).

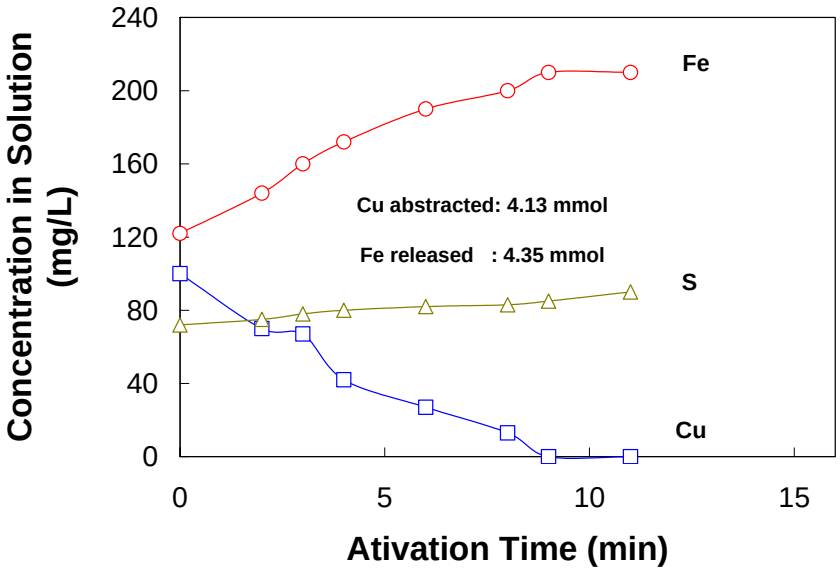

Figure 2.11: The change in Cu, Fe and S concentration during the activation of pyrrhotite with copper ions at pH 5.1 (Chang et al, 1954).

From this they concluded that the activation reaction could be represented by:

$$Cu^{2+} + FeS \leftrightarrow CuS + Fe^{2+} \quad (2.16)$$

Buswell and Nicol (2002) investigated the anodic decomposition rate of CuS on a pyrrhotite surface and found that the anodic rate became significant above 0.4V (vs. SHE). When no copper was present one of the anodic peaks of pyrrhotite was found at a much lower potential (0.1V vs. SHE). Based on this observation they concluded that copper stabilised the pyrrhotite surface.

At alkaline pH the activation of pyrrhotite is not fully understood leading to many controversial conclusions. Nicol (1984) showed that in alkaline pH (>8) copper activation is not possible because of the insoluble nature of the copper hydroxides forming under this condition. However, other researchers (Kelebek et al, 1996; Senior et al, 1995; Leppinen, 1990) have shown that copper improves pyrrhotite recovery. They found traces of copper on pyrrhotite particles in the concentrate from a plant operating at pH 9.

The controversy between laboratory and real industrial observations was explained by Finkelstein (1997) to be in part due to the presence of iron. The contact between sulphide minerals and metallic iron (such as grinding media) reduces the rest potential of the minerals and this significantly increases the adsorption of copper ions. This also points to the role of grinding media during milling and copper sulphate addition.

Copper in most cases is used to activate pyrrhotite, but it can also be activated by nickel in the pulp of massive nickel deposits (Yoon et al, 1995). The mechanism can be represented by:

$$Fe_7S_8 + 4.5Ni^{2+} + 4e^- \leftrightarrow (Fe_{4.5},Ni_{4.5})S_8 + 2.5Fe^{2+} \quad (2.17)$$

This indicates that nickel-activated pyrrhotite may act as if it were pentlandite.

2.3 Pyrrhotite

2.3.1 Properties

Because of the non-stoichiometric nature of pyrrhotite ($Fe_{1-x}S$; x varying from 0 to 0.2) it has a distorted NiAs structure. The crystal structure with the lowest Fe:S ratio (Fe_7S_9) is monoclinic while the intermediates (Fe_8S_9; Fe_9S_{10} and $Fe_{10}S_{11}$) are hexagonal. The equimolar crystal structure (FeS) is orthorhombic. Although it is reported that hexagonal pyrrhotite is more reactive, pyrrhotite rarely exists as a pure phase but usually consists of a mixture between hexagonal and monoclinic phases. The rate of pyrrhotite oxidation is also believed to increase with an increase in the S:Fe ratio (Janzen et al, 2000).

Pyrrhotite is often found in large Cu-Ni deposits where it is associated with chalcopyrite and pentlandite. In most flotation plants pyrrhotite is rejected (Chanturiya et al, 2004; Bozkurt et al, 1998; Fornasiero et al, 1995) as an undesirable mineral that only increases the iron and sulphur content of the concentrate sent to the smelters. For this reason most research on pyrrhotite is conducted with the aim of improving its rejection to the flotation tails.

2.3.2 Flotation with Thiocarbonate Collectors and Inhibiting Factors

It has been established that although pyrrhotite is a poor catalyst for oxygen reduction and dithiolate formation (Woods, 1976) its flotation response is still due to the formation of the dithiolate (Khan et al, 2004; Bozkurt et al, 1998). One of the inhibiting factors however is pH (Montalti, 1994).

The interaction of xanthate with pyrrhotite is first the attachment of ionic xanthate to the positively charged pyrrhotite surface followed by oxidation to the dithiolate (Khan et al, 2004; Bozkurt et al, 1998). A qualitative measure of the amount of positive surface sites (cationic) on a mineral is the calculation of the zeta potential for a specific surface. This zeta potential is calculated as the sum of all the surface charges (positive + negative), thus a positive zeta potential indicates that more cationic surface sites are present and visa versa for a negative zeta potential. Montalti (1994) investigated the pH dependence of zeta potential on pyrrhotite as a function of ethyl xanthate concentration (figure 2.12).

The point of zero charge (PZC) for this specific pyrrhotite sample was found by Montalti (1994) to be around pH 6.5 suggesting that above this pH the mineral develops more negative (anionic) surface species. It was also found that the electrokinetic response of this sample was not greatly affected by the low ethyl xanthate concentrations and argued that these results can be expected if the surface is oxidised and $Fe(OH)_3$ is stabilised on the surface since $Fe(OH)_3$ is known to have a PZC of about pH 6.5 (Montalti, 1994). A series of flotation tests at different values of the slurry pH demonstrates the effect of pH on pyrrhotite recovery (figure 2.13).

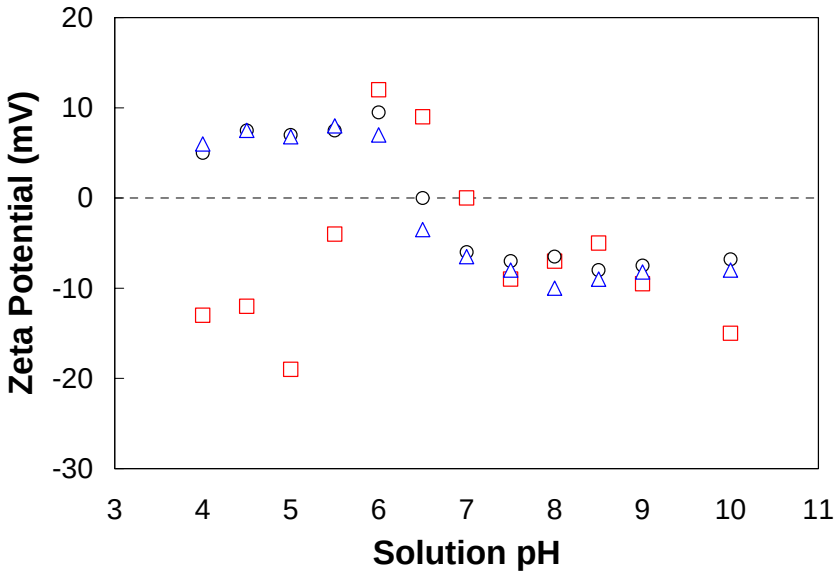

Figure 2.12: Zeta potential–pH plot for pyrrhotite in the presence of different concentrations of ethyl xanthate of 0 mol/L (O), $5.0x10^{-4}$ mol/L (Δ), $1x10^{-3}$ mol/L (□). [FeS] = 2.0 g/l in $2x10^{-3}$ mol/l KNO_3 (Montalti, 1994).

During the selective separation of pentlandite from pyrrhotite, Khan and Kelebek (2004) identified a second factor inhibiting the flotation of pyrrhotite. They found that at reduced potentials pyrrhotite recovery was inhibited and they attributed this to the preferential formation of DTC surface species on pentlandite at lower potentials.

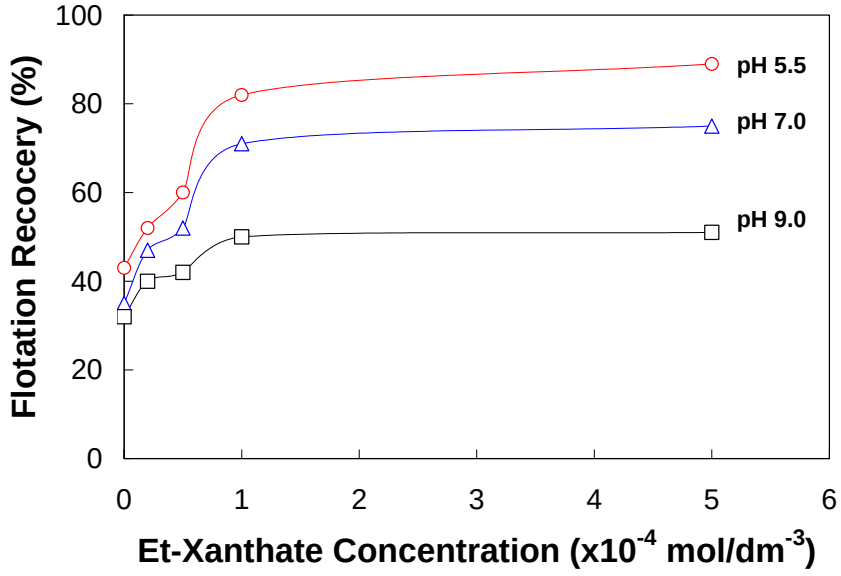

Figure 2.13: The effect of slurry pH on the flotation recovery of pyrrhotite (Montalti, 1994).

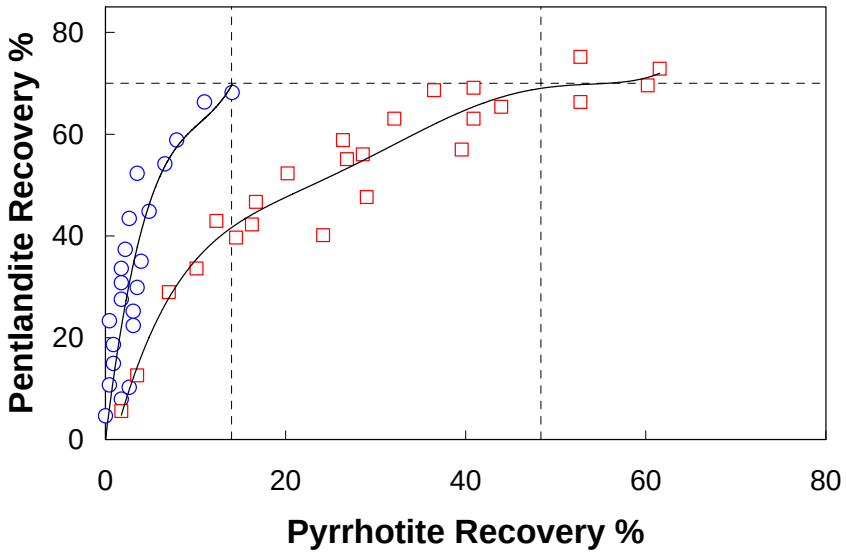

Figure 2.14: Selective flotation of pentlandite from pyrrhotite for different potential conditions. (O) indicates controlled potentials between -0.095 to -.0055V vs. SHE and (□) indicates uncontrolled potentials between 0.25 to 0.3V vs. SHE. (Khan and Kelebek, 2004).

2.4 Factors Influencing Flotation Kinetics

The rate at which the valuable minerals report to the flotation concentrate is the key to circuit design. In general when the flotation rate is slow, more residence time is required to achieve acceptable recoveries. Factors such as the relative rate of gangue recovery to the concentrate can lead to the design of a rougher-cleaner or a rougher-cleaner-recleaner circuit instead of a straight forward rougher circuit. All of which have significant implications in the amount of capital required for a concentrator.

This rate of flotation is influenced by a number of factors ranging from physical to mechanical and thirdly chemicals factors.

2.4.1 Grind and Liberation

The physical factors include particle size or degree of liberation. For a specific ore type the optimum metallurgical performance will be in a certain size range and for PGM flotation this is between approximately 106um and 53um. When the particle size is below that, slime coatings cause the valuable minerals to be floated less selectively and above 106um the particle/bubble interaction becomes too weak to maintain attachment long enough to allow particle collection.

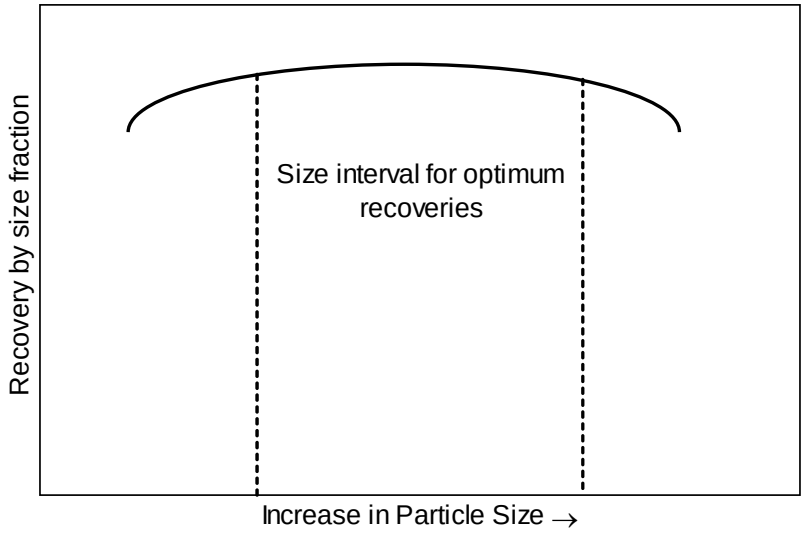

Figure 2.15: Hypothetical curve showing the effect of particle size on recovery.

Apart from the influence of particle size on the rate of flotation of valuable minerals it also plays a major role on gangue recovery. Kirjavainen (1996) described four mechanisms in which gangue can report to the flotation concentrate. Three of which is directly affected by particle size.

With regards to gangue minerals, particle size and inter-micellar water viscosity are important in the froth zone transportation of particles by ***entrainment***. This mechanism is strongly dependant on the particle size with an increase in recovery via entrainment for smaller particles (Savassi et al, 1998).

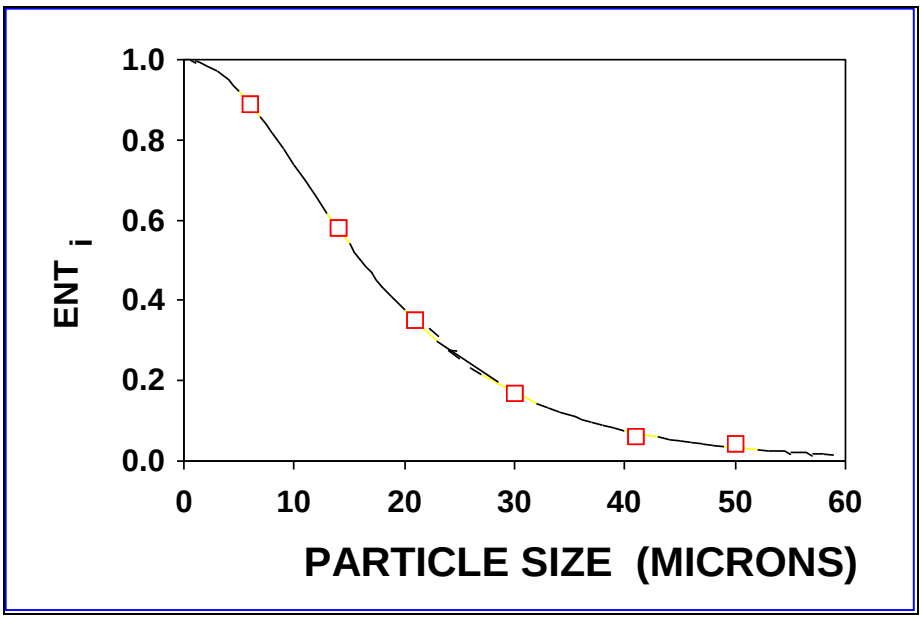

Figure 2.16: The effect of particle size on gangue entrainment (Savassi et al, 1998).

A second mechanism of gangue recovery is that of ***composite particles***. In ores with relatively course valuable mineral grain sizes, i.e. Nkomati massive sulphide ore, good liberation is normally easily achieved. However, ores having a fine valuable mineral grain size, such as the Merensky and UG-2, have to be ground very fine to achieve an acceptable degree of liberation. Grinding fine has a marked effect on froth flotation with complete liberation seldom achieved. Incomplete liberation therefore always leads to composite sulphide-gangue particles being recovered to the froth zone and this effect increases the intrinsic rate of gangue flotation (Kirjavainen, 1996).

When one mineral breaks faster during crushing/milling than others, over grinding or sliming could occur. These fine particles (particularly below 10 micron) have the ability to form

slime coatings on sulphide minerals that inhibits their flotation response. In this way the gangue is also transported into the concentrate (Kirjavainen, 1996). In sulphdes flotation, pentlandite is known to break quicker than the rest and will easily over grind. Slime gangue must be able to attach to sulphides for slime coating or piggy-back flotation. This normally takes place through an electrical charge or magnetism.

2.4.2 Molecular Structure and Collector Surface Coverage

When considering the different phases (gas, liquid solid) in flotation systems it is agreed that for a particle to be recovered to the froth phase complete separation between the solid and liquid interface must take place along with the simultaneous attraction between the solid/air interfaces. Flotation is thus a system where separation between two phases is required: that of the mineral surface from water and since the mineral surface is covered with collector molecules the predominant interactions take place between the collector molecules and water.

The free energies of interaction between the collector molecules and water have been studied in detail (Davidtz, 1999; Steyn, 1996) and it was concluded that a direct relationship holds between the calculated interaction energies and the initial rate of flotation. The interaction energies are calculated as follow: (Davidtz, 1999);

$$G^{ex}/RT = \sum_{i=1}^{n} X_i \cdot \ln\gamma_i + X_w \cdot \ln\gamma_w \qquad (2.18)$$

with X_i and γ_i the mole fraction and activity coefficients for the various collectors, respectively, and X_w and γ_w those properties for water.

For a specific particle size then when all else is kept constant two factors are important in flotation kinetics. The first is the amount of collector on the surface (X) and the second the activity of the collector on the mineral surface (γ).

In earlier work (Steyn, 1996; Slabbert, 1985) it was concluded that in TTCs all three sulphur atoms bond to the mineral surface and are assumed to be part of the mineral structure. In this case little or no interaction occurs between the polar function of the molecule and adjacent

water. For xanthates, the oxygen does not bond to the mineral surface and interacts with water. This lowers the surface hydrophobicity relative to the corresponding TTC. Because of this higher hydrophobicity of the TTC when attached to the mineral surface it produces a higher flotation rate compared to DTC at equal dosages (Steyn, 1996; Slabbert, 1985). This factor has a constant contribution with respect to the polar function of collector molecules. However the contribution relative to chain length changes as the hydrocarbon chain contribution to hydrophobicity increases. What is clear is that the mole fraction term has a direct proportionality to hydrophobicity while the activity coefficient term is logarithmically related. The increased contribution to G^{ex} as a result of the third sulfur atom varies with chain length. Table 2.5 below gives the percent increase in G^{ex} for different lengths of hydrocarbon chains between C_2 and C_4.

Table 2.5: Percent increase in G^{ex} between DTC and TTC molecules for different hydrocarbon chain lengths.

Chain length	**G^{ex} (DTC) Joules/Mole**	**G^{ex} (TTC) Joules/Mole**	**Increase (%)**
C_2	932	2380	155
C_3	1240	2770	123
C_4	1470	3030	106

The calculation of interaction energies with water for molecules having six or more carbons in the hydrocarbon tails is not straight forward (Davidtz, 2004). When the tail gets too long coiling can take place. This affects the interaction with the water phase. Also, at high dosages interactions as hydrophobic bonding between the hydrocarbon tails can occur and this further affects their interactions with water. Non of these issues are addressed by the UNIFAC method that is used to calculate the activity coefficient and for this reason the interaction with water will always be over predicted (more hydrophobic with long-chain molecules). Also, when mineral surfaces are partially oxidised the apparent surface coverage will also be lower and poorer recoveries than calculated results.

CHAPTER 3

Fourier Transform Infrared Spectroscopy and Contact Angle Measurements

3.1 Introduction

For the purpose of this study two fundamental techniques have been applied to evaluate the collectors SIBX and nC_{12}-TTC on a pyrrhotite surface. The first was External Reflectance Fourier Transform Infrared Spectroscopy (ERS FTIR) and the second was electrochemically controlled contact angle measurements.

3.1.1 External reflectance Fourier transform spectroscopy

This technique is often referred to as Specular Reflectance FTIR and measures the radiation that is reflected from a surface (George, 1987). This makes this technique particularly useful in studying adsorbed layers on metallic sulphide surfaces. Drawbacks of this technique however are:

- The inability to obtain the *in-situ* characterisation of the absorbed species, and
- The low sensitivity at monolayers and submolayer coverages (Leppinen et al, 1989).

However, this technique does not require extreme experimental conditions such as ultra high vacuums as is the case for other surface sensitive techniques such as XPS and TOF-SIMS (Mielczarski et al, 1996). Furthermore, Montalti et al (1991) claimed that infrared spectroscopy is the only technique that is able to show the adsorbed species of xanthate onto pyrite and other sulphide minerals.

In her study on thiocarbonate adsorption on pyrite, Du Plessis (2003) used the relative peak intensities of the mid infrared region to quantify the amounts of collector species on the surface of pyrite. In the same manner will these peaks be used to quantify the relative amounts of collector on the surface of pyrrhotite in the presence of SIBX, nC_{12}-TTC, and a combination of the two.

3.1.2 Electrochemically controlled contact angle measurements

This technique can be successfully applied to measure the wettability (hydrophilicity) of a mineral surface by water (Du Plessis, 2003). When a mineral surface has a low affinity for water, or put in another way, the surface is hydrophobic, an air bubble will attach to the mineral surface upon contact and the stability of attachment can be measured as a contact angle between the three phases: liquid, solid and gas (Fuerstenau et al, 1985).

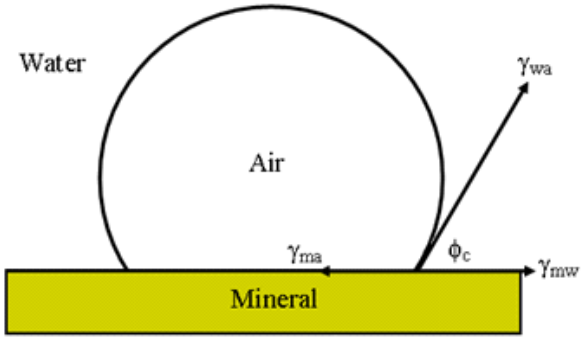

Figure 3.1: A schematic illustration of the equilibrium contact angle (ϕ_c) between an air bubble and a mineral surface immersed in a liquid (Adapted from Kelly and Spottiswood, 1989).

For flotation to occur it is thus agreeable that a mineral-air interface must be created with the simultaneous destruction of the water-air and mineral-water interfaces of equal area. Thus for bubble attachment to be achieved (Kelly and Spottiswood, 1989):

$$\gamma_{ma} - \gamma_{mw} < \gamma_{wa} \tag{3.1}$$

The change in free energy associated with the creation of this mineral-air interface is given by:

$$\Delta\gamma = \gamma_{ma} - (\gamma_{wa} + \gamma_{mw}) \tag{3.2}$$

When combined with the Young equation the free energy can be expressed in terms of the measured contact angle (ϕ_c).

$$\Delta\gamma = \gamma_{wa}.(\cos(\phi_c) - 1) \tag{3.3}$$

For flotation to be possible $\Delta\gamma$ must be negative, thus a higher value for the contact angle.

In this thesis the contact angle measurements were used to gain quantitative information regarding the change in surface hydrophobicity of a pyrrhotite surface when contacted with SIBX, nC_{12}-TTC and a combination of the two.

3.2 Materials and Methods

3.2.1 Materials

A massive pyrrhotite sample was obtained from the Geology Curator, College of Mines and Earth Science, University of Utah. A powder sample was characterised by XRD and the result is presented below. The pyrrhotite content was greater than 95%.

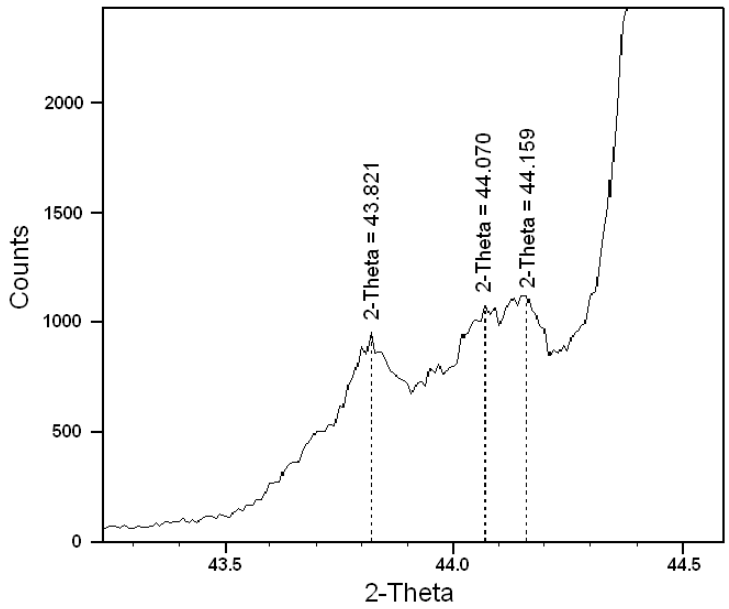

Figure 3.2: X-ray diffractogram of the pyrrhotite sample used in this investigation.

From figure 3.2 both the monoclinic phase (2-theta of 43.8) and the two peaks for the hexagonal crystal structure (2-theta of 44.0 and 44.2) are identifiable.

Sodium isobutyl xanthate and nC_{12}-trithiocarbonate were used as collectors. Analytical grade $CuSO_4.5H_2O$ and $PbNO_3$ was used as sources of copper and lead for activation.

3.2.2 Methods

The SIBX and nC_{12}-TTC were prepared according to the procedures described by Du Plessis (2003), and 1% stock solutions of lead nitrate and copper sulphate were prepared using deionised water.

Before any adsorption and experimental measurements were done, the pyrrhotite surface was polished with fine carbon paper and a 1um corundum (Al_2O_3) suspension.

3.2.2.1 Contact Angle Measurements

The apparatus used for the captive bubble contact angle measurements is given in figure 3.3, and the procedure described by Du Plessis (2003) was applied during contact angle measurements. The potential was controlled in the range (-0.5V to 0.1V vs. SCE).

3.2.2.2 Surface Spectroscopy (ERS-FTIR)

A pyrrhotite crystal was contacted with a xanthate and/or trithiocarbonate solution for predetermined times. This was done by placing a pyrrhotite crystal in a solution containing collector and when the trithiocarbonate was used the crystal was contacted for 10 minutes prior to adding xanthate. The xanthate was also contacted for 10 minutes. The crystal was then removed from the solution and dried with ultra pure nitrogen before it was placed in the spectrometer. Care was taken not to contaminate the surface.

The C-H stretching spectra were collected using a Biorad-Digilab FTS-6000 FTIR spectrometer with a liquid-nitrogen cooled detector having a wide band MCT. To flush the chamber before any spectra was obtained dried air was used and all absorbance spectra were the result of 512 co-added scans ratioed against 512 co-added background scans, all at a resolution of $4cm^{-1}$.

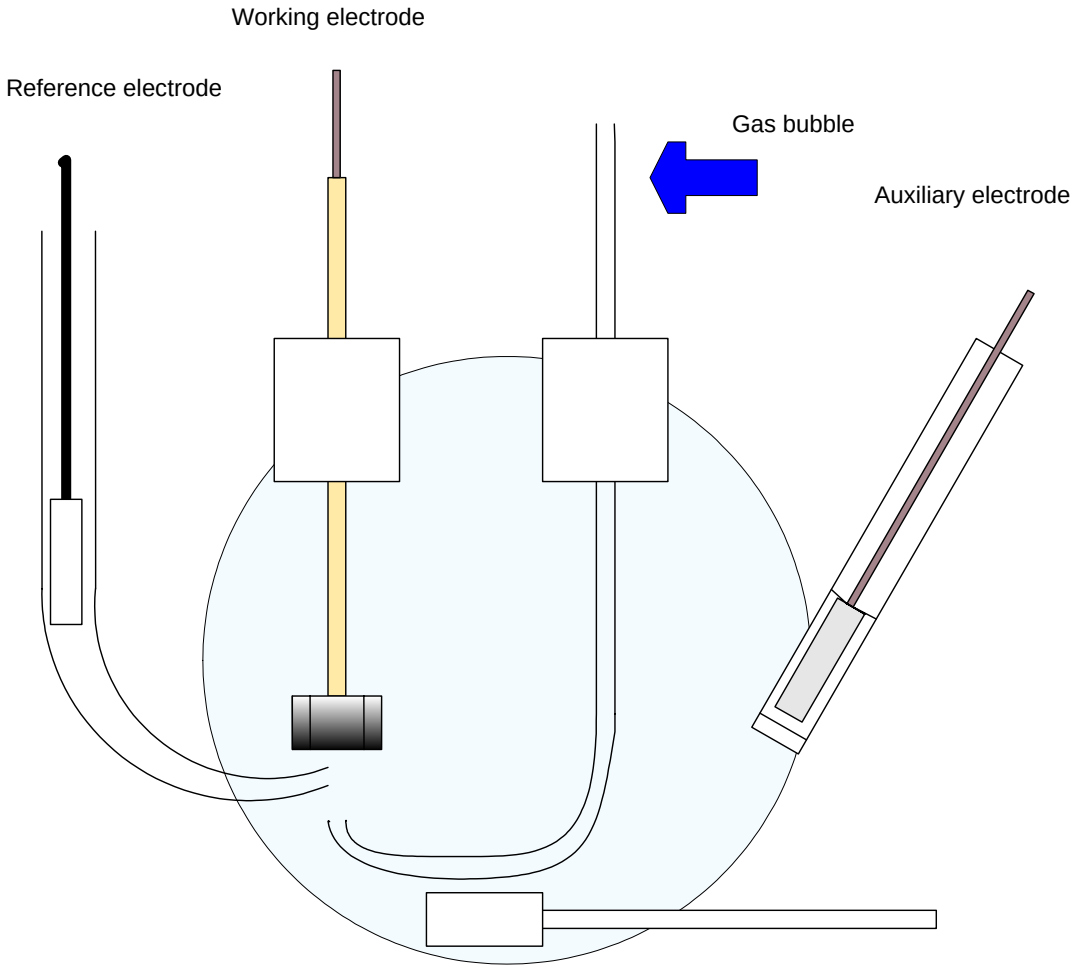

Figure 3.3: Set-up of the electrochemically controlled contact angle measurement experiments.

3.3 Results and Discussion

3.3.1 Contact Angle Measurements

3.3.1.1 Xanthate solutions

Contact angle measurements done on the pyrrhotite electrode in a collector-free solution (figure 3.4) indicated that pyrrhotite develops a self sustained hydrophobicity at a pH below 5. This solution pH agrees well with the value obtained from solution chemistry calculations. At this pH it is believed that hydrogen sulphide evolution becomes significant (1 atmosphere pressure). It is therefore expected that such a reaction (reaction 3.4) at the pyrrhotite surface is responsible for the collectorless flotation of pyrrhotite in acidic solutions (Miller et al, 2005). The reaction in acidic solutions can be summarised as follow:

$$FeS + 2H^{+} \leftrightarrow Fe^{2+} + H_2S \qquad (3.4)$$

This implicates that at Impala Platinum, operating at a pH value between 8 and 9 a poor, if any natural floatability of pyrrhotite will take place.

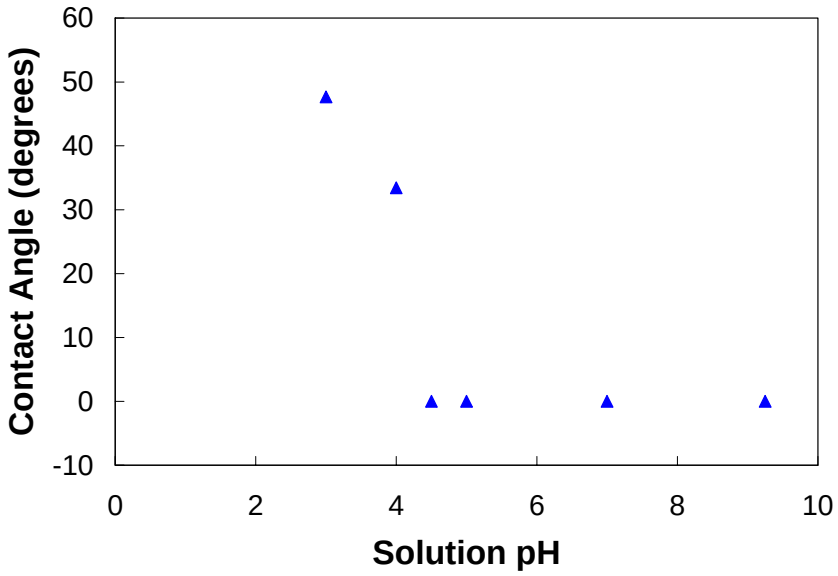

Figure 3.4: Effect of pH on pyrrhotite hydrophobicity in a collector-free solution.

As with the natural hydrophobicity of pyrrhotite, pH also plays an important role in xanthate adsorption onto pyrrhotite. With the addition of 10^{-4} molar xanthate the hydrophobicity of pyrrhotite is improved and the hydrophobic species is believed to be dixanthogen (Khan and Kelebek, 2004). Increasing the xanthate dosage to 10^{-3} molar has little further effect on the hydrophobicity of pyrrhotite at pH 5 and above.

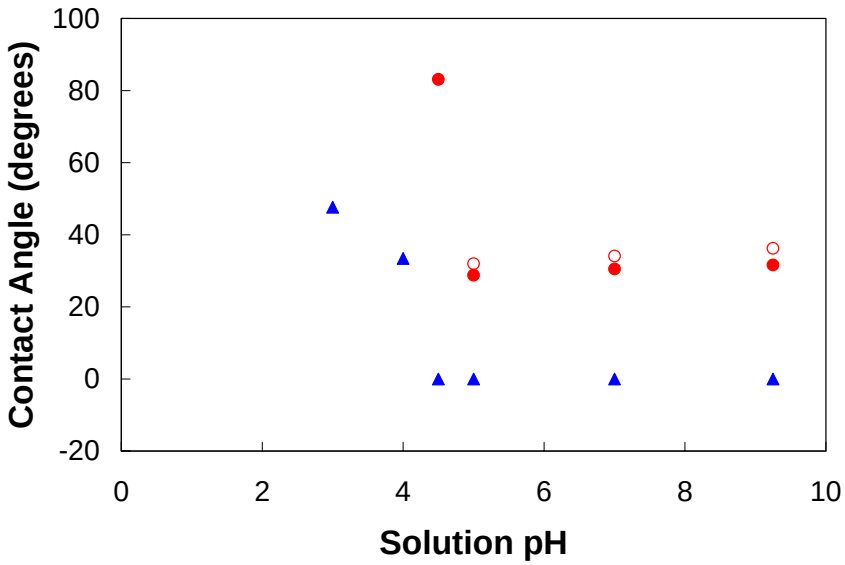

Figure 3.5: Contact Angle measurements showing the effect of pH and xanthate concentration on pyrrhotite hydrophobicity. ▲ = no xanthate; ● = 10^{-4} molar xanthate; O = 10^{-3} molar xanthate.

Although the addition of SIBX did have an improvement on the measured contact angle (increased from 0 to ~ 30°), this increase might still not be enough to reach the critical contact angle above which successful flotation recovery is achieved. During micro flotation experiments it was observed by Vermaak (2005) that even in the presence of SIBX (5 x 10^{-5} molar) pyrrhotite only recovered to approximately 3% while chalcopyrite and pyrite exhibited recoveries of 98% and 73% respectively for the same SIBX solution.

It also appears that the effectiveness of xanthate to create a hydrophobic pyrrhotite surface correlates with the zeta potential measurements reported by Montalti (1994). When the zeta potential is negative (pH above about 6) the surface of pyrrhotite predominantly consists of negative (anionic) charges. Since the initial step for xanthate adsorption onto pyrrhotite is believed to be physisorbed xanthate (Khan and Kelebek, 2004), the adsorption of anionic xanthate to the cationic sites is then limited and the reactivity is low. When the pH is lowered

the amount of surface cations are increased and the reactivity of pyrrhotite with xanthate is enhanced. The amount of cationic surface species is limited at a specific pH and because of this the increase in xanthate dosage does not have a significant effect on the surface hydrophobicity. Only a limited number of cationic sites are available for reaction with xanthate.

Although the use of heavy metal ions such as copper and lead have been proven to successfully improve the flotation rate of sulphides (Du Plessis, 2003), they have been unsuccessful in the activation of pyrrhotite in this study. They do have a dramatic improvement in more acidic solutions. In the previous example copper as an activator seemed to be slightly more effective (figure 3.6) than lead.

When examining the pyrrhotite, xanthate, metal ion system, a number of simultaneous reactions are possible:

- pyrrhotite activation by metal ions: $FeS + Pb^{2+} \rightarrow PbS + Fe^{2+}$
  $FeS + Cu^{2+} \rightarrow CuS + Fe^{2+}$
- dithiolate formation: $2X^{-} \rightarrow X_2$
- pyrrhotite oxidation: $FeS + 3OH^{-} \rightarrow Fe(OH)_3 + S^{0}$
- metal hydroxide precipitation: $Pb^{2+} + 2OH^{-} \rightarrow Pb(OH)_2$
  $Cu^{2+} + 2OH^{-} \rightarrow Cu(OH)_2$

In alkaline solutions pyrrhotite oxidation is very rapid. Also, copper and lead ions will form a hydroxide precipitate when the pH is above 8. The conclusion is that the rate of pyrrhotite oxidation and metal hydroxide precipitation exceeds that of the activation step. The result is that both copper and lead failed to activate the pyrrhotite surface for xanthate adsorption. Furthermore, in all the cases studied, the presence of a metal-xanthate precipitate was observed. Although the metal-xanthate species are hydrophobic, they must form on the mineral surface and not precipitate onto the surface from the solution phase. When in solution these species are non-polar and reacts very slow with the mineral surface.

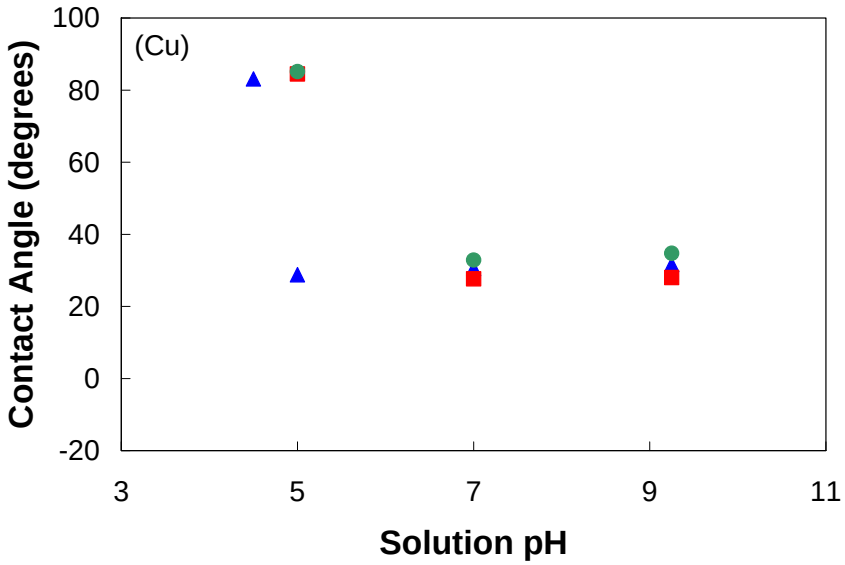

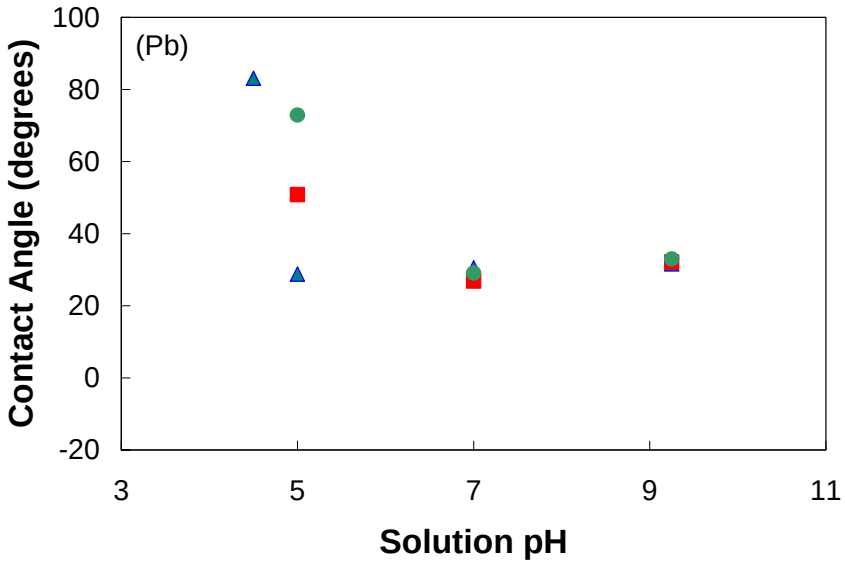

Figure 3.6: The effect of copper and lead activation of pyrrhotite as a function of solution pH with ▲ = no metal ions; ■ = 10^{-6} molar metal ions; ● = 10^{-5} molar metal ions.

3.3.1.2 Xanthate-nC_{12}-TTC solutions

The trithiocarbonates, although they also produce dithiolates and mercaptans after adsorption, function differently to xanthates under traditional flotation conditions (Du Plessis, 2003). The long chain trithiocarbonate has been applied as a collector in the recovery of auriferous pyrite. Here it was on pyrrhotite to evaluate its effect on surface hydrophobicity. A C_{12}-TTC/SIBX mixture was used in alkaline solutions. The contact angle results are presented in figure 3.7.

Under all conditions the TTC/SIBX mixture was better than SIBX alone however at high oxidising potentials (~ 0.3V vs. SHE) the effect of the TTC is best at a 5% substitution. When the potential is lowered to 0.15V (vs. SHE) the effect of the TTC becomes stronger even at more dilute concentrations. This is important since it appears that when the potential is slightly lower (less oxygen) the long chain TTC has a more pronounced effect on pyrrhotite hydrophobicity.

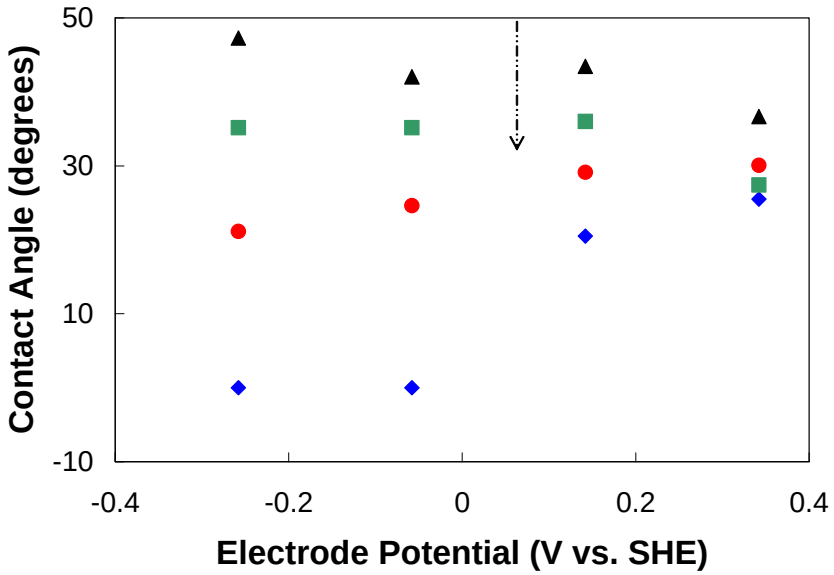

Figure 3.7: Effect of TTC addition on pyrrhotite hydrophobicity at pH 9.2. Initial [SIBX] = 10^{-3} molar. ◆ = no TTC addition; ● = 5% TTC addition without xanthate; ■ = 2.5% TTC addition with xanthate; ▲ = 5% TTC addition with xanthate. (⇢Indicates the reversible potential for the formation of dixanthogen)

When the potential is lowered further (< -0.2 V vs. SHE) another increase in the contact angle is observed. Khan and Kelebek (2004) reported that pyrrhotite floatability was severely inhibited when the potential was below 0V vs. SHE. They concluded that this was due to the

poor formation of the xanthate dithiolate on pyrrhotite. Figure 3.7 then implies that apart from the TTC dithiolate and mercaptan, some other species is also present at the mineral surface. This can possibly be ionic xanthate that is attached to the hydrophobic tail of the TTC or the xanthate dithiolate that formed in solution but not on the pyrrhotite surface.

3.3.2 ERS-FTIR Spectroscopy

IR spectroscopy was performed on a treated pyrrhotite surface and the spectra are presented below. For sodium isobutyl xanthate (SIBX) and nC_{12}-trithiocarbonate the following functional groups are important in this part of the mid infrared region (table 3.1).

Table 3.1: Group frequencies for selected saturated aliphatic (alkane/alkyl) functional groups (Coates, 2000).

Functional Group	Assignment	Group Frequency (cm^{-1})
Methyl CH_3--	Methyl C-H asymptotic stretching vibrations	2970-2950
	Methyl C-H symptotic stretching vibrations	2880-2860
Methylene --CH_2--	Methylene C-H asymptotic stretching vibrations	2935-2915
	Methylene C-H symptotic stretching vibrations	2865-2845
Methyne --CH--	Methyne C-H stretching vibrations	2900-2880

Although no in depth discussion about the different species present on the pyrrhotite surface can be made, the spectra do indicate that a change in the adsorption densities of the -CH2- functional groups occurred when the TTC was added with the SIBX. This effect is greater than the sum of the contributions from both the individual collectors and based on this it is concluded that some sort of collector crowding effect is taking place. A more in depth investigation is however required to establish the exact surface species and mechanisms of adsorption/attachment.

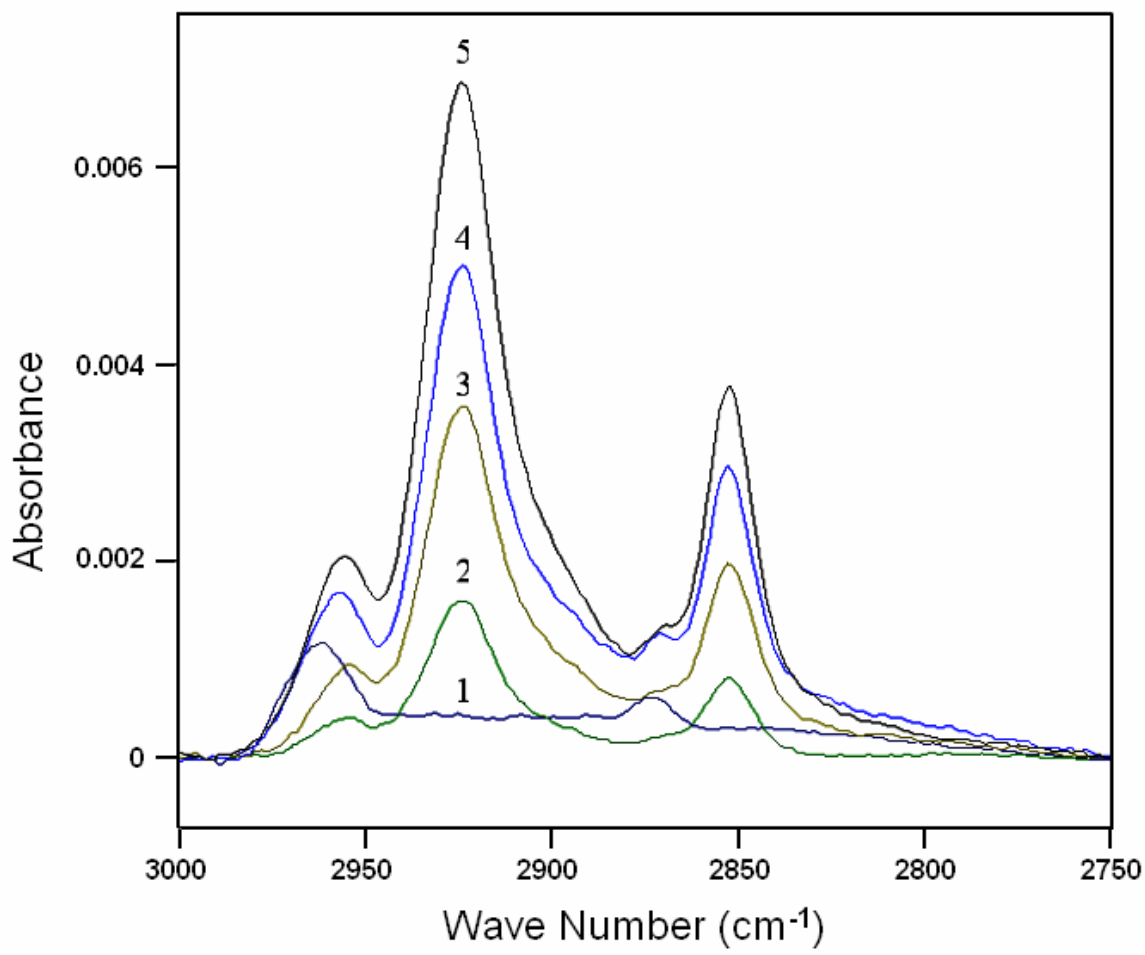

Figure 3.8: ERS-FTIR of the C-H stretching region on a treated pyrrhotite surface at pH 9.2 and open circuit potentials. 1) pure xanthate; 2) 5% pure TTC; 3) 10% pure TTC; 4) xanthate + 5% TTC; 5) xanthate + 10% TTC

3.4 Summary

Captive bubble contact angle measurements have shown that under traditional flotation conditions (air as flotation gas and oxidising potentials) the surface hydrophobicity of pyrrhotite can only be marginally improved by the addition of sodium isobutyl xanthate. The noted adsorption mechanism of xanthate onto pyrrhotite by Khan et al (2004) and Bozkurt et al (1998), along with the work of Montalti (1994), imply that it is the formation of excess anionic surface species that result in the slow reactivity of pyrrhotite with xanthate at alkaline pH. In this study only the effect of C_{12}-TTC was tested and hence DTP was not used. This might also explain the poor hydrophobicity of pyrrhotite with only SIBX compared to the SIBX/C_{12}-TTC mixtures. Although sufficient oxygen is present in the solution to form dixanthogen it may not adsorb to the mineral surface since no DTP is present to act as an anchor.

When the TTC is introduced at pH 9.2 and oxidising potentials (+ 0.3V vs. SHE) the increase in hydrophobicity is clear only at 5% molar replacement of SIBX. When the TTC is introduced at lower potentials an improvement in the surface hydrophobicity is achieved. This is true even at a low TTC dosage of 2.5 molar percent SIBX replacement. In the presence of TTC, a higher contact angle is measured even below the reversible potential for $(SIBX)_2$ formation. This indicates that even if no dixanthogen is formed on the mineral surface the TTC that is attached serves as an anchor for $SIBX^-$ and $SIBX_2$ in solution. The increase in contact angle is then due to the attraction of $SIBX^-$ and $SIBX_2$ to the tail of the TTC via hydrophobic bonding of the hydrocarbon groups.

Surface spectroscopy (ERS-FTIR) confirmed that the presence of small quantities of TTC resulted in an increase in the -CH2- groups on the pyrrhotite surface. This increase is even more evident when it is combined with SIBX. From this it is concluded that like DTP the C_{12}-TTC also acts as an anchor for $SIBX^-$ and $(SIBX)_2$ in solution.

Chapter 4

Bench-Scale Flotation Tests

4.1 Introduction

The objective of this chapter was to optimise a combination of C_{12}-TTC/SIBX/DTP as collector suite for later pilot plant testing and plant trial evaluation. The sequence of experimentation followed was:

1. Bench flotation tests (this chapter)
2. Pilot plant testing (chapter 5)
3. Plant trial (chapter 6)

As a precursor to the pilot plant trial, three levels of nC_{12}-TTC substitution for SIBX were evaluated. They were 5, 10 and 100% molar replacements of TTC for SIBX. No changes were made to the amount of DTP from the original SIBX-DTP mixture. The above replacements represent the following molar fractions:

Table 4.1: Mol fractions of SIBX/DTP/TTC mixtures for flotation tests.

SIBX Replacement (molar %)	**Mol Fraction**		
	SIBX	**DTP**	**nC_{12}-TTC**
0%	0.78	0.22	0.00
5%	0.74	0.22	0.04
10%	0.70	0.22	0.08
100%	0.00	0.22	0.78

4.2 Materials and Methods

4.2.1 Materials

A bulk Merensky sample from the hammer sampler at the central concentrator of Impala Platinum was used and collectors SIBX and DTP were obtained from the reagent inventory at Impala. The TTC solution was obtained from Wax-O-Lite. The remaining reagents (activator, frother and depressant) were from the reagent inventory at Impala.

4.2.2 Methods

4.2.2.1 Milling curve

The homogenised bulk sample was split into 3.3 kg samples for milling and flotation tests. Milling time necessary to produce a 60% passing 75 um at a mill speed of 65 rpm, was determined. The results are shown in figure 4.1.

The solids concentration in the mill was kept at 45% (wt/wt) with 3.3kg of solids and 4L of water. Nine stainless steel rods of various sizes were used as grinding media.

After milling, the slurry was filtered, dried and split into ten sub samples of which three were randomly selected and screened to calculate the percentage passing 75 micron material. The estimated time required for the grind was calculated from figure 4.1 to be 75 minutes.

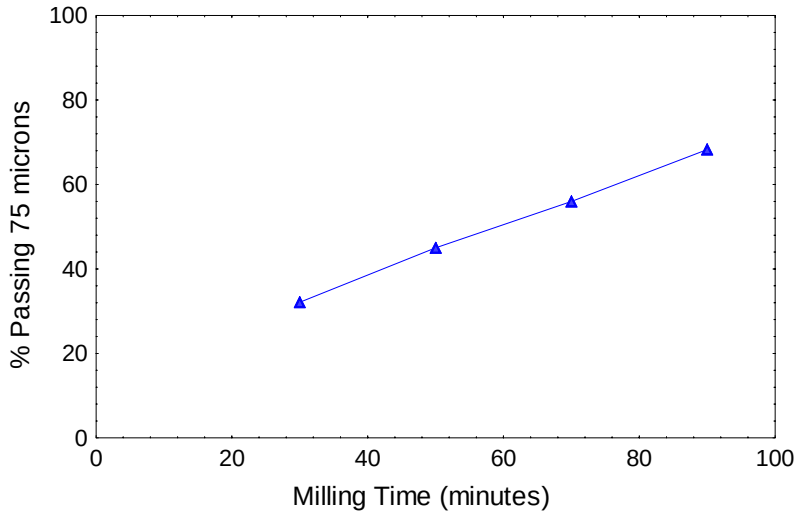

Figure 4.1: Merensky particle size distribution for various milling times.

4.2.2.2 Bench-scale flotation tests

The milled product was carefully emptied into a bucket and transferred into an 8L Denver flotation cell. The cell was filled to the 8-liter mark with fresh water to give the required pulp SG of 1.32. The float cell impeller speed was kept at 1200 rpm while the gas flow was self induced and always kept the same. Reagent dosage rates and locations are given in table 4.2. The SIBX/DTP mixture, activator and depressant were added as a 1% solution while the TTC was added as a 20% solution and the frother dosed as supplied. After conditioning, the airflow to the cell was open and timed concentrates were taken at 1, 6, 16 and 30 minute intervals by scraping every 15 seconds.

Table 4.2: Reagent conditions for bench-scale flotation tests.

Reagent	**Addition Point**	**Dosage (g/ton)**	**Conditioning Time**
Collector: (1) SIBX/DTP (2) SIBX/DTP/TTC	To mill	(1) 90 (SIBX + DTP) (2) TTC at 5,10 & 100% of initial SIBX dosage while DTP was constant	-
Activator	Float Cell	80	5 minutes
Collector spike	Float Cell	10	3 minutes
Depressant	Float Cell	90	1 minute
Frother	Float Cell	60	1 minute

4.3 Results and Discussion

4.3.1 Reproducibility

The statistical significance for each recovery benefit is given in appendix B. The recovery increase of 4.44% when 5 molar percent of the SIBX was replaced by C_{12}-TTC is statistically significant (>95%). The samples dosed at the higher levels of 10 and 100 molar percent SIBX replacement were below the 2.5% PGM recovery increase set by Impala on laboratory tests as significant improvements.

Table 4.3: Error summary for bench-scale flotation tests.

Test Condition	Standard Error %
Standard Test	0.6
5% TTC addition	0.2
10% TTC addition	1.5
100% TTC addition	0.9

4.3.2 Mass recovery

The mass recovery data for all four the flotation tests are presented in figure 4.2 and table 4.4.

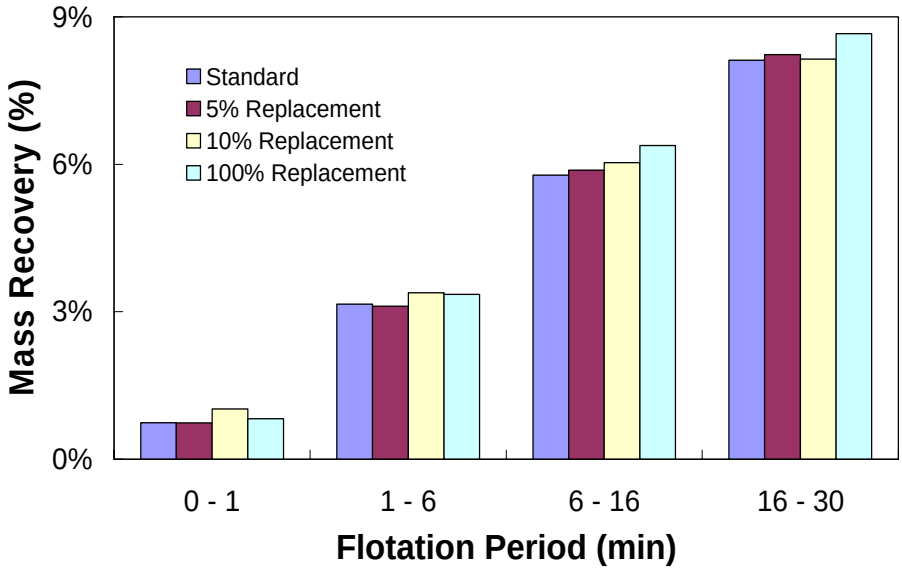

Figure 4.2: Mass recovery data for bench flotation tests.

Table 4.4: Summary of standard deviations (absolute value) on mass recovery calculations.

Period	Standard	5% TTC	10% TTC	100% TTC
0 - 1	0.12%	0.02%	0.14%	0.21%
1 - 6	0.13%	0.18%	0.11%	0.37%
6 - 16	0.17%	0.61%	0.22%	0.50%
16 - 30	0.24%	0.71%	0.26%	0.39%

During the whole flotation process the standard test and the 5 molar percent replacement test yielded the lowest mass recovery. When the TTC dosage was increased an increase in mass recovery was observed and more so in the intermediate stages of flotation. This effect can be related to an overdose of long chain collector in which the flotation process becomes unselective and this will slow down the recovery kinetics and ultimately reduce the final concentrate grade.

4.3.3 Grade recovery relationships

The effects of systematic replacement of SIBX by nC_{12}-TTC on PGM and base metal recovery and grades are reported in table 4.5 and figure 4.3.

For the 5% substitution and relative to the standard there was a 4.4%, 8% and 10.1% increase in the ultimate recovery of PGMs, Ni and Cu respectively, but no significant improvement in the final grade. In terms of final recovery, all TTC replacements were better than the standard. However, at intermediate recoveries only the 5% replacement grade-recovery curve was always above that of the standard. For copper there seemed to be an increase in recovery as the TTC dosage was increased. The 5% replacement by TTC was eventually selected as the median composition for the pilot plant trial to follow.

Table 4.5: Summary of Bench-scale flotation test results.

	PGM		Nickel		Copper	
Test Condition	**Recovery (%)**	**Grade (g/ton)**	**Recovery (%)**	**Grade (%)**	**Recovery (%)**	**Grade (%)**
Standard	86.1%	40.2	53.1%	1.1	61.5%	0.6
5% TTC	90.5%	41.6	61.0%	1.0	71.6%	0.6
10% TTC	86.2%	36.5	56.8%	1.1	73.2%	0.6
100% TTC	87.8%	36.1	60.0%	1.1	78.2%	0.6

This synergistic effect (table 4.5) at low TTC concentrations was the same as that reported by Breytenbach et al (2003) who investigated the effect of TTC addition on the sulfur recovery from a Merensky sample. In their work it was concluded that approximately 7.5% molar SIBX replacement resulted in the best sulfur grade and recovery improvement.

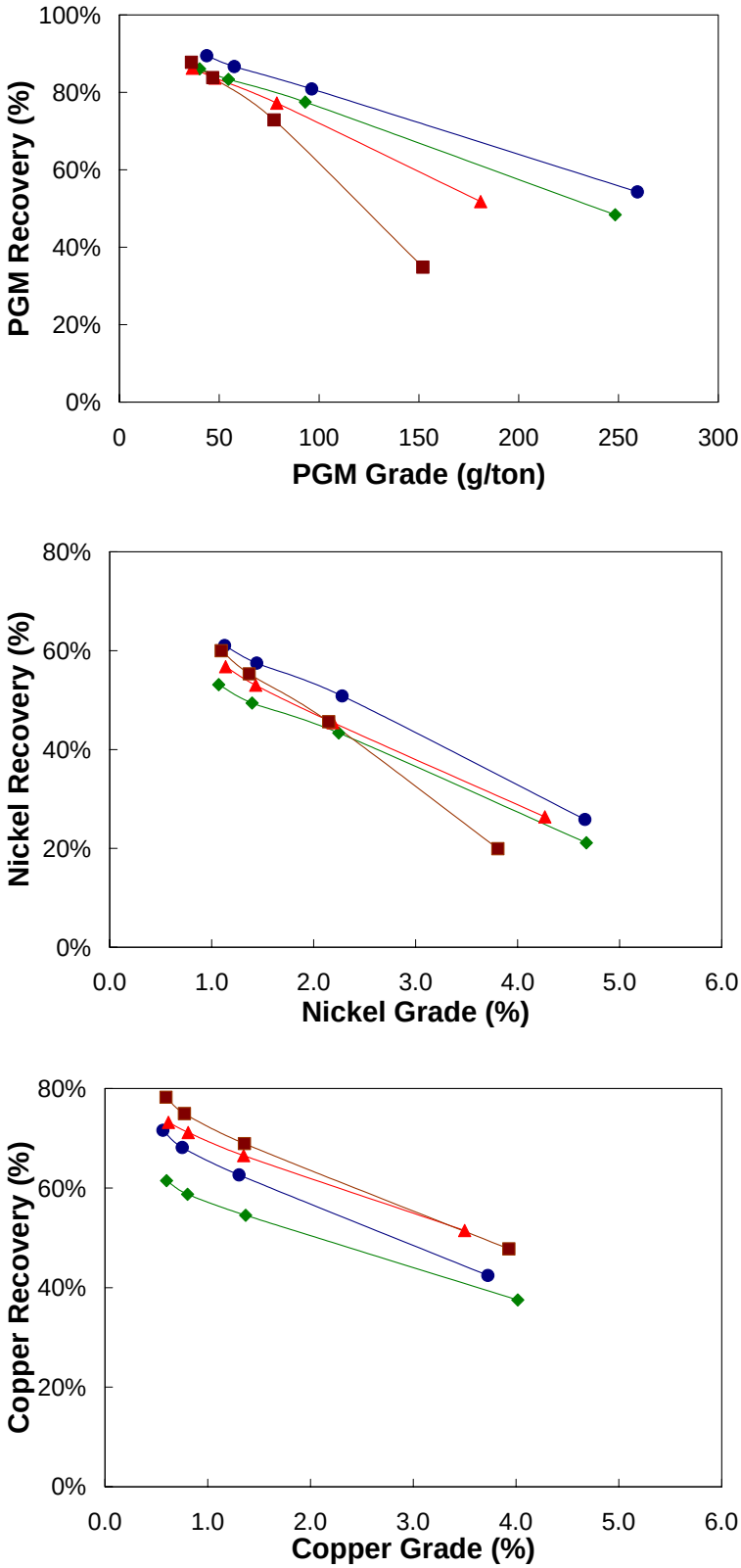

Figure 4.3: Grade-recovery relationships for various degrees of nC_{12}-trithiocarbonate substitution. ◆ = Standard test; ● = 5% TTC addition; ▲ = 10% TTC addition; ■ = 100% TTC addition.

4.3.4 Initial flotation rate (K) and final recovery (R)

The flotation rate constants (K) were calculated from the Klimpel equation (Klimpel, 1980) with the assistance of Excel's solver function. R represents the recovery after infinite time and r the recovery after a fixed time, t.

$$r = R \cdot \left(1 - \frac{(1 - \exp(-K \cdot t))}{K \cdot t}\right) \tag{4.1}$$

The initial (after 1 minute) recovery, grade and flotation rate constants are reported in table 4.6.

In general the initial rates and initial recoveries are strongly related. This holds for PGM, nickel and copper at all levels of substitution. The linear correlation coefficient (R^2) between initial rate constant and initial recovery for PGMs at all collector combinations was 0.98.

Table 4.6: Initial recovery, grade and flotation rate constants (K).

	PGM			**Nickel**		
TTC Substitution	**Recovery %**	**Grade g/ton**	**Rate Constant min-1**	**Recovery %**	**Grade %**	**Rate Constant min-1**
0%(STD)	48.4%	248.3	1.851	21.1%	4.67	0.961
5%	54.3%	259.5	2.176	24.3%	4.66	1.082
10%	51.8%	181.0	1.897	26.4%	4.27	1.184
100%	34.8%	152.0	1.001	19.9%	3.81	0.686

	Copper		
TTC Substitution	**Recovery %**	**Grade %**	**Rate Constant min-1**
0%(STD)	37.5%	4.02	1.678
5%	42.4%	3.73	2.216
10%	51.5%	3.50	3.043
100%	47.8%	3.93	2.329

Although the first order expression of Klimpel suggests a dependence of the final recovery on the initial rate, this does not necessarily hold if fast and slow floating minerals are simultaneously present.

The general trend for all metals recovered is an increase in initial rate and recovery as TTC concentration increases. However, when the amount of SIBX is further reduced the amount

of SIBX dithiolate also decreases. So either the decreasing amount of $(SIBX)_2$ or the increasing amount of TTC or both have a negative effect on flotation.

If it is assumed that no multi-layer adsorption of collector takes place, and that all collector molecules added are adsorbed, then it is possible to calculate the G^{ex} values for the interaction between collector molecules and interacting water when the mole fraction of water is given as $X_w = 0{,}5$ (Davidtz, 1999). The calculated G^{ex}/RT values at the respective mole fractions for the different substitutions are given in table 4.7. These were obtained from the UNIFAC program in Sandler (1999). The appropriate substitutions were made in the following equation:

$$G^{ex}/RT = X_{SIBX}\ln\gamma_{SIBX} + X_{DTP}\ln\gamma_{DTP} + X_{TTC}\ln\gamma_{TTC} + X_{H2O}\ln\gamma_{H2O} \qquad (4.2)$$

Table 4.7: Actual and predicted initial recoveries by Gibbs Excess Free Energy.

Collector/Water Mol Fractions				G^{ex}/RT	Actual Recovery (%)	Predicted Recovery (%)
nC_{12}-TTC	SIBX	DTP	Water			
0.00	0.39	0.11	0.50	0.550	48.4	--
0.02	0.37	0.11	0.50	0.588	54.3	51.8
0.04	0.35	0.11	0.50	0.626	51.8	55.0
0.39	0.00	0.11	0.50	1.226	34.8	107.8

At 5 mole percent substitution of SIBX by TTC, calculations predict an increase of 6.7% in the initial recovery relative to the standard while the actual increase was 12.3%. At 10 mole percent substitution, the predicted increase was 13.8% while the actual was 7.05% and at 100% substitution the predicted increase was 123% and in actual fact a decrease of 27.9% was observed. The explanation offered is that when the hydrocarbon chain reaches six and above, aliphatic hydrocarbon groups involved in the calculations start to interact with each other by hydrophobic bonding (Slabbert, 1985). This means the groups do not fully interact with the adjacent water and an apparent higher G^{ex}/RT results.

Unless one operates at starvation dosage, the nC_{12}-TTC interaction with water is incomplete and incorrect concentration or mole fraction values are assumed. Because of this its interaction with water as predicted with the UNIFAC method is over estimated. Also,

hydrophobic bonding between the adjacent long tails can occur which further influences the interactions with water. This is also not accounted for by the UNIFAC method.

The role of DTP has long been speculated to be that of assisting or enhancing the collecting properties of xanthate via a synergistic effect (Wiese et al, 2005b; Helbig et al, 2000). The free energy calculations between water and DTP, actually shows a small negative contribution to the interactions of this collector and the water phase. The standard redox potential for DTP to $(DTP)_2$ (Chander, 1999) is significantly higher than that occurring in flotation circuits and therefore it can be expected that the adsorption of this molecule onto mineral surfaces is via attachment of the ionic species. This results in a strong bonding to the surface resulting in an immobile and anchored surface species.

Because the DTP itself does not appear to enhance hydrophobicity via the calculated activity coefficient term, it has to be concluded that an increase in the mole fraction term is responsible for the increase in G^{ex}/RT. This in turn is responsible for the increased hydrophobicity or flotation activity in DTP/SIBX mixtures. A quantitative explanation for this synergistic effect now is possible by crowding of the $(SIBX)_2$ dithiolate around the anchored DTP, resulting in a localised increase in X_{SIBX} and finally G^{ex}/RT.

The TTC contribution to the activity coefficient or water repulsion is very high because of the many hydrophobic $-CH_2$ groups in the molecule. At low doses this effect is strong and evidenced in the flotation results. The low dosage effect is pronounced because a more effective contact and interaction with water molecules is possible. This molecule also appears to be strongly bound (du Plessis, 2003). A clustering of $(SIBX)_2$ around the immobile C_{12}-TTC would also account for the increase in flotation activity.

The higher copper recoveries compared to nickel are qualitatively explained on a basis of sulphide affinity for metals. From the K_{sp} relationships between metals and different xanthates (In Chander, 1999), NiS is 10^{-14} and CuS is 10^{-27}. This is a thirteen orders of magnitude difference implying the bonding energy between SIBX and Cu^{++} to be much stronger than SIBX with Ni^{++}. There is also evidence that both chalcopyrite (Fuerstenau, 1982c; Mielczarski et al, 1998; Hicyilmaz et al, 2004) and pentlandite (Hodgson and Agar, 1989) form metal salts (chemisorbed SIBX) with SIBX as an initial step during adsorption.

If one uses this difference, to be indicative of the interaction energy between the dithiolate $(SIBX)_2$, and the metal sulphide surface, then the $(SIBX)_2$ should be bonded much stronger to the copper containing mineral than the nickel containing one. This simply implies a greater selectivity for copper than nickel minerals. It is for example well known that covalent "oily" collectors (e.g. Z200) are generally more selective collectors and require long residence times to attach to the selected mineral. This is also because migration of covalent or non-polar collector molecules between minerals is possible and the longest retention time is on those minerals with the lowest solubility product, and the highest density of packing results.

4.3.5 Flotation rates of slow and fast floating minerals

A very popular modeling equation which uses flotation rate data is the unmodified Kelsall equation which has the following mathematical form (Hay et al, 2006):

$$r = 1 - \varphi_f \cdot e^{-K_f \cdot t} - \varphi_s \cdot e^{-K_s \cdot t} \qquad (4.3)$$

In this expression ϕ_f and ϕ_s represent the fraction of fast and slow floating minerals respectively and K_f and K_s their rate constants. In this expression $\phi_f + \phi_s$ sums to one.

This expression was used to calculate the fractions of the different floatable PGM minerals based on the data from the bench flotation tests. The results are presented in table 4.8.

At 5% molar replacement of SIBX an increase of 3.8% in the amount of PGM's in the fast floating fraction is observed with a simultaneous increase of 15.2.% and 27.1% in the flotation rate constants for the fast and slow floating minerals respectively.

When SIBX replacement was increased to 10% molar the amount of slow floating minerals was increased by 0.7%.

Table 4.8: Results of two-component floatability analysis.

SIBX Replacement	ϕ_f	ϕ_s	K_f	K_s
0%	0.754	0.246	1.007	0.021
5%	0.782	0.218	1.160	0.026
10%	0.748	0.252	1.153	0.022
100%	0.694	0.306	0.663	0.034

The final recovery was however still higher than the standard. This is explained in part by the fact that even if the amount of slow floating minerals increased, their flotation rate constant increased by 7.2%. More slow floating minerals are therefore expected to be recovered at the same residence times. The flotation rate of the faster floating fraction also increased by 14.5%.

When complete SIBX replacement was tested the amount of slow floating PGMs increased by 24%. At the same time the flotation rate for the fast fraction decreased by 34.2% while that of the slow floating fraction increased significantly by 63.5%. Because of this the initial PGM flotation rate was lower than that of the standard but at the end gave similar results.

Figure 4.4 shows the relationship between initial PGM recovery and the fast floating rate constant (solid triangles), as well as the fast floating fraction (empty triangles).

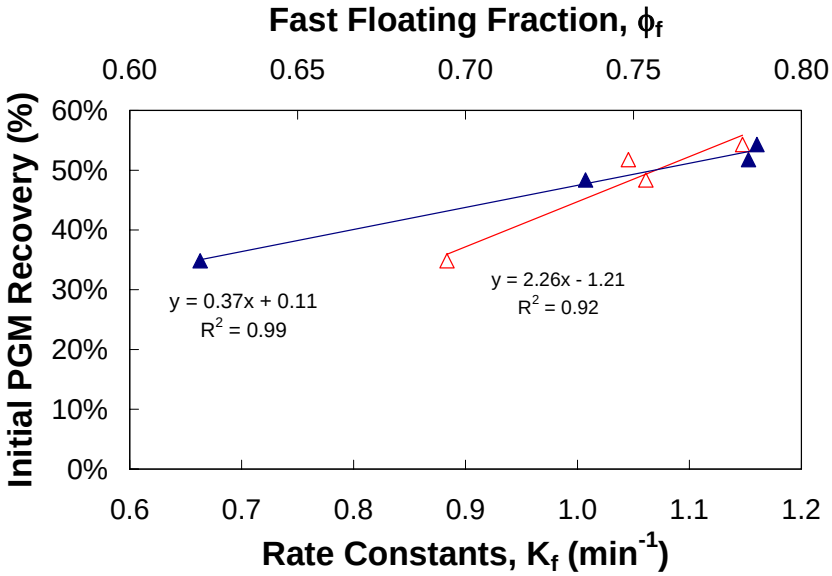

Figure 4.4: Relationship between initial PGM recovery and a) fast floating rate constant (solid triangles) and b) the fast floating fraction (empty triangles).

4.4 Summary

The effectiveness of C_{12}-TTC as a collector is dependent on the degree of SIBX replacement. It also implies that both TTC and SIBX have to be present to find an improvement in rate, recovery and grade. The optimum performance is close to 5 molar percent replacements, or one TTC molecule per 20 DTC molecules.

By using G^{ex}/RT calculations on the theoretical interaction calculations between water and DTP, it is concluded that DTP itself does not contribute a great deal to surface hydrophobicity. Using the concept of strong ionic interaction of DTP with mineral surfaces and ionic DTP adsorption with immobilisation, it is concluded that the synergistic behavior of the SIBX/DTP combination is due to higher densities of $(SIBX)_2$ packing around anchored DTP molecules. This is in agreement with proposals by Helbig et al (2000).

Based on the results of this investigation and those of Du Plessis (2003) it is believed long-chain TTCs are strongly held to the surface. One therefore has to assume the mechanism of higher recovery and rate at least partially results from higher density of $(SIBX)_2$ packing around TTC. The improved copper recovery compared to that of nickel has been related to differences in the interaction energies between the mineral surfaces and the SIBX dithiolate.

In general an increase in valuable mineral recovery is expected with an increase in mass recovery. Yet from figures 4.2 and 4.3 it appears that the first three tests showed similar mass recoveries while the 5 molar percent replacement tests yielded a significantly higher PGM recovery. This effect is attributed to an increased selectivity in recovering valuable minerals. This is the result of collecting more slow floating fine and course minerals. When complete replacement of SIBX was tested a higher mass recovery resulted without a significant benefit to PGM recovery. This effect suggests a less selective flotation process.

The linear relation (figure 4.4) between the initial PGM recovery, the rate constant and the amount of minerals in the fast floating fraction emphasises the importance of flotation kinetics in PGM recovery.

The increase in the flotation rate constants (table 4.5) with 5 molar percent TTC can be explained by the co-adsorption of TTC with SIBX and DTP and this increased the collector surface coverage. However, at higher collector dosages Klimpel (1999) also reported a decrease in flotation rate constants. By investigating the R/K relationship, Klimpel (1999) noted that increased collector dosages increased R while the value of K reached a maximum and this maximum depended on particle size. At courser particle sizes higher collector dosages increased the rate constant while it decreased for finer size fractions. This in part can now explain why the finer grained PGMs reached a maximum rate at lower TTC dosages compared to courser grained nickel and copper minerals. For all cases the final recovery was higher compared to the standard.

The fact that a modification of the chemical suite relative to the standard also changes the apparent fractions of fast and slow floating minerals, poses serious problems to predictions of the effect of particle size on kinetic energy effect only. The same holds for plant design parameters.

Chapter 5

Pilot Plant Trial on Underground Merensky Ore

5.1 Introduction

Before a plant trial is commissioned at Impala, pilot plant trial details are needed as intermediate between bench scale work and a large operation. These requirements include flotation kinetics, final grade and recovery as set by Impala. The primary objective in this chapter is to evaluate whether the proposed conditions arrived at from the bench scale work apply to up-scaling.

Based on the results from the bench scale test work, the 5 molar percent replacement of the current SIBX/DTP mixture by C_{12}-TTC was the best. Furthermore, a recent increase in CMC depressant dosage from 100g/ton to 350g/ton on the Merensky flotation section prompted an inclusion of high depressant dosages as an additional variable with TTC tests.

5.2 Test Procedure and Pilot Plant Flow Diagram

Impala's Merensky comminution circuit consists of fifteen (15) Semi-Autogenous (SAG) mills in closed circuit with cyclones. Compared to traditional run-of-mine SAG mills these mills all operate at relatively high critical speeds (~90%) and ball loads (~20%). The cyclone overflows from mills 1 – 7 and 15 are combined as feed to bank 1 of the Merensky float section while the cyclone overflows from mills 8 – 14 feed bank 2.

The current practice at Impala is to add most of the collector into the mill feed. Part of the reasoning is to assure an early attachment of collectors to rapid oxidising iron sulphides. Mill number 6 was selected for the pilot plant trial and the procedure of adding collectors to the mill was also applied during the trithiocarbonate trials. Five molar percent of the current SIBX-DTP collector combination was replaced with the nC_{12}-TTC.

The ***Floatability Characteristic Test Rig*** (FCTR) consists of 6x150L rougher cells in series

(figure 5.1). All six concentrates were combined to form the final concentrate. The final tails for assay were taken from the last rougher tail stream.

Initially a bleed-off stream from mill 6's cyclone overflow was used to fill the feed tank but this resulted in the stream being bias towards fine particles. Because of this, two valves were placed as is indicated on the flow sheet and the whole overflow stream was directed to fill the feed tank.

Activator, depressant and frother were added to the conditioning tank before the slurry was pumped to the first rougher cell.

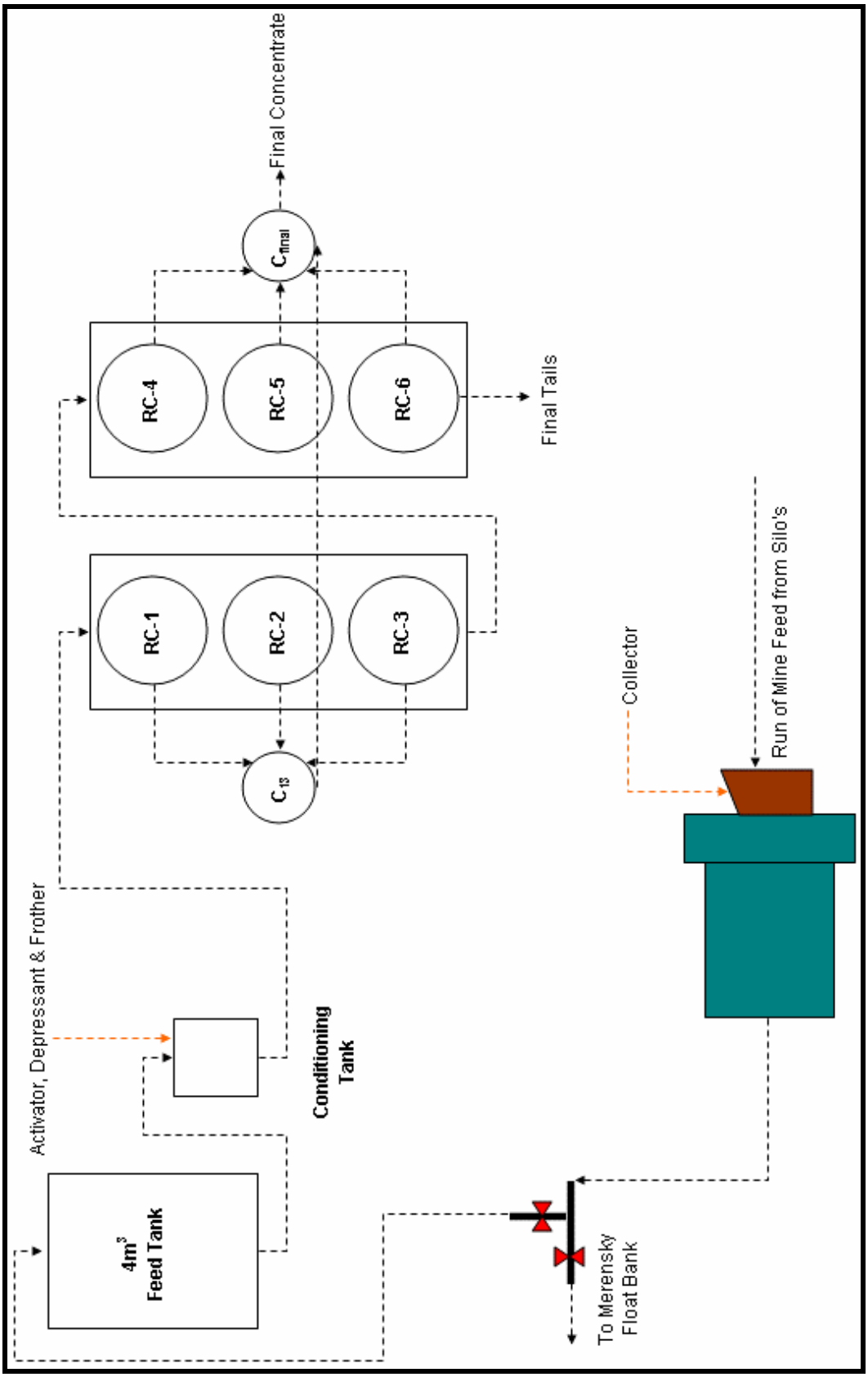

Figure 5.1: Schematic Representation of the Pilot Plant Setup.

After the changes to the collector suite were made the mill was left for 90 minutes before the cyclone overflow was directed to the pilot plant. This time delay was to allow the new collector suite to mix in the cyclone recirculating load (underflow).

The time from start-up to sampling was approximately 150 minutes. Of this time, 90 minutes were for all the cells to reach their individual level set points and another 60 minutes to make sure the plant was at steady state. Steady state was determined from tailing sump levels and cell level stability.

To ensure a good mass balance, as many streams as possible were sampled and analysed, they were:

- Pilot plant feed
- Final tails
- Final concentrate and
- Individual concentrates from cells 1 to 6.

Timed sampling on the individual concentrate streams was done to allow for the calculation of the actual mass recovery compared to the mass recovery calculated using the two-product formula.

The mass-balance procedure is described in detail in Appendix C. The parity graphs for the different stream assays indicate that a successful mass-balance was achieved for all the tests done.

5.3 Results and Discussion

TTC was tested over a period of 2 weeks and eight feed, final concentrate and final tails samples were collected during this time, as well as numerous concentrate samples for the individual cells. The high (350 g/ton) depressant tests with standard SIBX/DTP collectors were run before the TTC tests and the normal 100g/ton depressant trials after the TTC tests. For both the standard tests eight sets of feed, final concentrate and final tails samples were also collected with flotation rate data for the last series of tests as well.

Before a comparison between the different series of tests could be made it was necessary to compare the head grades because large differences in head grades can lead to recoveries being wrongly interpreted.

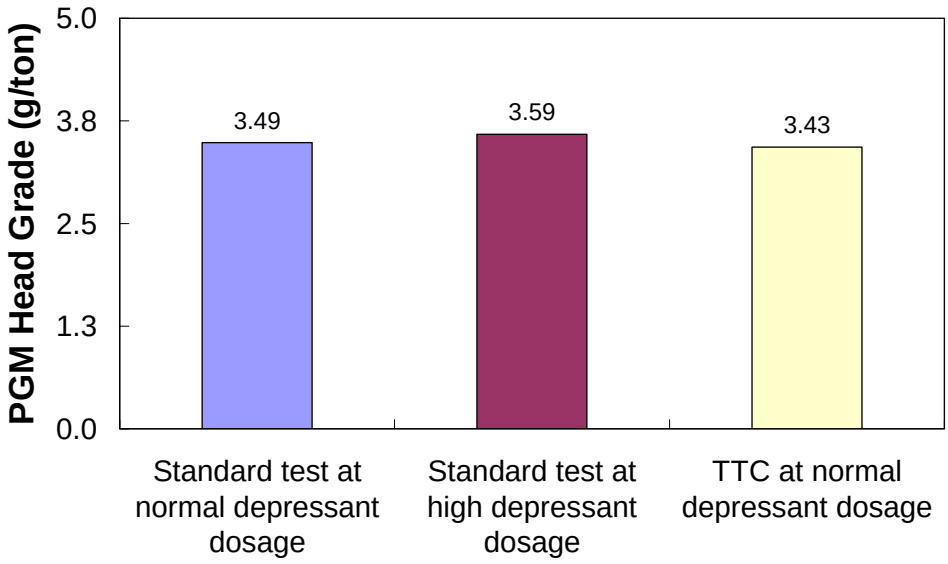

Figure 5.2: Comparison of average head grades for different tests.

Statistical evaluation of the twenty-four data sets using the paired t-test (method used for less than 40 data points) indicated that there was no significant difference between the three reported head grades. This implied that valid comparisons on metallurgical performances could be made.

5.3.1 Bubble loading and entrainment

A serious problem during flotation is the presence of a very stable froth phase (figure 5.3 (I)). This stability is normally attributed to excess fine minerals (-10um), and rapid floating gangue such as serpentine, talc and chlorites. Talc crystals in particular have hydrophobic surface planes and polar edges. The polar edges that project into the water phase and aggregate as particles of gangue, increase the inter-lamellar viscosity. The result is poor water drainage and increased bubble stability (Davidtz, 2004) leading to high mass recoveries and ultimately, poorer grade or selectivity.

To overcome this problem at Impala, high depressant dosages are used to ensure a hydrophilic gangue. Although the primary role of depressants is to control the natural floatability of gangue minerals, (mainly feldspar and pyroxenes for Merensky) the dosage of 350 g/ton CMC depressant also exhibits dispersing properties (Ryan, 2005). In contrast, gangue dispersion in the froth phase also reduces particle-particle bonding between gangue minerals with an increased overlap of electrical double layers. The increased repulsive forces between particles reduce viscosity with more free-flowing of water between bubbles, resulting in improved gangue drainage and valuable mineral grade. Small bubbles with clear windows normally indicate higher grades and gangue exclusion. In contrast cloudy and large bubbles suggest lower grades.

Concentrate grades from the first rougher cell for the various reagent combinations are reported in table 5.1. This increase in concentrate grade for the last two scenarios suggests a change in the relative floatability of valuables to gangue minerals. Preferential attachment of the valuable particles to the bubbles resulted in higher bubble loading with sulphide minerals.

Table 5.1: Concentrate grade comparison for the first rougher cell during various tests.

Collector Combination	**Concentrate Grade (g/ton PGM)**
Xanthate/DTP (low depressant)	~ 120
Xanthate/DTP (high depressant)	~ 200
Xanthate/DTP/TTC (low depressant)	~ 175

Figure 5.3 is froth images from the first rougher cell during the three different tests. At a 5 molar percent replacement of SIBX/DTP by TTC, the froth characteristics changed from a cloudy opaque froth seen for the flotation suite containing no TTC (figure 5.3 (I)) to small, clear bubbles (II and III). The result was better gangue rejection. Mass recovery for the first rougher cell dropped from 2.0% for the standard collector suite at 100g/ton depressant to 1.4% after the TTC was introduced.

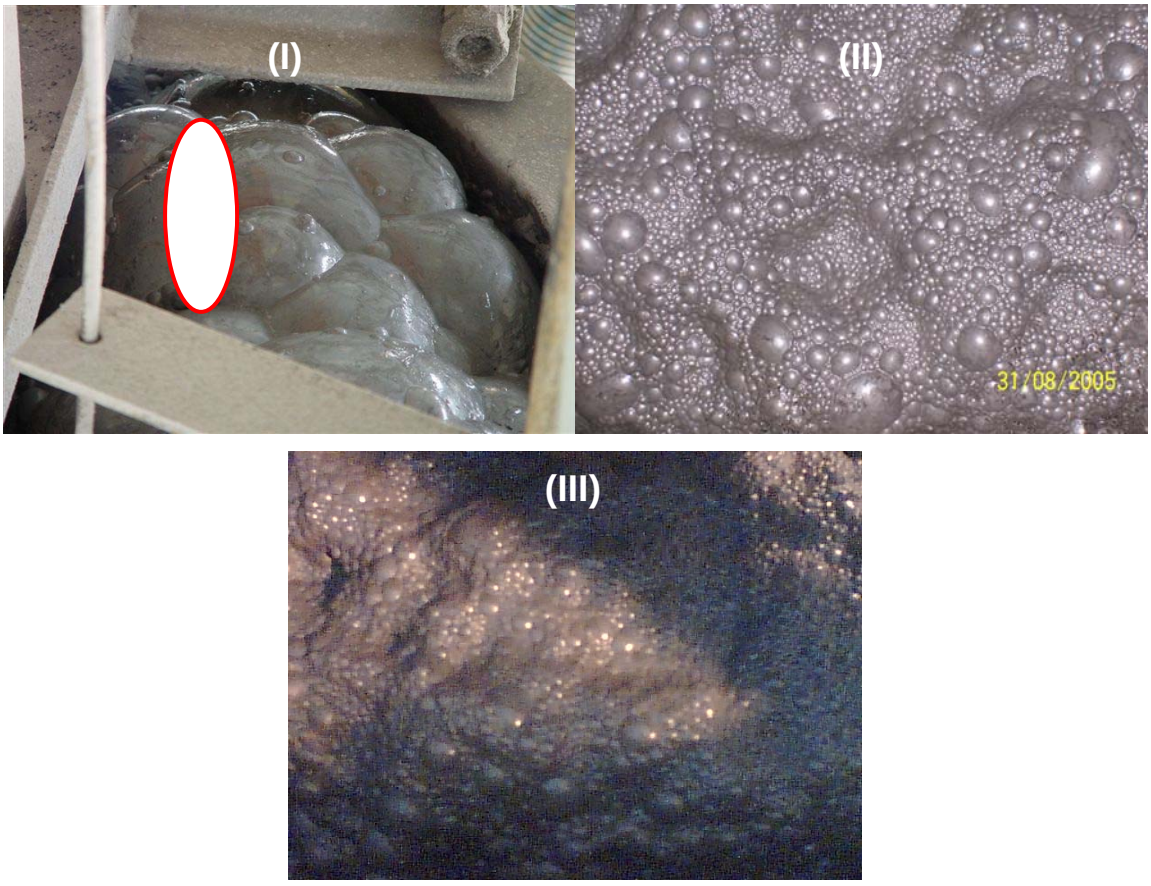

Figure 5.3: Froth Image of the first rougher cell on the pilot plant with: (I) the standard collector suite at low depressant dosage, (II) addition of 5 g/ton TTC with low depressant dosage and (III) the standard collector suite at high depressant dosage.

What is also clear from figure 5.3 (I) is the presence of what appears to be slime coatings (indicated by red oval). This is absent from figure 5.3 (II + III).

High doses of depressant visually looked like the TTC tests at 100g/ton depressant. From these observations also, a higher bubble loading by valuable minerals and improved intrinsic kinetics of the valuable minerals is expected.

The explanation for the increase in grade with high doses of depressant by Robertson et al (2003) was that of sulphide surface cleaning by the removal of the fine sliming gangue particles due to gangue dispersion. The increase in exposed surface area of sulphides results in an increase in the hydrophobic state and a corresponding increase in bubble attachment.

According to Dippenaar (1982) the increased hydrophobicity of the sulphide minerals at high depressant dosages is responsible for the increased rupture of water films when attached and because of this larger bubble do not grow at the expense of small ones. This could also be true when TTC as added. The increase in bubble instability due to rupturing results in less water being recovered to the concentrate and this lowers the amount of entrained gangue (Robertson et al, 2003).

5.3.2 Stage-by-stage comparison

The change in the metallurgical performance (grade-recovery relationship) with the addition of the long chain TTC at 100 g/ton depressant is reported in figure 5.4. Standard deviations for the calculated grades and recoveries are included.

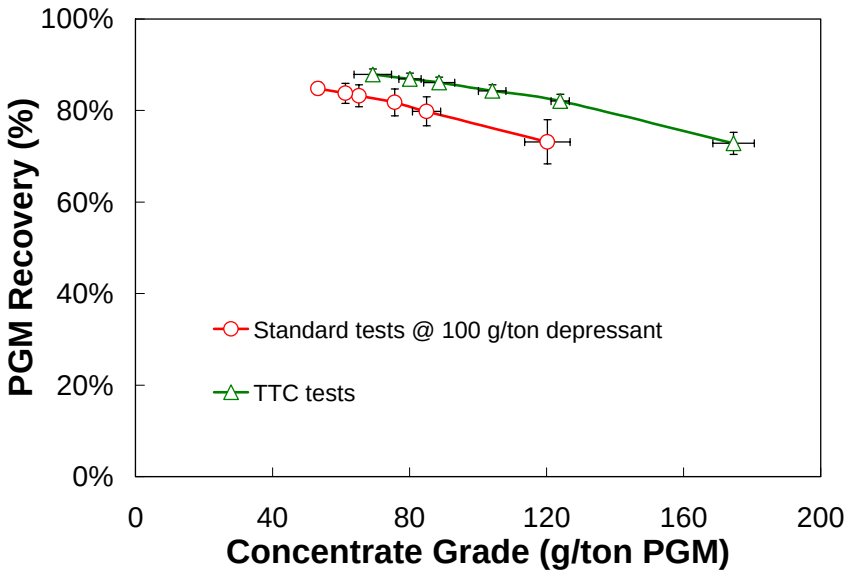

Figure 5.4: The effect of C_{12}-TTC on the PGM grade-recovery relationship when compared to the standard tests at 100 g/ton depressant.

The grade/recovery curve for the SIBX-DTP-TTC combination was always higher then the standard. This positive shift in the grade-recovery relationship implies a more selective

flotation process. An explanation is a higher loading of hydrophobic values due to higher intrinsic kinetics and the simultaneous exclusion of gangue.

Mass recoveries from the different rougher cells are reported in Table 5.2. Apart from the first two cells there seems to be no difference in the mass recovery from the rest of the cells. This shows that the long-chain TTC is responsible for a more selective flotation process during the initial stages of flotation which ultimately ends in higher final concentrate grades.

The increase in selectivity can be explained by combined effects of solution and froth phases. Firstly an increase in G^{ex} which is a collector/particle effect in the solution phase (Steyn, 1996; Davidtz, 1999) and secondly a particle/bubble effect which is in the froth phase (Leja, 1989; Adamson, 1990). These two effects are not necessarily always directly dependent on each other. The synergistic effect one sees with dithiolate formation in the presence of an immobile co-collector, is primarily a collector/particle effect and therefore dependent on surface coverage and molecular structure of the collector.

Table 5.2: Increase in solids recovery for individual cells.

	Increase in Mass-pull	
	Standard	**TTC**
Cell 1	2.0%	1.4%
Cell 2	1.1%	0.8%
Cell 3	0.5%	0.4%
Cell 4	0.6%	0.6%
Cell 5	0.4%	0.3%
Cell 6	0.7%	0.7%
Total	5.3%	4.2%

The bubble effect is primarily the result of the ease of frother/collector interactions (Schubert, 2005; Adamson, 1990). This in turn is related to film thinning and bubble capture. These two are direct consequences of molecular structure and primarily diffusion and mixing between the collector and frother (Leja, 1989). It can be appreciated that a mobile species such as dixanthogen would more easily mix with a frother than an immobile DTP. It appears therefore that the TTC in some way also catalyses this diffusion and mixing of the collector and frother phase. This would mean the long-chain TTC in some way affects a rapid bubble attachment that excludes gangue as well. These effects can explain most of the flotation activity differences encountered.

5.3.3 Overall performance

Figure 5.5 is a summary of the average tails grades for the three pilot plant tests.

A drop in the average tails grade is seen after the introduction of TTC into the collector suite, or with the addition of higher amounts of depressant. Although a significant change in tails grade was not expected with the addition of the TTC, the reported results can be explained as follow: the ore is known to have both slow and fast floating material and down the bank of flotation cells it becomes increasingly difficult to recover valuable minerals.

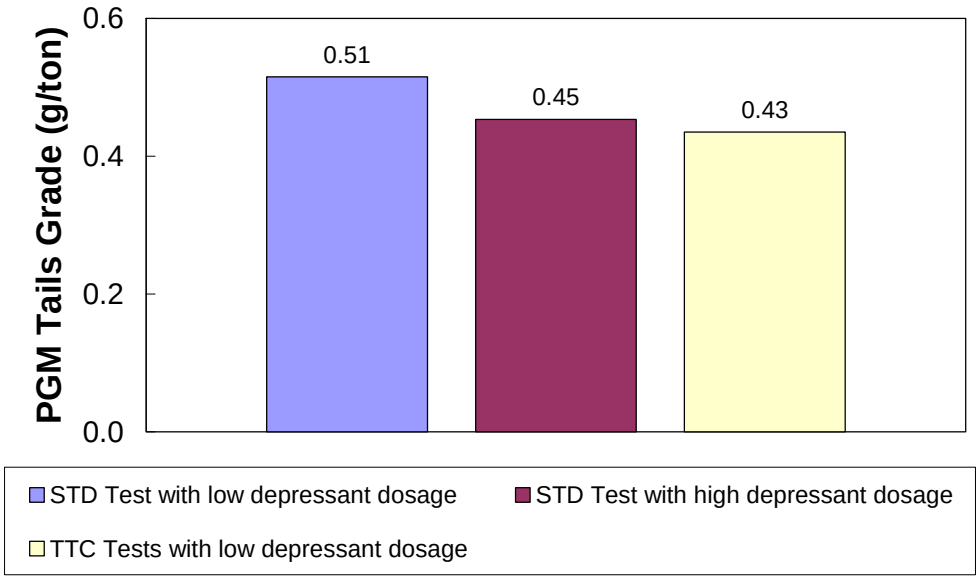

Figure 5.5: Average final tails grades for the three different pilot plant tests.

With such high residence time (± 80 minutes) on the pilot plant it can be argued that whatever minerals are not recovered for a specific condition, will never be recovered. However, after introduction of the long chain TTC a portion of very slow (either fine or poorly liberated) floating minerals are recovered. This is supported by the observed changes in the amount of fast and slow floating PGMs as was calculated from the laboratory flotation tests in chapter 4.

Based on statistical evaluations of the twenty-four data sets, it is concluded that the approximate drop in tails grade of 0.1g/ton (for the latter two scenarios) is statistically significant with 98.95% confidence.

Figure 5.6 shows the average overall recovery for the three tests. The conclusion is that either the introduction of TTC at low depressant dosages or the increase in depressant dosages resulted in a higher average PGM recovery. This agrees with the consistently lower final tails grade and was concluded to result at least partially from the recovery of slower floating valuable minerals.

A faster and stronger bubble attachment by the valuable minerals appears to be a consequence of TTC addition, the result is improved gangue depression or increased selectivity resulting in improved recovery of the valuables.

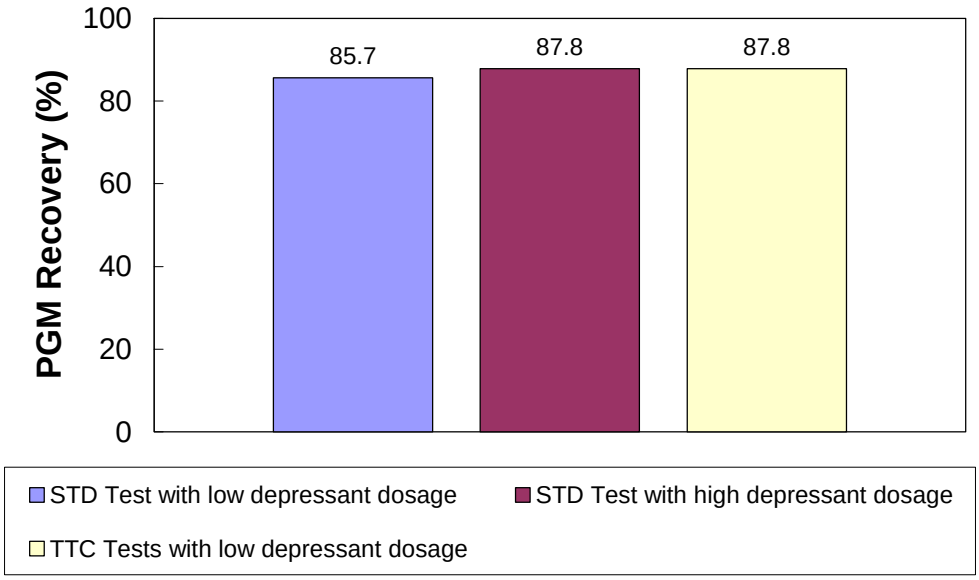

Figure 5.6: Recovery comparison of standard tests and TTC tests.

Since the overall flotation rate will depend on the relative flotation rates of valuables and gangue (figure 5.7) it may also be argued that because both adsorption and desorption of valuable and gangue particles occur in the froth phase, the ratio of the two rate constants will determine the final equilibrium or bubble loading of valuable and gangue particles. This phenomenon is also known as froth recovery.

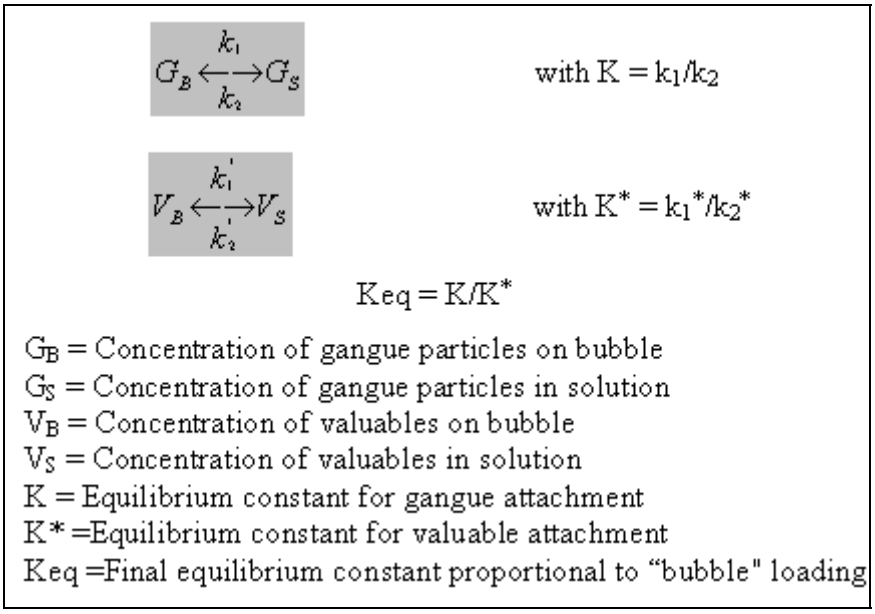

Figure 5.7: Representation of gangue and valuable mineral kinetics in the froth phase.

If this model is used to explain the higher PGM recoveries with TTC it can be concluded that the equilibrium constant for valuable mineral attachment (K*) increased, which means that the relative rate of PGM de-sorption (k_2*) decreased or the relative rate of adsorption (k_1*) increased. Both these scenarios will result in a higher value of equilibrium bubble attachment for valuable minerals.

If one considers the adsorption of the long chain TTC to be strong (immobile), resulting in a localised increase in collector concentration it can be surmised that the formation of patches or islands of collector improves mineral-bubble attachment (Leja, 1989). This can have two froth phase effects. It can increase the rate of valuable mineral-bubble attachment and/or improve the bubble attachment of slower floating minerals (composite particles). It can thus be concluded that in this study TTC affected both parameters and by doing so increased the equilibrium constant for valuable mineral attachment. The ultimate result was improved recoveries.

When considering the gangue minerals it can be argued that the TTC did not affect the gangue directly but by increasing the equilibrium constant for the valuable minerals resulted in improved gangue rejection due to preferred valuable mineral bubble attachment.

The mass recoveries for the three tests are reported in figure 5.8. TTC addition as well as higher depressant dosages resulted in a significant decrease in mass recovery, translating to a more selective separation process. As a result, the PGM concentrate grades increased from 57 g/ton to 73 g/ton for the TTC tests and to 85g/ton when high depressant dosages were used.

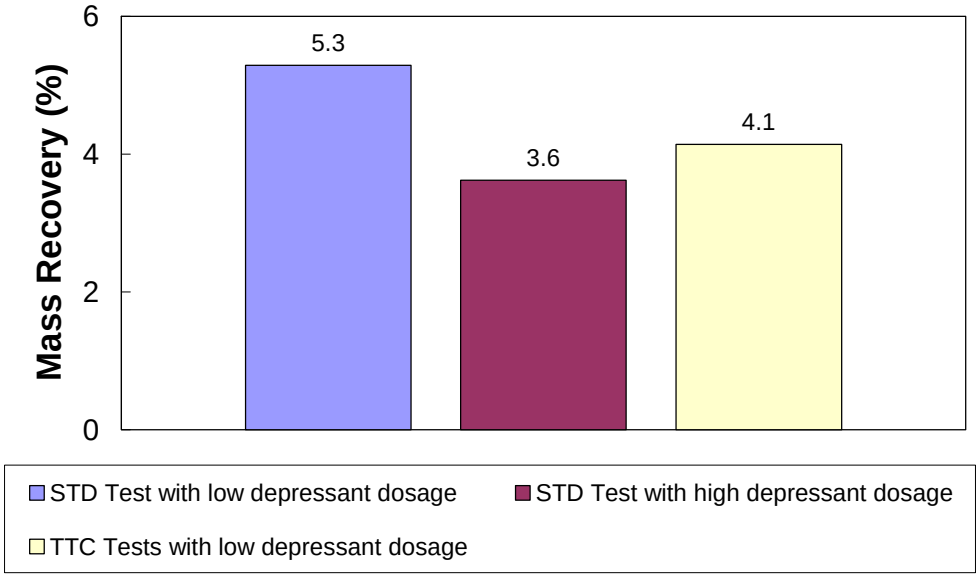

Figure 5.8: Mass recovery comparison of standard tests and TTC tests.

The mass recovery was calculated using the PGM assays (after mass balancing) as follow:

$$\text{Mass recovery}\,(\%) = \frac{f - t}{c - t} \times 100 \qquad (5.1)$$

where f, c and t represent the PGM grades in the feed, concentrate and tails respectively.

5.4 The Effect of Mild Steel Grinding Media

A second part of the pilot plant trial was to investigate the effect of chemical performance with forged and high chrome steel balls as grinding media. Previous work by Impala's grinding media supplier, Magotteaux (Greet, 2004), has shown that when Merensky ore is floated with SIBX-DTP after being milled with mild steel balls, a significant loss in PGM recovery and grade resulted. It was concluded that due to oxygen scavenging by iron in solution, the dithiolate of SIBX was unable to form. However, TTC has proven to improve

sulphide surface hydrophobicity at low oxygen concentrations or reduced potentials. For the TTC tests, only the TTC was added to the mill feed, other reagents were added down-stream. During the standard tests the SIBX-DTP was introduced to the mill feed.

5.4.1 Results and discussion

Figure 5.9 is a summary of the final concentrate grades achieved from the four tests.

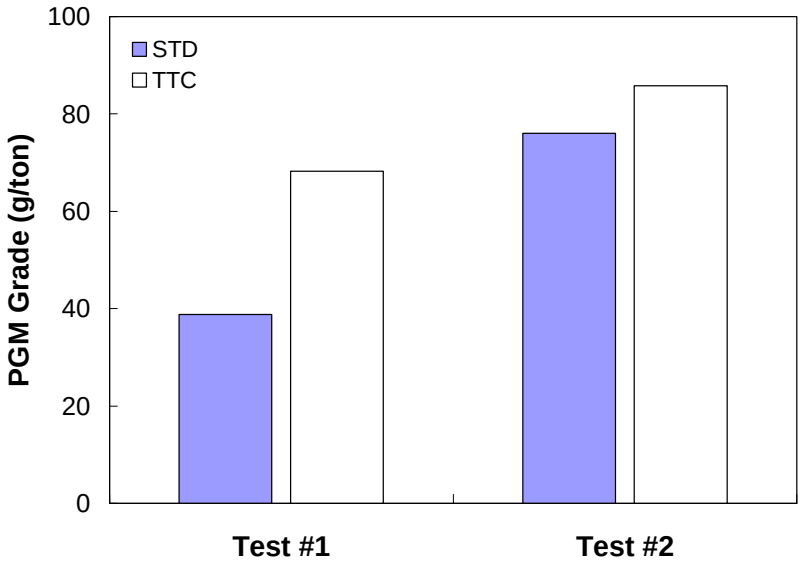

Figure 5.9: The effect of TTC addition on the flotation activity of SIBX and DTP with mild steel grinding media.

In both tests, improvements in PGM grade resulted. An explanation for this improved grade with TTC is twofold: Firstly it is based on the ability of TTC to produce a hydrophobic state at very low oxygen concentrations. Xanthate in turn cannot convert to dixanthogen under depleted oxygen conditions but this is needed to produce a good collector combination for effective bubble attachment. Secondly, the reduced oxygen atmosphere in the mill prevents base metal sulphides associated with PGMs from oxidation and loss. The argument is that TTC firstly attaches to pre-oxidised sulphide minerals in the mill and so doing creates surface sites with hydrophobic “tails”. The mobile dixanthogen formed under oxidative conditions hydrophobically can bond to the adsorbed TTC “tails”, so doing increasing the mineral’s ability to float by effective bubble capture. From this it is concluded that the detrimental effect of mild steel grinding media on the oxidation of SIBX during milling is not the case with the addition of TTC which improves the flotation process as a whole.

- ***A cost implication***

Table 5.3: Possible cost implications of using TTC with forged steel grinding media.

Grinding Media	Cost		Consumption	
Forged steel	4.80	R/kg	0.64	kg/ton
High chrome steel (12%)	6.80	R/kg	0.56	kg/ton
Tones Merensky milled		7.9	million tones per annum	
Grinding media cost				
Forged steel	R 24.34	million per annum		
High chrome steel	R 30.17	million per annum		
Savings on grinding media	R 5.83	million per annum		
TTC cost (5% replacement)	R 7.43	million per annum		
Saving (Loss)	R -1.60	million per annum		

Although a loss of R1.6 million per annum is predicted, it must be recognised that only a slight improvement in PGM recovery and grade is required to have the loss turned into a substantial benefit. The Lone Tree operation in Nevada, USA, employs an oxygen free atmosphere with the specific intention of avoiding fine-grained pyrite losses due to oxidation. The mild steel milling may have similar effects with respect to PGM recovery, especially readily oxidised sulphides such as pyrrhotite and fine pentlandite. These hidden effects can have a significant effect on the process viability. A TTC break even dosage is 5.9 g/ton before any optimisation has been done.

5.5 Summary

The pilot plant testing of TTCs has yet again unraveled some of the unique properties of this long-chain molecule. It was found that only a third of the current depressant dosage was required to have a similar metallurgical performance. For the first time the froth phase effect of the long-chain TTC was identified and found to be an important indicator of grade and kinetics. It was also identified that the negative effect of mild steel grinding media with SIBX and DTP is diminished when TTC is added.

The dramatic change in bubble properties on Merensky ore also suggests a change in bubble capture and growth in the presence of long-chain TTCs. If some of the reasons for this can be identified, it would help understand the forces operating in bubble capture. There has been a great deal of success with the factors responsible for phase separation of collectors on particle surfaces and adjacent water in a flotation system with G^{ex} calculations. These thermodynamic factors led to the design and prediction that TTCs should theoretically be the most effective molecule in securing the phase separation of a particle from solution. Now for example, what is the best frother with a particular collector suite? Certain mixing rules applied to frother-collector interactions should apply. Is it simply the long chain, or is this a variable?

There is much speculation regarding nano-bubbles and their effect on bubble attachment. Does the non-polar nitrogen molecule for example concentrate in pores between hydrophobic groups and is it possible that branched hydrophobic groups at a surface would enhance nitrogen adsorption to the degree that nano-bubbles form?

CHAPTER 6

Preliminary Plant Trial on Underground UG-2 Ore

6.1 Plant Trial at Impala's MF-2 Plant

6.1.1 Introduction

Uncertainty regarding the availability of Merensky ore at section 16 of the MF-2 plant led to the postponement of TTC evaluation on Merensky ore until the new float upgrade is complete. It was decided to continue on underground UG-2 ore at section 20/21 at the MF-2 side of Impala's Central concentrator. This section consists of both a primary and secondary milling and flotation section. After milling and classification, the product is sent to conditioning tanks for reagent addition. The collector suite consists of pre-mixed, 70/30 mass-ratio, SIBX and DTP. For this trial a 5 molar percent replacement of the total collector addition to the primary section was made with TTC and the TTC was dosed with the primary mill feed.

During the trial, representative samples of the first two primary rougher concentrates were collected over a period of time for screening and assaying. Daily shift results were used for overall comparisons.

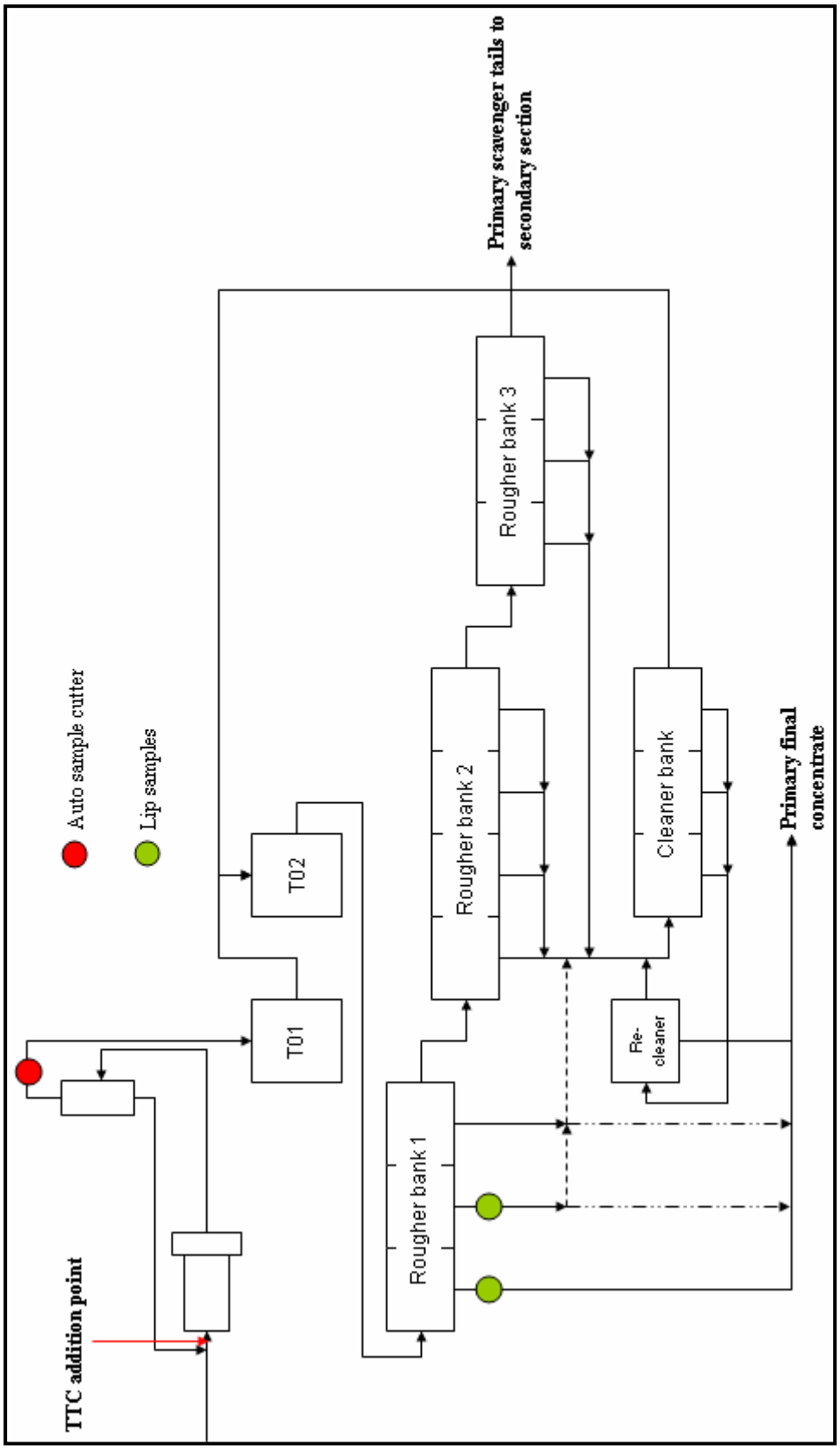

Figure 6.1: Flow diagram of the primary section 21 at MF-2.

6.1.2 Results and Discussion

6.1.2.1 Effect on particle size distribution

From 300 um down to approximately 53 um there was a consistent decrease in the amount of particles in the respective size classes after TTC was dosed with SIBX and DTP. The conclusion is that during the initial stages of rougher flotation, more composite particles were rejected with the new collector combination.

Table 6.1: Discrete size distribution of concentrate samples.

	% Retained on screen			
	Rougher 1		Rougher 2	
Aperture (um)	**Standard**	**TTC**	**Standard**	**TTC**
300	0.37	0.28	2.51	1.03
212	0.52	0.24	1.25	0.57
150	0.85	0.28	1.50	0.55
106	1.75	0.34	2.25	0.67
75	3.52	0.63	3.61	1.31
53	5.98	2.50	5.30	2.87
38	8.28	6.15	6.86	5.37
10	43.43	49.95	38.03	44.82
0	35.30	39.63	38.69	42.80

The cumulative percentage mass passing, versus screen size is plotted in figure 6.2. From this it is estimated that the amount if course material (+53 um) decreased from 13% to 4.3% for the first rougher cell and from 16.4% to 7% for the second rougher cell.

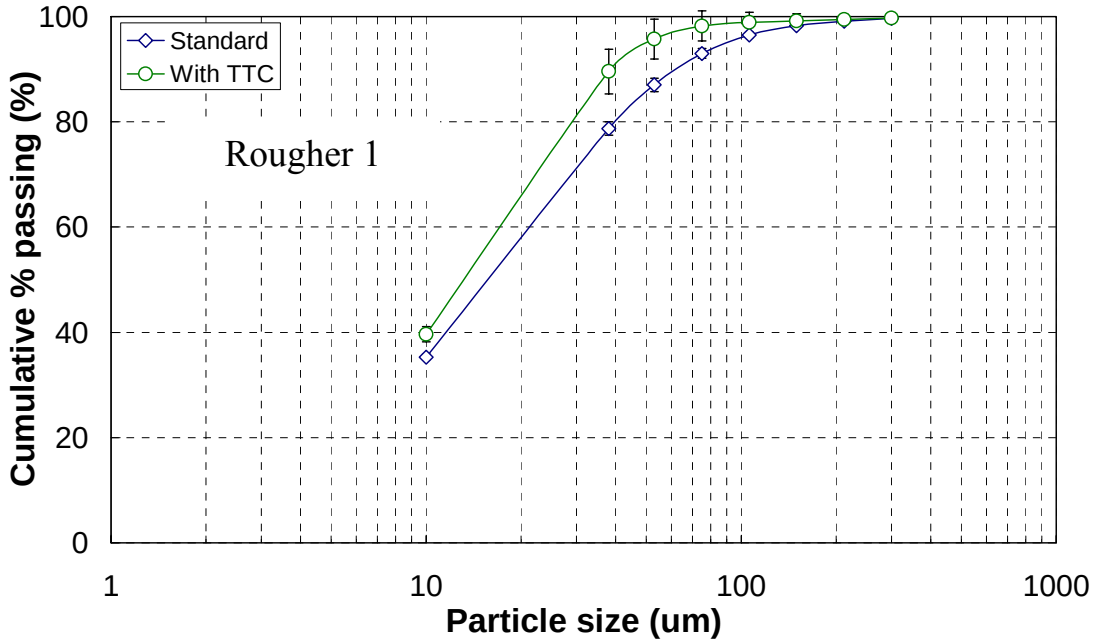

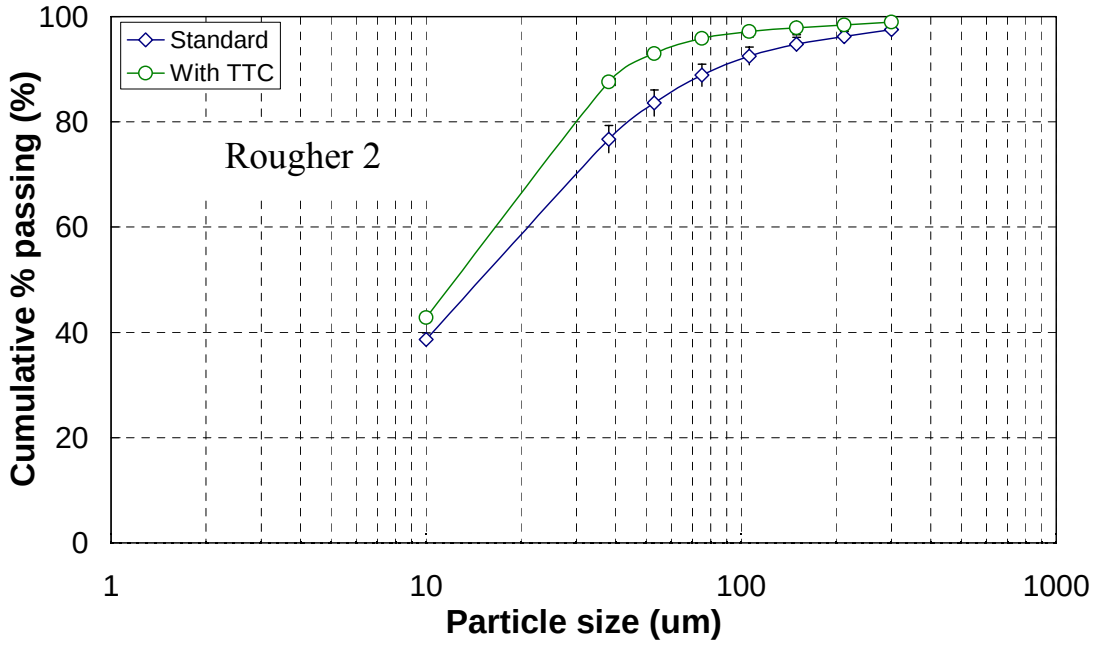

Figure 6.2: The effect of TTC on the particle size distribution of the rougher concentrates.

6.1.2.2 Initial concentrate grades of PGMs and chromite.

Figure 6.3 below shows the change in concentrate grades for the rougher cells.

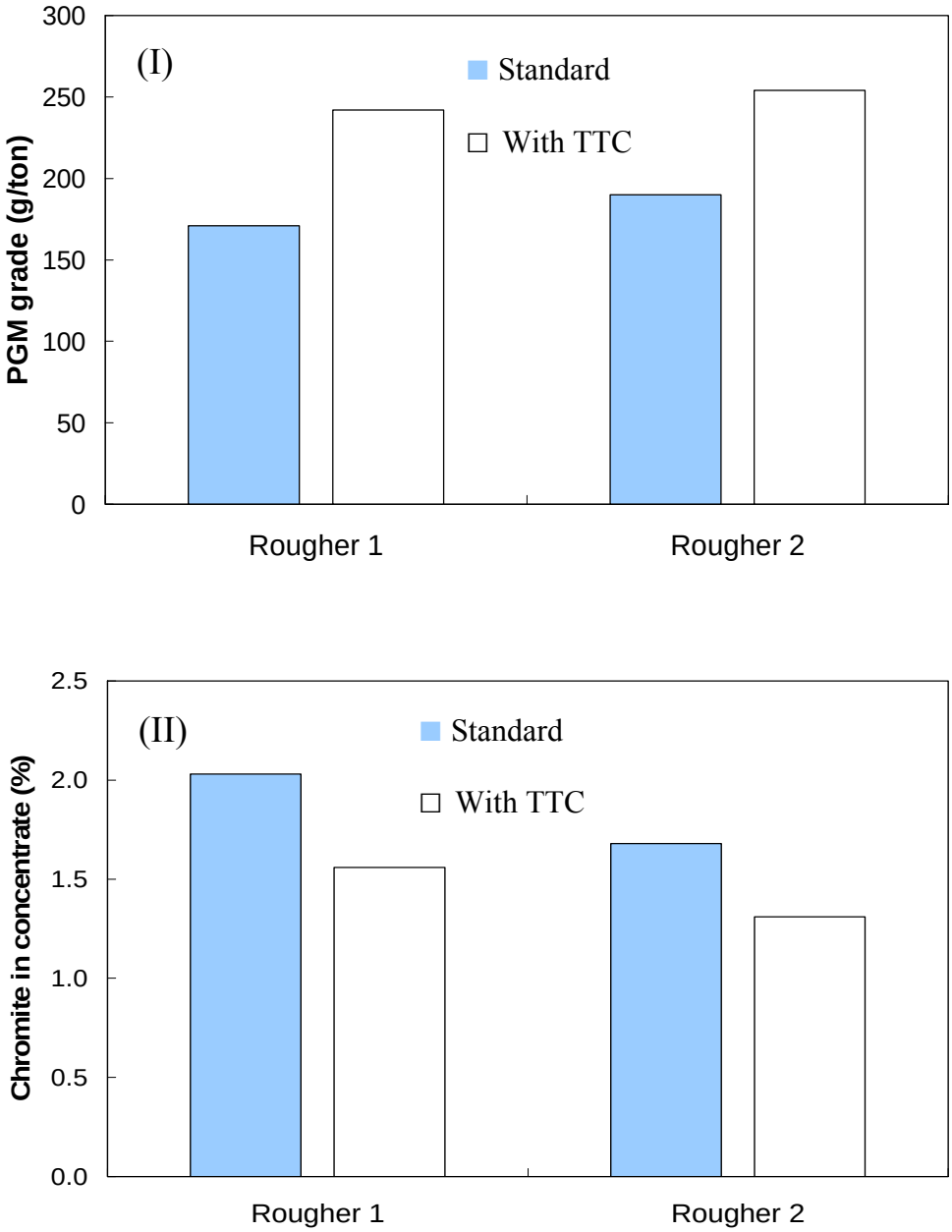

Figure 6.3: Change in concentrate grade from the first two primary rougher cells with TTC addition.

Two important differences to note is the increase in initial PGM grade and reduction in the amount of chromite in the concentrate. The concentrate from these two rougher cells is primarily sent to final concentrate. With such an improvement in concentrate grade it can be expected that the grade from the primary section will also improve. Although the remainder

of rougher and scavenger concentrates are sent to cleaners and finally a re-cleaning stage, with the apparent increase in intrinsic PGM floatability (relative to gangue) it can further be expected that the cleaner and ultimately, re-cleaner concentrates will also benefit from TTC addition.

To further address the issue of course particle rejection with TTC, concentrate samples were screened at 53 um and sent for analyses. These results are reported in table 6.2.

Table 6.2: Size-by-size assay results for concentrate samples.

	Rougher 1			Rougher 2		
	PGM (g/ton)	**Cr2O3 (%)**	**SiO2 (%)**	**PGM (g/ton)**	**Cr2O3 (%)**	**SiO2 (%)**
Standard +53 um	160	1.21	41.9	170	2.39	49.6
With TTC +53 um	420	1.04	37.5	312	0.70	37.0
Standard -53 um	162	1.41	42.1	186	1.71	50.2
With TTC -53 um	232	1.48	50.9	200	2.03	49.4

For the +53 um fraction TTC addition improved both chromite and siliceous gangue exclusion. This resulted was an improvement in PGM concentrate grade for this size fraction.

For the -53 um fraction the concentrates from the TTC trial had equal or higher chromite and siliceous gangue content than the samples from the standard trial. The PGM grade was still higher although not by the same margin as the +53 um fraction.

From this data it appears that the TTC had a two-fold effect: the exclusion of courser gangue material to improve PGM grade but also improved fine grained PGM recovery. Hence the increase in PGM grade for the fine size fraction with higher gangue content.

6.1.2.3 Overall performance

Figure 6.4 shows the Q-Sum calculations for the head grade data. The values indicated on the graph are the average values for the corresponding period. A definite increase in PGM head grade is seen between the periods marked with the vertical solid lines. The period between the vertical dashed line and the right-hand-side solid line represents the TTC trial period.

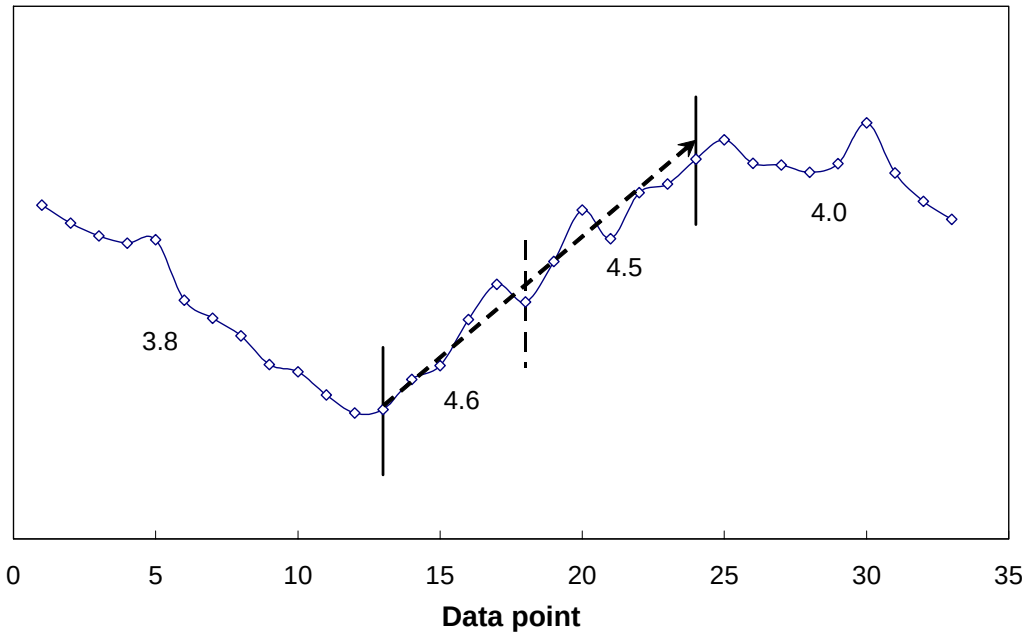

Figure 6.4: Calculated head grade Q-Sum for the MF-2 trial.

Although no significant difference is seen between the head grades from the TTC trial and the days just before, the head grades before and after the marked period show lower values and care must be taken when comparing PGM recovery and concentrate grades. The same calculations on the concentrate grades are shown in figure 6.5.

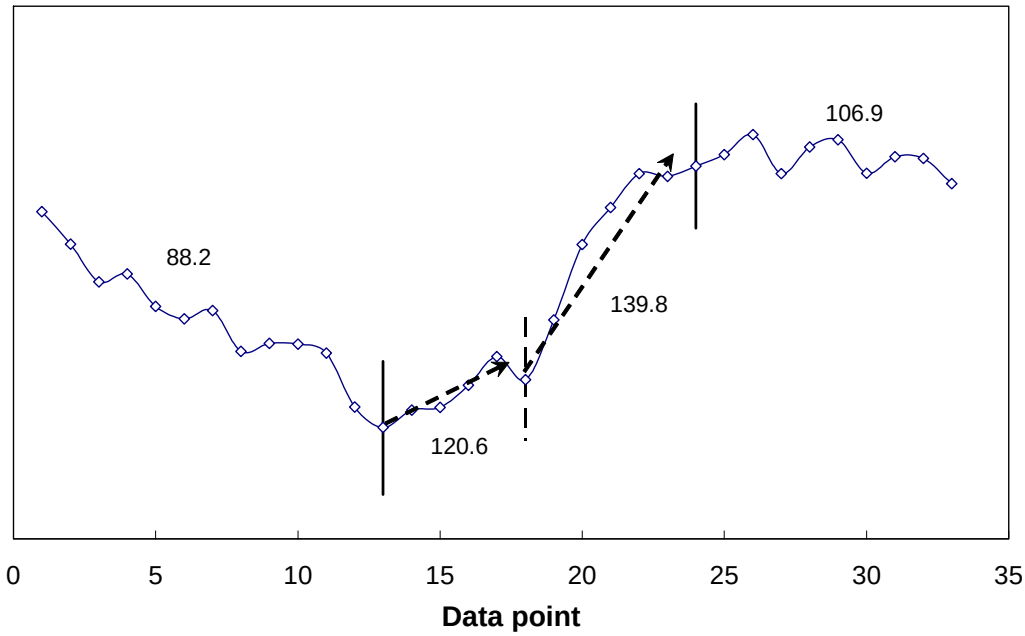

Figure 6.5: Calculated concentrate grade Q-Sum for the MF-2 trial.

Similar to the head grade, an increase in concentrate grade is seen for the period marked between the solid lines. This can be attributed to higher head grades. However, unlike the head grade where the increase had a constant slope throughout, the concentrate grade shows an increase in gradient when the TTC was introduced. This means that apart from the head grade effect, another factor contributes to the improvement in final concentrate grade. This factor is probably the introduction of the long-chain TTC with the SIBX-DTP mixture.

Prior to TTC addition there was an increase in tailing grade and it decreased till after the trial was terminated (figure 6.6). Sustained residual effects due to TTC or TTC decomposition products have been reported on auriferous pyrite flotation (Davidtz, 2006) and this effect can be argued to be in part responsible for the lower tails grades even after the trial was terminated.

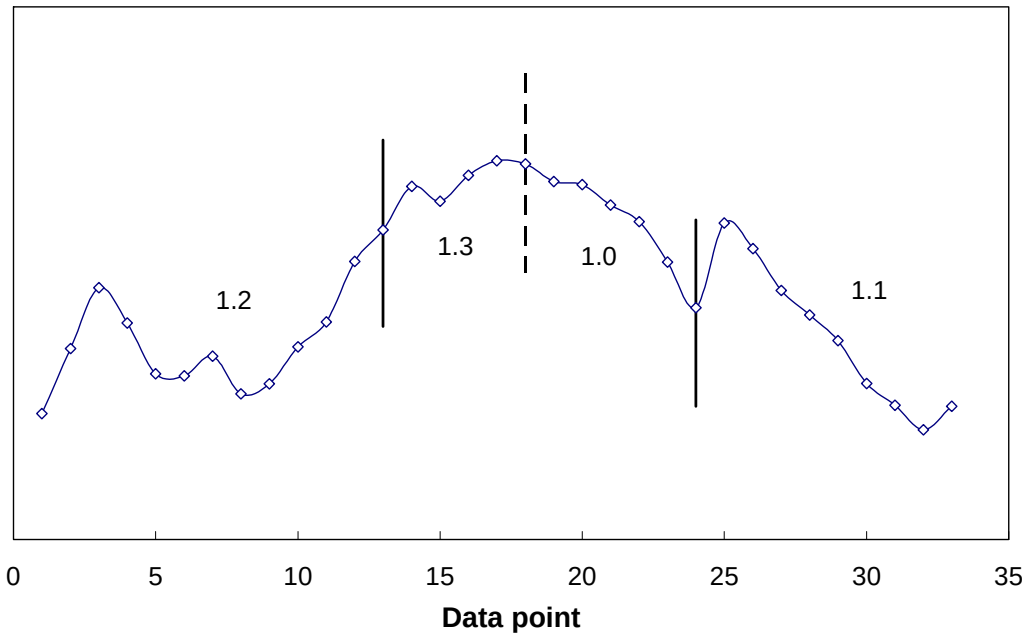

Figure 6.6: Calculated tailings grade Q-Sum for the MF-2 trial.

In summary, Q-Sum calculations indicate that the addition of TTC showed a significant improvement in final PGM concentrate grade. The effect on final PGM tails grade is debatable.

A pronounced effect of the TTC is most noticeable in concentrates from the primary rougher cells. The effect was characterised by significantly higher PGM grades and a reduction in gangue recovery for +53 um material.

6.2 Summary

Although this was only a two-week preliminary plant trial, indicators are that TTCs are beneficial. Unlike the Merensky pilot plant tests, the UG-2 trial was not preceded by any bench scale optimisation.

The following conclusions have been drawn:

- There was a large improvement in primary rougher concentrate grade when TTC was added to the existing flotation suite.
- This improvement was charaterised by higher PGM grades and lower chromite grade in the concentrate.
- Particle size analysis of the concentrates showed that the TTC produced a finer concentrate. Above 53 um the TTC recovered much less material.
- The higher rougher concentrate grades can in part be attributed to an increased courser gangue rejection coupled with an improvement in liberated valuable mineral recovery.
- For the +53 um size fraction more chromite and siliceous gangue was rejected from the bubbles. This effect was most pronounced in PGM grades in the coarse fraction.
- Although the TTC improved the rougher performance, the overall performance of the TTC on the section was shadowed by the presence of the regrind mill material. It is recommended that TTC be added to the secondary float section as well but at lower quantities, approximately 2.5 molar percent as a start.
- Overall, in terms of unit cost and storage capacity, the smelter should benefit most.

Chapter 7

Conclusions and Recommendations

It is unusual that a single chemical shows as much promise to sulphide mineral processing as the TTC does, especially on Merensky ore with more base metal sulphides than UG-2. With cautious optimism, one can expect the large improvements seen on Merensky, to at least in part extend to UG-2 operations, and possibly oxidised sulphide ore bodies.

Factors such as kinetics and grade are expected to result in large savings in chemical costs, and downstream processing costs such as smelting. Final recovery has the potential to also improve but the added chemical cost is overwhelmingly justified by the return in revenue from predictions on reagent cost alone. This also brings into question the economic significance before and after the processing of tails. Although very simplistically a rough calculation on reagent cost savings is shown below.

Table 7.1: Simplified cost benefit calculation for using TTC on Merensky ore.

Information		
Tonnes Merensky milled (BP FY07)	358800	tones floated per month for bank 2
Bank 2 running time	92%	
	3961152	tones floated for bank 2 per year
KU-47 price	R 10.50	R/kg
nC12-trithiocarbonate price	R 125.00	R/kg
Senario #1 - High depressant dosages		
Depressant usage	1386.4	tones per year
Depressant cost	R 14.6	million per year
Total Cost	R 14.6	million per year
Senario #2 - Low depressant dosage with ~ 5% TTC addition		
Depressant usage	396.1	tones per year
Depressant cost	R 4.2	million per year
TTC usage	29.7	tones per year
TTC cost	R 3.7	million per year
Total Cost	R 7.9	million per year
Total Savings	*R 6.7*	*million per year for Bank 2*

A further R2.9 million can be added to this saving if the same calculations are done for bank

1 of the Merensky circuit which uses slightly less depressant. This brings the potential cost saving to approximately R9.6 million per annum. These calculations do not include any potential financial gain from improved metal recoveries. If one assume a Merensky PGM head grade of approximately 3.8g/ton PGM and a PGM basket price of approximately R 150 000 per kilogram, the financial gain from a 1% increase in PGM recovery amounts to approximately R45 million per annum. This is a staggering increase in the amount of revenue generated.

7.1 Conclusions

- A 5 mole percent substitution of the standard SIBX-DTP collector suite by nC_{12}-TTC on Merensky ore proved most effective. The improvement in overall performance was substantial and consistently found.

- A two rate-constant (Kelsall equation) model showed that the TTC substitution improved the flotation rate constants for both slow and fast floating PGM minerals on Merensky ore, and therefore the overall recovery when compared to the standard SIBX-DTP collector suite.

- During pilot plant testing only one third of the high depressant dosage used was needed to obtain an equivalent metallurgical performance on Merensky ore.

- A very unique effect on the froth phase was identified which significantly affected valuable and gangue mineral recovery to the concentrate.

- Based on thermodynamic reasoning, (G^{ex}/RT), the synergistic effect of $(SIBX)_2$/DTP is due to the high concentration of $(SIBX)_2$ around immobilised DTP. TTC probably does the same but more efficiently and it does not have an oxygen atom in the molecule that interacts stronger with water than the added sulphur atom in TTC. This results in a localised increase in X_{SIBX} and finally G^{ex}/RT in equation (4.2).

- Under electrochemically controlled conditions, and pH 9.2 an improved surface hydrophobicity on pyrrhotite was found with TTC and SIBX than SIBX alone. This effect

increased at lower potentials.

- In the presence of forged mild steel balls, the efficiency of SIBX-DTP increased considerably when TTC was added to the mill. This means an increase in flotation activity at lower levels of dissolved oxygen in the mill.

- Cost savings on reagents alone used on Merensky has been calculated to be approximately R9.6 million per annum.

- The 5 molar percent TTC in SIBX-DTP on UG-2 produced a finer concentrate from the first two primary rougher cells.

- The +53 um and -53 um size fractions from UG-2 concentrates produced a higher PGM grade for the courser size fraction. There was also an increase in PGM grade for the finer size fraction.

- The addition of TTC improved the exclusion of course gangue minerals from the bubbles, and improved the recovery of fine minerals.

- Overall, TTC addition to a UG-2 collector suite significantly improved the final concentrate grade with no clear effect on final tailings grade.

7.2 Recommendations

- It is recommended that a full plant scale testing of TTC with SIBX and DTP be undertaken for Merensky ore on Impala's section 15 after the upgrades.

- When TTC is used on Merensky ore, stage addition of depressant should be investigated to minimise gangue entrainment in the scavenger section.

- The testing of mercaptan-TTC mixtures applied to the mill feed of Merensky and UG-2 should have a high priority. Included should be the effect of long-chain isomers of TTCs.

- Further investigation of grinding media should be done, and passivation of minerals that

are easily oxidised. Particularly the effect of copper and lead cations on freshly fractured and aged surfaces. In particular on pyrrhotite and fine grained semi-conducing metal sulphides which include pentlandite.

- It is necessary to identify and quantify forces involved in bubble capture and in particular the role of long-chain, branched and linear collectors and frothers.
- Molecular structure effects on interaction energies between frother and collector molecules and water by G^{ex} methods should be correlated with bubble capture results.
- The effect of collector and frother structure be related to N_2 adsorption and parameters involved in bubble capture.

APPENDICES

Appendix A

Thermodynamic Calculations

The production of iron ions and hydrogen sulphide by pyrrhotite in acidic solutions can be represented by:

$$Fe_{(1-x)}S + 2H^{+} \rightarrow H_2S + Fe^{2+} \quad \text{(A1)}$$

Thermodynamically the equilibrium reaction can be represented by:

$$\Delta G_f = -R_i.\log(\kappa) \quad \text{(A2)}$$

were:

ΔG_f : Gibbs free energy of formation,

R_i : Ideal gas constant.

κ : Constant.

The energy of formation for the various species is given in table A1, below:

Table A.1: Free energies of formation for various species (Garrels et al., 1990).

	Species	**Energy of formation (kCal/mol.K)**
Reagents	$Fe_{(1-x)}S$	-23.320
	H^{+}	0.000
Products	H_2S	-7.892
	Fe^{2+}	-20.300

ΔG_f is calculated from the differences between the energies of formation for the product and the reagents as follow:

$$\Delta G_f = \Delta G_{products} - \Delta G_{reagents}$$
$$\Delta G_f = \left(\Delta G_{H_2S} + \Delta G_{Fe^{2+}}\right) - \left(\Delta G_{pyrrhotite} + 2 \cdot \Delta G_{H^+}\right)$$
$$\Delta G_f = \left(-7.892 - 20.3000\right) - \left(-23.3200\right)$$
$$\Delta G_f = -4.872 \text{kCal/mol.K}$$

The value for log(κ) is then calculated accordingly:

$$\log(\kappa) = \frac{\Delta G_f}{-R} = \frac{-4.872}{-1.987} = 2.45$$

Log(κ) is related to the activities of the species as follow:

$$\kappa = \frac{P_{H_2S} \cdot a_{Fe^{2+}}}{\left(H^+\right)^2}$$
$$\log(\kappa) = \log(P_{H_2S}) + \log\left(a_{Fe^{2+}}\right) - 2 \cdot \log\left(H^+\right)$$

The assumption is made that the concentration of the Fe^{2+} species in solution is very low (ppm level) because a pyrrhotite crystal is used for only a short time in pure water i.e. $a_{Fe2+} = 1e^{-6}$ molar. It is also general knowledge that $\log(H^+) = -pH$, thus, the above formula can be simplified as follow:

$$\log\left(P_{H_2S}\right) = \log(\kappa) - \log[Fe^{2+}] - 2pH = A$$
$$P_{H_2S} = 10^A$$

From this a plot of pH vs. the fugacity of hydrogen sulphide (P_{H2S}) can be constructed (Figure A1).

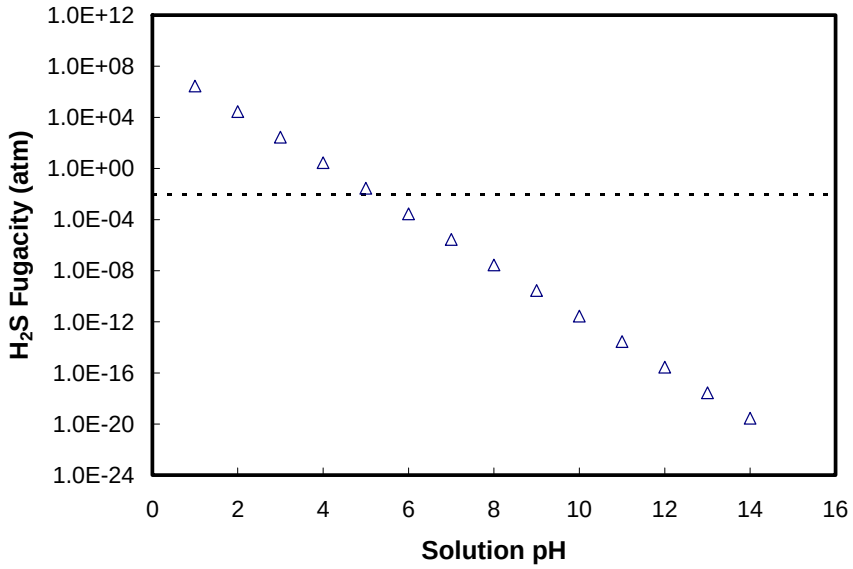

Figure A.1: Fugacity of H_2S for pyrrhotite as a function of pH at a Fe^{2+} concentration of $1.0e^{-6}$ molar.

From figure A1 it is clear that thermodynamically, pyrrhotite will start to produce H_2S gas at the mineral-water interface in acidic media due to oxidation at a pH of approximately 5 and lower. This strongly correlates to the pH values obtained in chapter 4 where pyrrhotite starts to develop a self-sustained natural hydrophobicity.

Appendix B

Bench-Scale Flotation Test Data

Assay Data

Table B.1: Bench Scale Flotation Results for Standard Test on Merensky Ore.

Standard Test #1

	Dry mass (g)	Cum. % Mass pull	PGM Grade (g/ton)	Ni Grade (%)	Cu Grade (%)	Cum. PGM Rec	Cum. Ni Rec	Cum. Cu Rec
Conc 1	20.07	0.63%	274.0	5.00	4.32	45.2%	19.5%	35.3%
Conc 2	76.93	3.03%	51.0	1.64	0.68	77.5%	44.1%	56.6%
Conc 3	82.58	5.60%	9.0	0.39	0.13	83.6%	50.4%	61.0%
Conc 4	71.80	7.84%	4.7	0.26	0.10	86.4%	54.0%	63.9%
Tails	2954.91	100.00%	0.56	0.08	0.03	100.0%	100.0%	100.0%
Calculated Head			3.79	0.16	0.08			

Standard Test #2

	Dry mass (g)	Cum. % Mass pull	PGM Grade (g/ton)	Ni Grade (%)	Cu Grade (%)	Cum. PGM Rec	Cum. Ni Rec	Cum. Cu Rec
Conc 1	27.95	0.87%	229.0	4.42	3.81	51.7%	22.4%	37.6%
Conc 2	73.86	3.15%	41.0	1.47	0.53	76.2%	42.1%	51.4%
Conc 3	85.53	5.80%	8.2	0.37	0.13	81.9%	47.9%	55.4%
Conc 4	78.63	8.23%	4.4	0.26	0.10	84.7%	51.6%	58.1%
Tails	2964.24	100.00%	0.64	0.09	0.04	100.0%	100.0%	100.0%
Calculated Head			3.83	0.17	0.09			

Standard Test #3

	Dry mass (g)	Cum. % Mass pull	PGM Grade (g/ton)	Ni Grade (%)	Cu Grade (%)	Cum. PGM Rec	Cum. Ni Rec	Cum. Cu Rec
Conc 1	23.98	0.74%	242.0	4.60	3.92	48.1%	21.5%	39.6%
Conc 2	82.17	3.28%	45.0	1.40	0.46	78.8%	43.8%	55.6%
Conc 3	85.84	5.93%	8.2	0.37	0.12	84.6%	50.0%	59.9%
Conc 4	75.51	8.27%	4.1	0.26	0.08	87.2%	53.8%	62.5%
Tails	2968.48	100.00%	0.52	0.08	0.03	100.0%	100.0%	100.0%
Calculated Head			3.73	0.16	0.07			

Table B.2: Bench Scale Flotation Results for 5% C12-TTC on Merensky Ore.

5% C12-TTC substitution Test #1

	Dry mass (g)	Cum. % Mass-pull	PGM Grade (g/ton)	Ni Grade (%)	Cu Grade (%)	Cum. PGM Rec	Cum. Ni Rec	Cum. Cu Rec
Conc 1	23.36	0.72%	268.0	4.72	3.78	49.1%	23.7%	40.8%
Conc 2	81.18	3.24%	53.2	1.52	0.62	83.0%	50.3%	64.0%
Conc 3	99.18	6.31%	7.0	0.36	0.12	88.4%	58.0%	69.5%
Conc 4	78.45	8.74%	3.8	0.23	0.09	90.8%	61.9%	72.8%
Tails	2948.11	100.00%	0.4	0.06	0.02	100.0%	100.0%	100.0%
Calculated Head			3.95	0.14	0.07			

5% C12-TTC substitution Test #2

	Dry mass (g)	Cum. % Mass-pull	PGM Grade (g/ton)	Ni Grade (%)	Cu Grade (%)	Cum. PGM Rec	Cum. Ni Rec	Cum. Cu Rec
Conc 1	24.29	0.75%	251.0	4.60	3.67	52.1%	24.9%	44.1%
Conc 2	72.21	2.98%	46.4	1.46	0.48	80.7%	48.4%	61.3%
Conc 3	79.94	5.45%	10.0	0.40	0.14	87.5%	55.6%	66.8%
Conc 4	73.79	7.73%	4.4	0.27	0.10	90.3%	60.0%	70.4%
Tails	2986.66	100.00%	0.38	0.06	0.02	100.0%	100.0%	100.0%
Calculated Head			3.62	0.14	0.06			

5% C12-TTC substitution Test #3

	Dry mass (g)	Cum. % Mass-pull	PGM Grade (g/ton)	Ni Grade (%)	Cu Grade (%)	Cum. PGM Rec	Cum. Ni Rec	Cum. Cu Rec
Conc 1	23.83	0.74%	259.5	4.66	3.73	50.6%	24.3%	42.4%
Conc 2	76.70	3.11%	49.8	1.49	0.55	81.8%	49.4%	62.6%
Conc 3	89.56	5.88%	8.5	0.38	0.13	88.0%	56.8%	68.2%
Conc 4	76.12	8.23%	4.1	0.25	0.10	90.5%	61.0%	71.6%
Tails	2967.39	100.00%	0.39	0.06	0.02	100.0%	100.0%	100.0%
Calculated Head			3.78	0.14	0.06			

Table B.3: Bench Scale Flotation Results for 10% C12-TTC on Merensky Ore.

10% C12-TTC substitution Test #1

	Dry mass (g)	Cum. % Mass-pull	PGM Grade (g/ton)	Ni Grade (%)	Cu Grade (%)	Cum. PGM Rec	Cum. Ni Rec	Cum. Cu Rec
Conc 1	29.70	0.92%	210.0	4.62	3.72	53.6%	25.4%	49.7%
Conc 2	77.87	3.33%	38.0	1.38	0.49	79.1%	45.3%	66.9%
Conc 3	79.08	5.78%	8.6	0.47	0.12	84.9%	52.2%	71.1%
Conc 4	67.12	7.86%	4.0	0.30	0.07	87.2%	55.9%	73.2%
Tails	2973.70	100.00%	0.5	0.08	0.02	100.0%	100.0%	100.0%
Calculated Head			3.60	0.17	0.07			

10% C12-TTC substitution Test #2

	Dry mass (g)	Cum. % Mass-pull	PGM Grade (g/ton)	Ni Grade (%)	Cu Grade (%)	Cum. PGM Rec	Cum. Ni Rec	Cum. Cu Rec
Conc 1	38.33	1.18%	114.0	3.55	3.05	45.4%	25.7%	52.4%
Conc 2	75.86	3.51%	35.8	1.29	0.42	73.5%	44.1%	66.7%
Conc 3	87.54	6.19%	7.8	0.46	0.12	80.6%	51.7%	71.4%
Conc 4	64.45	8.17%	3.9	0.26	0.06	83.2%	54.9%	73.2%
Tails	2991.17	100.00%	0.54	0.08	0.02	100.0%	100.0%	100.0%
Calculated Head			2.96	0.16	0.07			

10% C12-TTC substitution Test #3

	Dry mass (g)	Cum. % Mass-pull	PGM Grade (g/ton)	Ni Grade (%)	Cu Grade (%)	Cum. PGM Rec	Cum. Ni Rec	Cum. Cu Rec
Conc 1	31.06	0.96%	219.0	4.63	3.73	56.3%	28.0%	52.3%
Conc 2	76.22	3.31%	36.0	1.27	0.40	79.1%	46.9%	66.0%
Conc 3	90.90	6.12%	8.6	0.46	0.12	85.5%	55.1%	70.9%
Conc 4	73.00	8.37%	4.4	0.31	0.07	88.2%	59.5%	73.2%
Tails	2967.27	100.00%	0.48	0.07	0.02	100.0%	100.0%	100.0%
Calculated Head			3.73	0.16	0.07			

Table B.4: Bench Scale Flotation Results for 100% C12-TTC on Merensky Ore.

100% C12-TTC substitution Test #1

	Dry mass (g)	Cum. % Mass-pull	PGM Grade (g/ton)	Ni Grade (%)	Cu Grade (%)	Cum. PGM Rec	Cum. Ni Rec	Cum. Cu Rec
Conc 1	34.20	1.05%	154.0	3.87	3.29	42.2%	26.1%	54.8%
Conc 2	86.68	3.72%	48.2	1.45	0.50	75.7%	50.9%	75.9%
Conc 3	97.75	6.72%	12.4	0.49	0.13	85.4%	60.3%	82.1%
Conc 4	71.29	8.92%	6.4	0.33	0.10	89.1%	65.0%	85.6%
Tails	2961.57	100.00%	0.46	0.06	0.01	100.0%	100.0%	100.0%
Calculated Head			3.84	0.16	0.06			

100% C12-TTC substitution Test #2

	Dry mass (g)	Cum. % Mass-pull	PGM Grade (g/ton)	Ni Grade (%)	Cu Grade (%)	Cum. PGM Rec	Cum. Ni Rec	Cum. Cu Rec
Conc 1	25.22	0.78%	142.0	3.70	3.78	32.2%	19.3%	49.6%
Conc 2	83.77	3.35%	54.4	1.66	0.57	73.1%	48.0%	74.4%
Conc 3	105.80	6.61%	12.0	0.49	0.13	84.5%	58.7%	81.6%
Conc 4	72.41	8.84%	5.9	0.31	0.08	88.3%	63.3%	84.6%
Tails	2961.83	100.00%	0.44	0.06	0.01	100.0%	100.0%	100.0%
Calculated Head			3.43	0.15	0.06			

100% C12-TTC substitution Test #3

	Dry mass (g)	Cum. % Mass-pull	PGM Grade (g/ton)	Ni Grade (%)	Cu Grade (%)	Cum. PGM Rec	Cum. Ni Rec	Cum. Cu Rec
Conc 1	20.83	0.64%	160.0	3.85	4.72	30.2%	14.4%	38.9%
Conc 2	76.18	2.99%	57.6	1.72	0.58	69.9%	38.0%	56.4%
Conc 3	91.66	5.81%	14.0	0.54	0.13	81.5%	46.9%	61.2%
Conc 4	77.94	8.21%	6.3	0.34	0.11	86.0%	51.7%	64.6%
Tails	2982.55	100.00%	0.52	0.09	0.03	100.0%	100.0%	100.0%
Calculated Head			3.40	0.17	0.08			

Statistical Analysis

The bench-scale flotation tests will be evaluated using the null-hypothesis. This is a standard technique that can be applied to a small number of data points to give a statistical significance, or confidence, in the conclusions drawn from the data.

For a small number of samples ($n < 40$) this hypothesis can be tested using the t-distribution. This analysis will be illustrated by using the data from the *Standard Test* as well at the test with *5% SIBX replacement with C_{12}-TTC*.

The null-hypothesis (H_o) is that there is no significant difference between the average recovery from the standard test (R_1) and the average recovery obtained with 5% C_{12}-TTC (R_2).

The average recovery for each test is calculated as follow:

$$\bar{R}_i = \frac{\sum R_i}{N} \qquad \text{(B1.1)}$$

Values for $\bar{R}_i$: Standard Test - 86.1%
5% TTC Test - 90.5%

The standard deviation (s_d) for each data set is calculated with the following equation:

$$s_d = \sqrt{\frac{\sum_{N=1}\left(d - \bar{d}\right)^2}{N-1}} \qquad \text{(B1.2)}$$

Values for s_d: Standard Test - 1.29%
TTC Test - 0.22%

The mean standard deviation (S_{dm}) for the two pairs of tests can be calculated as follow:

$$S_{dm} = \sqrt{\frac{s_{d1}^{\ 2} + s_{d2}^{\ 2}}{2}} \qquad \text{(B1.3)}$$

This calculates to a value for S_{dm} of 0.93%. The degrees of freedom are now calculated as follow:

$d_f = N_1 + N_2 - 2$. Thus, $d_f = 3 + 3 - 2 = 4$.

Using these values of S_{dm} and d_f, the value of t can be calculated that indicates the statistical significance in the observed recovery difference of 4.4%.

$$t = \frac{\bar{R}1 + \bar{R}2}{S_{dm} \cdot \sqrt{\frac{1}{3} + \frac{1}{3}}} \qquad \text{(B1.4)}$$

This calculates to 5.87. Using a table with values of t as a function of degrees of freedom, a probability of more than 99.5% is obtained. This means that the recovery increase of 4.4% for the specific data set is statistically significant at more than 99.5%.

Table B.5: Summary of the statistical analysis of bench-float data on PGM recovery.

Test Condition	Recovery Increase	Confidence Level	Significant?
5% TTC Addition	4.44%	99.8%	YES
10% TTC Addition	0.13%	53.0%	NO
100% TTC Addition	1.69%	90.0%	NO

Appendix C

Pilot Plant Data

The feed pump to the pilot plant is operated at 650 RPM with a volumetric feed rate of 10L/min. Using the SG of the feed the solids flow rate to the first rougher cell was calculated.

Knowing the solids flow to the pilot plant the individual reagent dosage rates were calculated as follow:

$$\text{Dosage rate (mL/min)} = \frac{F_{solids} \cdot D}{1000 \cdot S} \qquad \text{(C1.1)}$$

with:

F_{solids} = solids feed rate to the first rougher cell (kg/min)
D = required reagent dosage (g/ton)
S = reagent solution strength (g/mL)

Table C.1: Reagent conditions for pilot plant trials.

Reagent	**Dosage (g/ton)**	**Solution Strength (mg/mL)**
Activator	80	0.14
Depressant	90 & 350	0.01
nC_{12}-TTC	6	0.20
Frother	50	1.00

The TTC was dosed with the current xanthate/DTP mixture into the mill feed and for this the dry mill feed rate was used to calculate the required dosage rate of the trithiocarbonate. The average mill feed rate was approximately 75 TPH. The xanthate/DTP dosage rate was changed from the control room.

Assay Data

Individual cells for normal depressant and TTC tests

Table C.2: Individual cell data for standard tests and TTC tests 1 and 5.

Stream	Test Number	PGM g/ton	Cr2O3 %
Cell 1 Conc	STD 1	127.0	0.55
Cell 2 Conc	STD 1	27.0	0.82
Cell 3 Conc	STD 1	14.0	1.18
Cell 4 Conc	STD 1	10.4	1.41
Cell 5 Conc	STD 1	7.2	1.64
Cell 6 Conc	STD 1	6.9	1.65
Cell 1 Conc	STD 2	118.0	0.55
Cell 2 Conc	STD 2	18.2	0.82
Cell 3 Conc	STD 2	14.6	1.18
Cell 4 Conc	STD 2	5.2	1.41
Cell 5 Conc	STD 2	4.3	1.64
Cell 6 Conc	STD 2	2.5	1.65
Cell 1 Conc	STD 3	115.0	0.50
Cell 2 Conc	STD 3	15.2	0.83
Cell 3 Conc	STD 3	13.6	1.11
Cell 4 Conc	STD 3	6.7	1.16
Cell 5 Conc	STD 3	5.9	1.60
Cell 6 Conc	STD 3	3.6	1.31
Cell 1 Conc	TTC 1.1	142.0	0.37
Cell 2 Conc	TTC 1.1	23.0	0.52
Cell 3 Conc	TTC 1.1	18.2	0.73
Cell 4 Conc	TTC 1.1	7.5	0.74
Cell 5 Conc	TTC 1.1	5.0	0.84
Cell 6 Conc	TTC 1.1	3.6	0.92

Stream	Test Number	PGM g/ton	Cr2O3 %
Cell 1 Conc	TTC 1.2	210.0	0.49
Cell 2 Conc	TTC 1.2	56.0	0.77
Cell 3 Conc	TTC 1.2	23.7	1.19
Cell 4 Conc	TTC 1.2	12.8	1.31
Cell 5 Conc	TTC 1.2	7.6	1.74
Cell 6 Conc	TTC 1.2	4.6	1.68
Cell 1 Conc	TTC 5.1	209.0	0.36
Cell 2 Conc	TTC 5.1	46.5	0.59
Cell 3 Conc	TTC 5.1	20.0	1.00
Cell 4 Conc	TTC 5.1	15.3	0.89
Cell 5 Conc	TTC 5.1	8.9	1.25
Cell 6 Conc	TTC 5.1	6.4	0.96
Cell 1 Conc	TTC 5.2	193.0	0.33
Cell 2 Conc	TTC 5.2	42.5	0.77
Cell 3 Conc	TTC 5.2	12.2	0.91
Cell 4 Conc	TTC 5.2	10.1	0.90
Cell 5 Conc	TTC 5.2	7.2	1.08
Cell 6 Conc	TTC 5.2	5.5	1.43
Cell 1 Conc	TTC 5.3	140.0	0.32
Cell 2 Conc	TTC 5.3	27.5	0.59
Cell 3 Conc	TTC 5.3	12.4	0.82
Cell 4 Conc	TTC 5.3	9.2	0.87
Cell 5 Conc	TTC 5.3	5.0	1.00
Cell 6 Conc	TTC 5.3	2.6	1.20

Table C.3: Individual cell data for TTC tests 2 and 4.

Stream	Test Number	PGM g/ton	Cr2O3 %
Cell 1 Conc	TTC 2.1	150.0	0.35
Cell 2 Conc	TTC 2.1	29.0	0.53
Cell 3 Conc	TTC 2.1	11.4	0.75
Cell 4 Conc	TTC 2.1	9.0	0.78
Cell 5 Conc	TTC 2.1	7.3	0.74
Cell 6 Conc	TTC 2.1	4.6	0.72
Cell 1 Conc	TTC 2.2	207.0	0.33
Cell 2 Conc	TTC 2.2	44.5	0.51
Cell 3 Conc	TTC 2.2	7.0	0.79
Cell 4 Conc	TTC 2.2	11.6	0.60
Cell 5 Conc	TTC 2.2	6.5	0.74
Cell 6 Conc	TTC 2.2	5.0	0.58
Cell 1 Conc	TTC 2.3	182.0	0.48
Cell 2 Conc	TTC 2.3	44.0	0.70
Cell 3 Conc	TTC 2.3	17.5	0.85
Cell 4 Conc	TTC 2.3	13.4	0.97
Cell 5 Conc	TTC 2.3	11.7	1.03
Cell 6 Conc	TTC 2.3	7.0	1.16
Cell 1 Conc	TTC 2.4	158.0	0.52
Cell 2 Conc	TTC 2.4	51.0	0.68
Cell 3 Conc	TTC 2.4	18.3	0.79
Cell 4 Conc	TTC 2.4	14.3	0.94
Cell 5 Conc	TTC 2.4	10.1	1.10
Cell 6 Conc	TTC 2.4	5.8	1.28

Stream	Test Number	PGM g/ton	Cr2O3 %
Cell 1 Conc	TTC 4.1	183.0	0.38
Cell 2 Conc	TTC 4.1	18.0	0.60
Cell 3 Conc	TTC 4.1	7.2	0.90
Cell 4 Conc	TTC 4.1	8.7	0.86
Cell 5 Conc	TTC 4.1	5.9	0.96
Cell 6 Conc	TTC 4.1	4.9	1.02
Cell 1 Conc	TTC 4.2	200.0	0.46
Cell 2 Conc	TTC 4.2	46.0	0.63
Cell 3 Conc	TTC 4.2	17.8	0.88
Cell 4 Conc	TTC 4.2	15.6	1.02
Cell 5 Conc	TTC 4.2	10.8	1.12
Cell 6 Conc	TTC 4.2	7.5	1.13
Cell 1 Conc	TTC 4.3	148.0	0.61
Cell 2 Conc	TTC 4.3	35.5	0.75
Cell 3 Conc	TTC 4.3	13.0	1.26
Cell 4 Conc	TTC 4.3	11.8	1.47
Cell 5 Conc	TTC 4.3	7.8	1.68
Cell 6 Conc	TTC 4.3	5.3	1.80
Cell 1 Conc	TTC 4.4	171.0	0.57
Cell 2 Conc	TTC 4.4	28.5	0.75
Cell 3 Conc	TTC 4.4	11.2	1.22
Cell 4 Conc	TTC 4.4	10.3	1.25
Cell 5 Conc	TTC 4.4	5.0	1.96
Cell 6 Conc	TTC 4.4	2.9	2.88

Selected Data Points for Comparison with High Depressant Tests

Table C.4: Selected data points for overall comparisons.

	Standard tests at high depressant dosage				
	Feed grade	**PGM Recovery**	**Mass-pull**	**Concentration ratio**	**Concentrate grade**
	3.20	90.3	3.07	33	94.2
	4.28	90.1	4.18	24	92.2
	3.84	90.0	3.60	28	96.0
	3.64	89.9	3.31	30	98.8
	3.20	88.5	3.46	29	82.0
	3.62	83.0	3.62	28	62.3
	3.40	87.1	4.30	23	68.8
	3.52	83.5	3.41	29	86.2
Average	*3.59*	*87.8*	*3.62*	*28*	*85.1*

	TTC tests at normal depressant dosage				
	Feed grade	**PGM Recovery**	**Mass-pull**	**Concentration ratio**	**Concentrate grade**
	3.12	89.6	4.31	23	64.8
	3.48	86.7	3.68	27	82.0
	3.20	89.8	4.34	23	66.2
	3.52	89.7	4.20	24	75.2
	3.24	85.8	4.41	23	63.0
	3.92	87.8	4.11	24	83.8
	3.32	84.9	3.58	28	78.8
	3.64	88.5	4.50	22	71.6
Average	*3.43*	*87.8*	*4.14*	*24*	*73.2*

	Standard tests at normal depressant dosage				
	Feed grade	**PGM Recovery**	**Mass-pull**	**Concentration ratio**	**Concentrate grade**
	4.02	87.8	5.39	19	65.5
	3.16	84.9	4.71	21	57.0
	3.66	86.1	5.73	17	55.0
	2.92	85.0	4.68	21	53.0
	3.64	88.0	5.34	19	60.0
	2.92	80.5	5.00	20	47.0
	4.48	89.3	7.47	13	53.5
	3.08	83.8	3.97	25	65.0
Average	*3.49*	*85.7*	*5.29*	*19*	*57.0*

Mass Balance Procedure

To obtain a mass balance around the FCTR a technique known as connection matrices was used. This technique relies on the feed sample having a high degree of confidence as far as flow rates are concerned. From here on, split factors (g_i) are then used to calculate the individual concentrate and tail flow rates as follow:

$$g_i = \frac{\text{conc flow}}{\text{tails flow}} \qquad \text{(C1.2)}$$

As an initial guess a value of 1 was assigned to g_i for all the different components in every stream.

A connection matrix was then set up for every piece of equipment. When a concentrate stream leaves the piece of equipment it is donated a g_i at the piece of equipment it enters. In this case none exists since all go to final concentrate. When it is tails it is represented by a 1 at the piece of equipment it enters. In this case Cell 1 tails is going to Cell 2, hence the 1 in the row of Cell 2 but the Column of Cell 1. At a specific piece of equipment the cell is represented by $-(1+ g_i)$. In this case C_1 to C_6 represents rougher cells 1 to 6.

Table C.5: Example of a connection matrix.

Connection Matrix

	Cell1	**Cell2**	**Cell3**	**Cell4**	**Cell5**	**Cell6**
Cell1	$-(1+gC_1)$	0	0	0	0	0
Cell2	1	$-(1+gC_2)$	0	0	0	0
Cell3	0	1	$-(1+gC_3)$	0	0	0
Cell4	0	0	1	$-(1+gC_4)$	0	0
Cell5	0	0	0	1	$-(1+gC_5)$	0
Cell6	0	0	0	0	1	$-(1+gC_6)$
Feed split	1	0	0	0	0	0

The bottom row (Feed spilt, δ) is an indication of the fraction of new feed that is fed to the individual cells. In this case all goes to cell 1. Once the matrix is set up the tails (**T**, a vector) is calculated according to:

$$T = -F \cdot \sum C^{-1} \cdot \delta \qquad \text{(C1.3)}$$

where $\mathbf{C^{-1}}$ is the inverse of the connection matrix formed by the rows and columns of the rougher cells. Once the value of **T** is known the concentrate flow is calculated from equation (C1.2).

Using solver in Microsoft Excel, the values of g_i were iterated to give the best fit to the measured mass flow rates. When the elemental assays are balanced, the flow of every elements in the individual streams are calculated and used to back-calculate the assay. The errors in the assays are then used as criteria. Finally, parity graphs (experimental values vs. balanced values) are plotted to view the integrity of the mass balance.

Parity Graphs for Pilot Plant Mass Balance

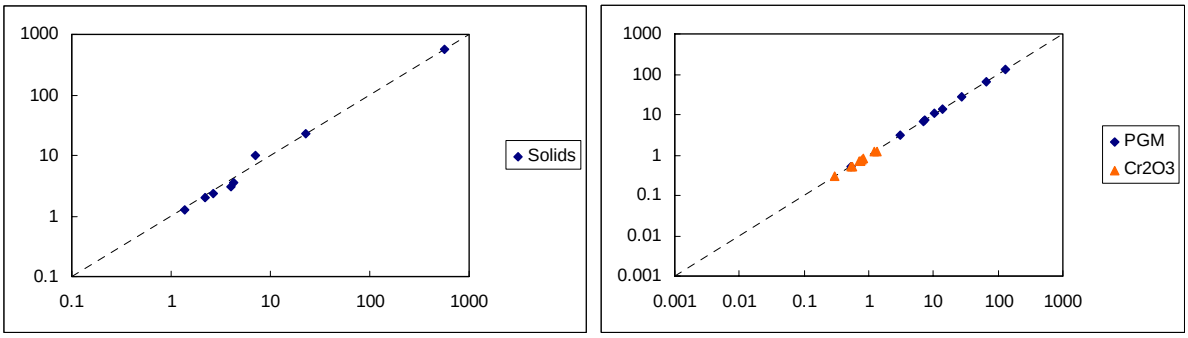

Figure C.1: Parity graphs on solids, PGM and Cr_2O_3 for standard test 1.

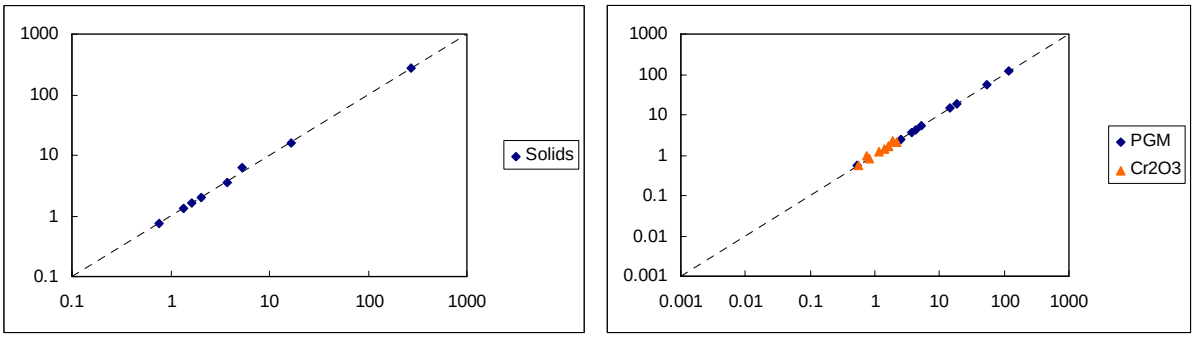

Figure C.2: Parity graphs on solids, PGM and Cr_2O_3 for standard test 2.

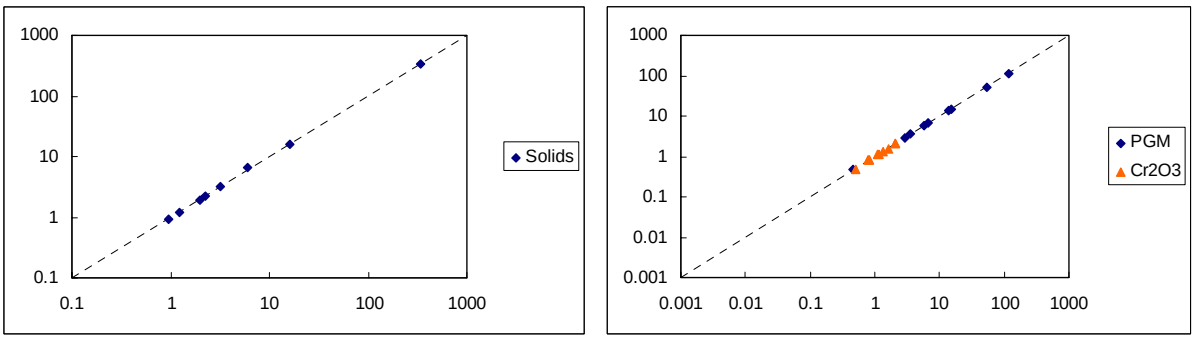

Figure C.3: Parity graphs on solids, PGM and Cr_2O_3 for standard test 3.

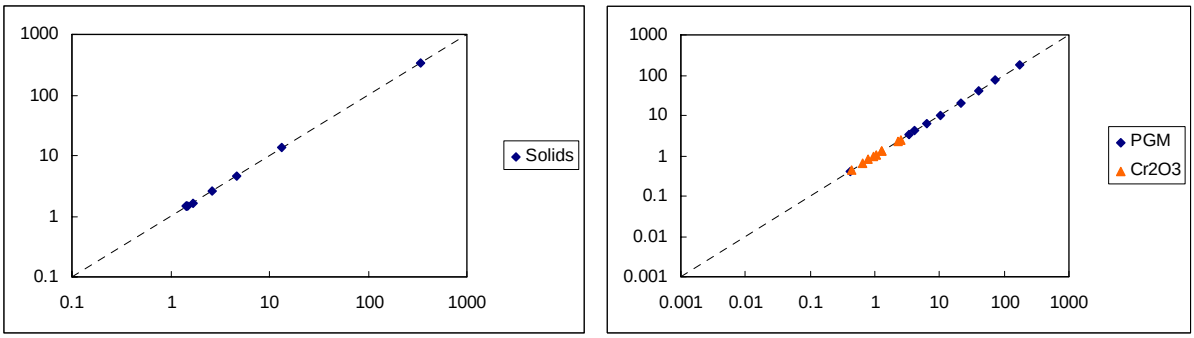

Figure C.4: Parity graphs on solids, PGM and Cr_2O_3 for TTC test 1.

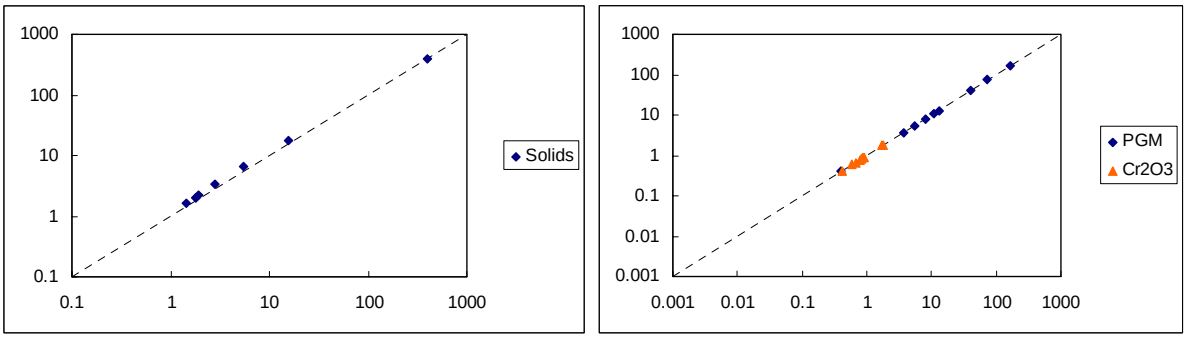

Figure C.5: Parity graphs on solids, PGM and Cr_2O_3 for TTC test 2.

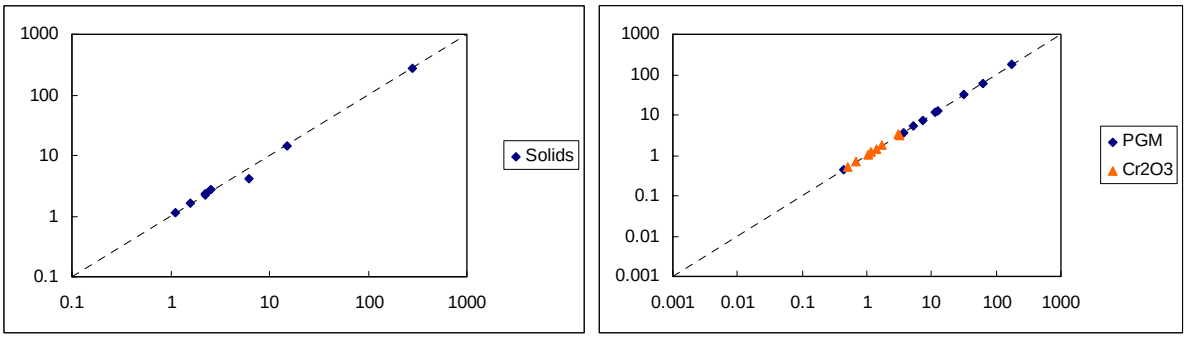

Figure C.6: Parity graphs on solids, PGM and Cr_2O_3 for TTC test 4.

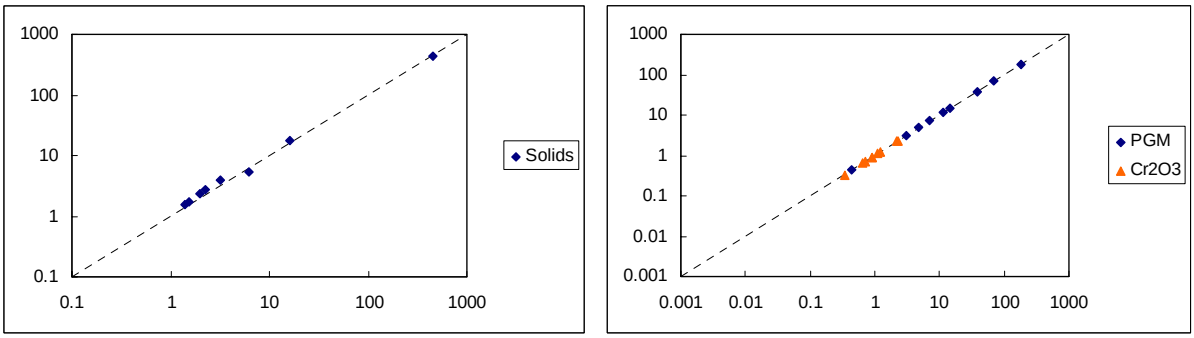

Figure C.7: Parity graphs on solids, PGM and Cr_2O_3 for TTC test 5.

Appendix D

Preliminary Plant Trial Data

Table D.1: Summary of plant trial shift results.

	Feed		Concentrate		Tails		Recovery		Cr in Concentrate	
	STD	**TTC**	**STD**	**TTC**	**STD**	**TTC**	**STD**	**TTC**	**STD**	**TTC**
1	4.4	5.1	77.7	194.2	1.09	1.12	76.3	78.5	1.48	1.44
2	4.0	4.3	118.1	120.7	0.88	0.80	78.6	81.9	2.07	1.48
3	4.7	3.6	128.6	150.7	1.38	0.99	71.4	73.0	2.75	1.33
4	4.8	4.6	141.6	106.3	1.34	0.84	72.8	82.4	2.09	1.8
5	3.8	3.8	63.2	82.7	0.86	1.12	78.4	71.5	1.36	5.2
6	3.9	4.9	66.5	176.6	0.76	1.01	81.4	79.8	2.40	2.98
7	4.2	5.0	86.4	147.3	1.03	1.02	76.4	80.2	2.11	1.37
Ave	*4.3*	*4.5*	*97.4*	*139.8*	*1.05*	*0.99*	*76.5*	*78.2*	*2.04*	*2.23*

Table D.2: Summary of rougher concentrate assays.

	PGM	
	Rougher 1	**Rougher 2**
Standard	171	190
With TTC	242	254

	Cr2O3	
	Rougher 1	**Rougher 2**
Standard	2.03	1.68
With TTC	1.56	1.31

Table D.3: Size-by-size assay results of concentrate samples.

	Rougher 1			Rougher 2		
	PGM (g/ton)	**Cr2O3 (%)**	**SiO2 (%)**	**PGM (g/ton)**	**Cr2O3 (%)**	**SiO2 (%)**
Standard +53 um	160	1.21	41.9	170	2.39	49.6
With TTC +53 um	420	1.04	37.5	312	0.70	37.0
Standard -53 um	162	1.41	42.1	186	1.71	50.2
With TTC -53 um	232	1.48	50.9	200	2.03	49.4

Particle Size Analyser Data

Table D.4: Particle size data obtained from particle size analyser.

	Standard Collector Suite					
	Rougher cell 1			Rougher cell 2		
	Run 1	**Run 2**	**Run 3**	**Run 1**	**Run 2**	**Run 3**
300 um	99.57	99.81	99.51	97.21	98.24	97.03
212 um	98.83	99.49	99.01	95.35	97.27	96.11
106 um	97.9	98.81	98.08	93.30	95.84	95.10
75 um	96.49	97.06	95.98	90.55	93.47	93.47
53 um	93.58	93.48	91.91	86.50	89.65	90.52
38 um	87.92	87.59	85.52	80.89	84.13	85.75
10 um	79.50	79.46	77.23	73.99	77.08	79.11
sub 10 um	35.86	35.18	34.87	37.54	38.53	40.01

	Standard Collector Suite with TTC					
	Rougher cell 1			Rougher cell 2		
	Run 1	**Run 2**	**Run 3**	**Run 1**	**Run 2**	**Run 3**
300 um	99.15	100.00	100.00	99.68	99.50	97.72
212 um	98.44	100.00	100.00	99.25	98.93	97.00
106 um	97.60	100.00	100.00	98.79	98.40	96.34
75 um	96.59	100.00	100.00	97.98	97.52	96.01
53 um	94.92	99.88	99.89	96.28	95.73	95.57
38 um	91.32	97.99	97.87	93.05	92.37	93.55
10 um	84.70	92.22	91.81	87.62	86.83	88.42
sub 10 um	38.00	40.09	40.79	42.61	42.00	43.80

Published Papers

- MILLER, J.D., LI, J., DAVIDTZ, J.C. & VOS, C.F. 2005. A review of pyrrhotite flotation chemistry in the processing of PGM ores. *Minerals Engineering*, July 2005, vol. 18, p. no. 2, p.855-865.

- VOS, C.F., DAVIDTZ, J.C. & MILLER, J.D. 2006. Trithiocarbonates for the flotation of PGM sulphides. *Paper presented at the 2nd Platinum Conference, 8-12 October 2006, Sun City, South Africa*.

References

ADAM, K. & IWASAKI, I. 1984. Grinding media-sulphide mineral interaction and its effect on flotation. *Trans SME-AIME*, p.66-80.

ADAMSON, A.W. 1990. Physical chemistry of surfaces. John Wiley and Sons Inc, 5th ed. New York, Chichester, Brisbane, Toronto, Singapore.

ANDREEV, G.N. & BARZEV, A. 2003. Raman spectroscopy study of some chalcopyrite-xanthate flotation products. *Journal of Molecular Structures*, 2003, vol.661-662, p.325-332.

BOZKURT, V., XU, Z. & FINCH, J.A. 1998. Pentlandite/Pyrrhotite interaction and xanthate adsorption. *International Journal of Mineral Processing,* February 1998, vol.52, no.4, p.203-214.

BOZKURT, V., XU, Z. & FINCH, J.A. 1999. Effect of depressants on xanthate adsorption on pentlandite and pyrrhotite: Single vs mixed minerals. *Canadian Metallurgical Quarterly,* April 1999, vol.38, no.2, p.105-112.

BRADSHAW, D.J. 1997. Synergistic effects between thiol collectors used in the flotation of pyrite. PhD Thesis. Faculty of Engineering and Built Environment, University of Cape Town, South Africa.

BRADSHAW, D.J., BUSWELL, A.M., HARRIS, P.J. & EKMEKCI, Z. 2006. Interactive effect of the type of milling media and copper sulphate addition on the flotation performance of sulphide minerals from Merensky ore. Part I: Pulp chemistry. *International Journal of Mineral Processing*, February 2006, vol. 78, no. 3, p.153-163.

BREYTENBACH, W., VERMAAK, M.K.G., & DAVIDTZ, J.C. 2003. Synergistic effects among dithiocarbonate (DTC), dithiophosphate (DTP) and trithiocarbonate (TTC) in the flotation of Merensky ores. *Journal of South African Institute of Mining and Metallurgy*, December 2003, vol.103, no.10, p.667-670.

BUCKLEY, A., HAMILTON, I.C. & WOODS, R. 1985. In Flotation of sulphide minerals. Developments in mineral processing, eds. E. Forssberg, Elsevier, Amsterdam, no.6, p.41-60.

BUCKLEY, A.N. & WOODS, R. 1993. Underpotential deposition of dithiophosphate on chalcocite. *Journal of Eletroanalytical Chemistry,* 1993, vol. 357, p. 387-405.

BUCKLEY, A.N. & WOODS, R. 1997. Chemisorption – the thermodynamically favoured process in the interaction of thiol collectors with sulphide minerals. *International Journal of Minerals Processing,* October 1997, vol.51, no.1-4, p. 15-26.

BUCKLEY, A.N., GOH, S.W., LAMB, R.N. & WOODS, R. 2003. Interaction of thiol collectors with pre-oxidised sulphide minerals. *International Journal of Mineral Processing,* 29 September 2003, vol.72, no.1-4, p.163-174.

BULATOVIC, S. 2003. Evaluation of alternative reagent schemes for the flotation of platinum group minerals from various ores. *Minerals Engineering,* October2003, vol.16, no.10, p. 931-939.

BUSWELL, A.M. & NICOL, M.J. 2002. Some aspects of the electrochemistry of the flotation of pyrrhotite. *Journal of Applied Electrochemistry*, December 2002, vol.32, no. 12, p.1321-1329.

CHANDER, S. 1999. Fundamentals of Sulphide Mineral Flotation. In *Advances in Flotation Technology*, ed. B.K. Parekh and J.D. Miller, p.129-165.

CHANG, C.S., COOKE, S.R.B. & IWASAKI, I. 1954. Flotation characteristics of pyrrhotite with xanthate. *Trans. AIME,* p.199-209.

CHANTURIYA, V., MAKAROV, V., FORSLING, W., MAKAROV, D., VASILEVA, T., TROFIMENKO, T. & KUZNETSON, V. 2004. The effect of crystallochemical peculiarities of nickel sulfide minerals on flotation of copper-nickel ores. *International journal of Mineral Processing,* 19 November 2004, vol.74. no.1-4, p.289-301.

COATES, J.P. 2000. Interpretation of infrared spectra: A practical approach. *Encyclopedia of Analytical Chemistry,* R.A. Meyers (Ed.). Copyright © John Wiley & Sons, Chichester, p.10815-10837.

COETZER, G. & DAVIDTZ, J.C. 1989. Sulfhydryl collectors in bulk and selective flotation. Part 1. Covalent trithiocarbonates. *Journal of South African Institute of Mining and Metallurgy,* October 1989, vol. 89, no. 10, p.307-311.

COETZER, G. 1987. A quantitative evaluation of sulphydryl collectors on the selective flotation of a copper-lead-zinc-iron ore. M.Eng Thesis. Potchefstroom University for Christian Higher Education.

CRAMER, L.A. 2001. The extractive metallurgy of South Africa's platinum ores. *JOM,* October 2001, vol.53, no.10, p.14-18.

CROZIER, R.D. & KLIMPEL, R.R. 1989. Frothers: Plant practice. *Minerals Processing and Extractive Metallurgy. Review*. vol. 5, p. 257-279.

DAVIDTZ, J.C. 1998. Design of molecules specific to base mineral recovery in typical PGM containing ores. 8th International Platinum Symposium, 28 June-3 July 1998.

DAVIDTZ, J.C. 1999. Quantification of the flotation activity by means of excess Gibbs Free Energies. *Minerals Engineering*, October 1999, vol.12, no.10, p.11471 – 1161.

DAVIDTZ, J.C. 2004. Research Professor, Pretoria University. South Africa. Personal Communications.

DAVIDTZ, J.C. 2006. Research Professor, Pretoria University. South Africa. Personal Communications.

DIPPENAAR, A. 1982. The destabilisation of froth by solids. I. The mechanism of film rupture. *International Journal of Mineral Processing,* January 1982, vol. 9, no. 1, p. 1-14.

DU PLESSIS, R. 2003. The thiocarbonate flotation chemistry of Auriferous Pyrite. PhD Thesis. University of Utah, Salt Lake City, Utah, USA.

EKMEKCI, Z., BRADSHAW, D.J., HARRIS, P.J. & BUSWELL, A.M. 2006. Interactive effect of the type of milling media and copper sulphate addition on the flotation performance of sulphide minerals from Merensky ore. Part II: Froth stability Chemistry. *International Journal of Mineral Processing*, February 2006, vol. 78, no. 3, p. 164-174.

FINKELSTEIN, N.P. 1997. The activation of sulphide minerals for flotation: a Review. *International Journal of Mineral Processing*, December 1997, vol.52, no.2-3, p.81-120.

FORNASIERO, D., MONTALTI, M. & RALSTON, J. 1995. Kinetics of adsorption of Ethyl Xanthate on pyrrhotite: In Situ UV and Infrared Spectroscopy studies. *Journal of Colloid and Interface Science,* 15 June 1995, vol.172, no.2, p.467-478.

FORSSBERG, K.S., SUBRAHMANYAM, T.V. & NILSSON, L.K. 1993. Influence of grinding method on complex sulphide ores flotation: a pilot plant study. *International Journal of Mineral Processing,* June 1993, vol.38, no.3-4, p.157-175.

FUERSTENAU, M.C. & SABACKY, B.J. 1981. On the natural floatability of sulphides. *International Journal of Mineral Processing,* March 1981, vol.8, no.1, p.79-88.

FUERSTENAU, M.C. 1982a. Adsorption of sulfhydryl collectors. *In Principals of Flotation, ed. R.P. King, SAIMM, Johannesburg.* p. 91-108.

FUERSTENAU, M.C. 1982b. Chemistry of collectors in solution. *In Principals of Flotation, ed. R.P. King, SAIMM, Johannesburg.* p. 1-16.

FUERSTENAU, M.C. 1982c. Sulphide mineral flotation. *In Principals of Flotation, ed. R.P. King, SAIMM, Johannesburg.* p. 159-182.

FUERSTENAU, M.C. 1982d. Activation in the flotation of sulphide minerals. *In Principals of Flotation, ed. R.P. King, SAIMM, Johannesburg.* p. 183-198.

FUERSTENAU, M.C., MILLER, J.D. & KUHN, M.C. 1985. Chemistry of flotation. SME, p. 1-5; 74-78.

GARRELS, R.M. & CHRIST, C.L. 1990. Minerals and equilibria. Jones and Bartlett Publishers, Boston and London.

GAUDIN, A.M. 1957. Flotation. 2nd Ed, McGraw-Hill, New York, N.Y, Chapter 9.

GEORGE, W.O. 1987. Infrared spectroscopy. John Wiley and Sons, Great Britain, p. 537.

GÖKTEPE, F. 2002. Effect of pH on pulp potential and sulphide mineral flotation. *Turkish Journal of Engineering and Environmental Science*, July 2002, vol. 26, no.4, p.309-318.

GREET, C.J. 2004. Impala Platinum Limited: Repeat Grinding Media Testing To Determine the Effects of High Chrome on Platinum Flotation. Report Number DP14. Submitted to Impala Platinum LTD, 31 August 2004.

GROBLER, W.A., SONDASHI, S. & CHIDLEY, F.J. 2005. Recent developments in flotation reagents to improve base metal recovery. *The South African Institute of Mining and Metallurgy. Paper presented at the third Southern African Conference on Base Metals.* In Press

GUO, H. & YEN, W.T. 2003. Pulp potential and floatability of chalcopyrite. *Minerals Engineering,* March 2003, vol.16, no.3, p.247-256.

HARRIS, P.J. 1982. Frothing phenomena and frothers. *In Principals of Flotation, ed. R.P. King, SAIMM, Johannesburg.* p. 237-250.

HAY, M.P., FRAGOMENI, D. & DiFEO, T. 2006. Determination of metal and mineral flotation performance at one of Falconbridge's base metal operations. *Paper presented at Canadian Mineral Processing 2006,* Ottawa, Canada.

HELBIG, C., BRADSHAW, D.J., HARRIS, P.J., O'CONNAR, C.T. & BALDAUF, H. 2000. The synergistic interactions of mixtures of thiol collectors in the flotation of sulphide minerals. *Presented at XXI International Mineral Processing Congress, Rome, Italy, 2000.*

HEYENS, G.W. & TRAHAR, W.J. 1984. The flotation of pyrite and pyrrhotite in the absence of conventional collectors. *Proceedings of the International Symposium on Electrochemistry in Mineral and Metal Processing*, P.R. Richardson, S.S. Srinivasan and R. Woods (Eds), Elecro. Chem. Soc., Pennington, N.J., 84-10, 219.

HICYILMAZ, C., ALTUN, N.M., EKMEKCI, Z. & GOKAGAC, G. 2004. Quantifying hydrophobicity of pyrite after copper activation and DTPI addition under electrochemically controlled conditions. *Minerals Engineering,* July-August 2004, vol.17, no.7-8, p.879-890.

HODGSON, M. & AGAR, G.E. 1989. Electrochemical investigations into the flotation chemistry of pentlandite and pyrrhotite: process water and xanthate interactions. *Canadian Metallurgy Quarterly,* vol.28, p.189-198.

IWASAKI, I., REID, K.J., LEX., H.A. & SMITH, K.A. 1983. Effect of autogenous and ball mill grinding on sulphide flotation. *Mining Engineering,* October 1983, vol. 35, no. 8, p.1184-1190.

JANZEN, M.P., NICHOLSON, R.V. & SCHARER, J.M. 2000. Pyrrhotite reaction kinetics: Reaction rates for oxidation by oxygen, ferric iron, and non-oxidative dissolution. *Geochimica et Cosmochimica Acta,* May 2000, vol.64, no.9, p.1511-1522.

KELEBEK, S., WELLS, P.F., FEKETE, S.O. 1996. Differential flotation of chalcopyrite, pentlandite and pyrrhotite in Ni-Cu sulphide ores. *Canadian Metallurgical Quarterly*, October - December 1996, vol.35, no.4, p.329-336.

KELLY, E.G. & SPOTTISWOOD, D.J. 1989. Introduction to mineral processing. Lamb Printers, Australia, 1st Ed reprint, 1989.

KHAN, A. & KELEBEK, S. 2004. Electrochemical aspects of pyrrhotite and pentlandite in relation to their flotation with xanthate. Part-I: Cyclic voltammetry and rest potential measurements. *Journal of Applied Electrochemistry,* August 2004, vol. 34, no. 8, p.849-856.

KIRJAVAINEN, V.M. 1996. Review and analysis of factors controlling the mechanical flotation of gangue minerals. *International Journal of Mineral Processing,* April 1996, vol.46, no.1-2, p.21-34.

KLIMPEL, R.R. & ISHERWOOD, S. 1992. The Interaction of size reduction and froth flotation in sulphide mineral processing. *Mineral Reagent International, Midland, MI 48640*.

KLIMPEL, R.R. 1999. A review of sulphide mineral collector practice. In Advances in Flotation Technology, ed. B.K. Parekh and J.D. Miller, p.183-195.

KLIMPEL, R.R. 2000. Optimising the industrial flotation performance of sulphide minerals having some natural floatability. *International Journal of Mineral Processing,* February 2000, vol.58, no.1-4, p. 77-84.

Klimpel, R.R., Selection of chemical reagents for flotation. *In Mineral Processing Design, Eds. A. Mular and R. Bhappu*. Society of mining engineers, Littleton, Colorado, 907-934 (1980).

KUOPANPORTTI, H., SUORSA, T. & PÖLLANEN, E. 1997. Effects of oxygen on kinetics of conditioning in sulphide flotation. *Minerals Engineering,* November 1997, vol.10, no.11, p1193-1205.

LEJA, J. & SCHULMAN, J.H. 1954. Flotation theory: molecular interaction between frothers and collectors at solid-liquid-air interfaces. *Transactions of the SME-AIME,* 1954, vol. 199, p. 221-228.

LEJA, J. 1968. On the mechanisms of surfactant adsorption. Presented at *VIII International Mineral Processing Congress, Leningrad.* vol S-1, p. 1-7.

LEJA, J. 1989. Interactions of surfactants. *Minerals Processing and Extractive Metallurgy. Review.* 1989, vol. 5, p. 1-22.

LEPPINEN, J.O. 1990. FTIR and flotation investigation of the adsorption of ethyl xanthate on activated and non-activated sulphide minerals. *International Journal of Mineral Processing*, 30 December 1990, vol.30, no.3-4, p.245–263.

LEPPINEN, J.O., BASILIO, C.I. & YOON, R.H. 1989. In-situ FTIR study of ethyl xanthate adsorption on sulphide minerals under conditions of controlled potential. *International Journal of Mineral Processing,* July 1989, vol. 26, no. 3-4, p. 259-274.

LOVELL, V.M. 1982. Industrial flotation reagents. *In Principals of Flotation, ed. R.P. King, SAIMM, Johannesburg.* p. 73-89.

MENDIRATTA, N.K. 2000. Kinetic study of sulphide mineral oxidation and xanthate adsorption. PhD Thesis. Virginia Ploytech Institute and State University.

MIELCZARSKI, J.A., CASES, J.M. & BARRES, O. 1996. In Situ infrared characterisation of surface products of interaction of an aqueous xanthate solution with chalcopyrite, tetrahedrite, and tennantite. *Journal of Colloid and Interface Science*, 25 March 1996, vol.178, no.2, p.740-748.

MIELCZARSKI, J.A., MIELCZARSKI, E. & CASES, J.M. 1998. Influence of chain length on adsorption of xanthates on chalcopyrite. *International Journal of Mineral Processing*, February 1998, vol.52, no.4, p.215-231.

MIELZARSKI, J.A., MIELZARSKI, E. & CASES, J.M. 1996. Interaction of amyl xanthate with chalcopyrite, tetrahedrite, and tennantite at controlled potentials. Simulation and spectroelectrochemical results for two-component adsorption layers. *Langmuir,* 25 December 1996, vol. 12, no. 26, p.6521-6529.

MILLER, J.D. 1988. The significance of electrochemistry in the analysis of mineral processing phenomena. *Seventh Australian Electrochemistry Conference*, Sydney, Australia, 14-19 February 1988.

MILLER, J.D., LI, J., DAVIDTZ, J.C. & VOS, F. 2005. A review of pyrrhotite flotation chemistry in the processing of PGM ores. *Minerals Engineering,* June 2005, vol.18, no.2, p.855-865.

MONTALTI, M. 1994. Interaction of ethyl xanthate with pyrite and pyrrhotite minerals. PhD Thesis. University of South Australia.

MONTALTI, M., FORNASIERO, D. & RALSTON, J. 1991. Ultraviolet-visible spectroscopic study of the kinetics of adsorption of ethyl xanthate on pyrite. *Journal of Colloid and Interface Science,* May 1991, vol. 143, no. 2, p. 440-450.

MONTE, M.B.M. & OLIVEIRA, J.F. 2004. Flotation of sylvite with dodecylamine and the effect of added long chain alcohols. *Minerals Engineering*, March 2004, vol.17, no.3, p.425-430.

NICHOLSON, R.V. & SHARER, J.M. 1994. Laboratory studies of pyrrhotite oxidation kinetics. In: Alpers, C.N., Blowes, D.W. (Eds), Environmental Geochemistry of sulphide oxidation. ACS Symposium series, vol.550, p.14-30. Washington, DC.

NICOL, M.J. 1984. In: Richardson, P.E., Srinivasan, S., Woods, R. (Eds.), International Symposium on Electrochemistry Mineral and Metal Processing. Electrochemical Society, pp. 152–168.

PANG, J. & CHANDER, S. 1993. Properties of surface films on chalcopyrite and pyrite and their influence in flotation. *Preceedings of the XVII International Mineral Processing Congress*. The Australasian Institute of Mining and Metallurgy in Parkville, no.3, p.669-677.

PLAKSIN, I.N. & BESSONOV, S.V. 1957. The role of gasses in flotation reactions. *Proceedings of the 2nd International Congress on Surface Activity*, 1957, vol.3, p.361-367.

POLING, G.W. 1976. Reactions between thiol reagents and sulphide minerals. In Flotation ed. M.C. Fuerstenau, AIME, New York, NY, p.334-363.

RAO, K.H. & FORSSBERG, K.S.E. 1997. Mixed collector systems in flotation. *International Journal of Mineral Processing*, October 1997, vol.51, no.1-4, p.67-79.

RICHARDSON, P.E. & WALKER, G.W. 1985. The flotation of Chalcocite, Bornite, Chalcopyrite and Pyrite in electrochemical flotation cell. Paper presented at the *XV International Minerals Processing Congress*, *Cannes*, vol. II, p.198-210.

ROBERTSON, C., BRADSHAW, D. & HARRIS, P. 2003. Decoupling the effect of depression and dispersion in the batch flotation of a platinum bearing ore. *Proceedings of the XXII International Mineral Processing Congress*, Cape Town, South Africa, 29 Sept-3 Oct, 920-928.

RYAN, M.A. 2005. Senior Metallurgical Engineer, Impala Platinum Mineral Processes, Rustenburg, South Africa. Personal Communications.

SANDLER, S.I. 1999. Chemical and engineering thermodynamics. 3nd Edition, Wiley & Sons, 1999.

SAVASSI, O.N., ALEXANDER, D.J., FRANZIDIS, J.P. & MANLAPIG, E.V. 1998. An empirical model for entrainment in industrial flotation plants. *Minerals Engineering*, March 1998, vol.11, no.3, p.243-256.

SCHUBERT, H. 2005. Nanobubbles, hydrophobic effect, heterocoagulation and hydrodynamics in flotation. *International Journal of Mineral Processing,* 15 December 2005, vol. 78, no. 1, p. 11-21.

SENIOR, G.D., TRAHAR, W.J., GUY, P.J., 1995. The selective flotation of pentlandite from a nickel ore. *International Journal of Mineral Processing,* June 1995, vol.43, no.3-4, p. 209-234.

SHACKLETON, N.J., MALYSIAK, V. & O'CONNOR, C.T. 2003. The use of amine complexes in managing inadvertent activation of pyroxene in a pentlandite-pyroxene flotation system. *Minerals Engineering,* September 2003, vol.16, no.9, p.849-856.

SLABBERT, W. 1985. The role of trithiocarbonates and thiols on the flotation of some selected South African sulphide ores. M.Eng Thesis. Potchefstroom University for Christian Higher Education.

STEYN, J.J. 1996. The role of collector functional groups in the flotation activity of Merensky Reef samples. M.Eng Thesis. Potchefstroom University for Christian Higher Education.

SWEET, J.A. 1999. Investigation of a methodology to decouple physical and chemical effects for flotation circuit performance evaluation. MSc Thesis. Faculty of Engineering and Built Environment, University of Cape Town, South Africa.

TAGGART, A.F., GIUDICE, G.R.M. & ZIEHL, O.A. 1934. The case for chemical theory of flotation. *Transactions of the American Institute of Mining and Metallurgical Engineers,* vol. 112, p. 348-381.

VAUGHAN, D.J., BECKER, U. & WRIGHT, K. 1997. Sulphide mineral surfaces: theory and experiments. *International Journal of Minerals Processing,* October 1997, vol. 51, no. 1-4, p. 1-14.

VERMAAK, M.K.G. 2005. Fundamentals of the flotation behaviour of Palladium Bismuth Tellurides. PhD Thesis. Department Material Science and Metallurgical Engineering, University of Pretoria.

VOS, N.F. 2004. Senior Geologist, Anglo Platinum, Rustenburg Section. Personal Communications.

VREUGDENHIL, A.J., BRIENNE, S.H.R., MARKWELL, R.D., BUTLER, I.S. & FINCH, J.A. 1997. Headspace analysis gas-phase infrared spectroscopy: a study of xanthate decomposition on mineral surfaces. *Journal of Molecular Structure,* 17 March 1997, vol. 405, no.1, p.67-77.

WIESE, J., HARRIS, P. & BRADSHAW, D. 2005a. The influence of the reagent suite on the flotation of ores from the Merensky reef. *Minerals Engineering*, February 2005, vol.18, no.2, p.189-198.

WIESE, J., HARRIS, P. & BRADSHAW, D.J. 2005b. Investigation of the role and interactions of a dithiophosphate collector in the flotation of sulphides from the Merensky reef. *Minerals Engineering*, May-June 2005, vol.18, no.6-8, p.675-686.

WILLS, B. A. 1997. Mineral Processing Technology: An introduction to the practical aspects of ore treatment and mineral recovery. 6th ed. Butterworth Heinemann.

WOODS, R. 1971. The oxidation of ethyl xanthate on platinum, gold, copper and galena electrodes. Relation to the mechanism of flotation. *Journal of Physical Chemistry,* 1971, vol. 75, no. 3, p.354-362.

WOODS, R. 1976. Electrochemistry of Sulphide Flotation. In Flotation ed. M.C. Fuerstenau, AIME, New York, NY, p.298-333.

WOODS, R. 1987. Flotation of sulphide minerals. *In Reagents in Mineral Technology*, eds., P. Somasundaran and B.M Moudgil, Marcel Dekker, New York, p.39-78.

YOON, R.-H., BASILIO, C.I., MARTICORENA, M.A., KERR, A.N. & STRATTON-CRAWLEY, R. 1995. A study of the pyrrhotite depression mechanism by diethylenetriamine. *Minerals Engineering,* July 1995, vol.8, no.7, p.807-816.

ZDZIENNICKA, A., JANCZUK, B. & WOJCIK, W. 1998. Influence of ethyl xanthate on the wettability and surface free energy of synthetic Chalcocite. *Powder Technology,* March 1998, vol.95, no.3, p.234-239.